

Inhibitory and oxidative effects of gossypol on MCF7 breast cancer cells *in vitro*

by

William Brandon Winfrey

20 August 2013

Principal Investigator: Baohong Zhang, Ph.D.

Department of Biology

East Carolina University

Abstract

Human cancer is the second leading cause of death in the United States and breast cancer is responsible for the second highest number of deaths in women with cancer worldwide. Today, cancer is becoming more and more resistant to current chemotherapeutic agents. In an effort to decrease this resistance, natural products like gossypol are being tested for efficacy as a natural chemotherapeutic agent with anti-cancer properties. Current literature demonstrates that gossypol is indeed an effective drug against breast cancer when used alone and when combined with other chemotherapeutic agents [1-5]. The majority of current literature focuses on the ability of gossypol to antagonize anti-apoptotic proteins like BCL-XL and induce apoptosis [6, 7]. This study helps understand previous data and goes beyond the current knowledge base and explores not only apoptosis induction, but also on other important effects like: oxidative stress, other possible avenues of cell death, growth and development, and cell cycle progression. Combining physiological, genotypic, flow cytometric and biochemical assays, a more complete understanding of gossypol's efficacy and mechanism of action

can be ascertained. In past studies, the focus of gossypol's efficacy has been too narrow and currently the study of gene regulators like microRNAs (miRNAs) has not been incorporated. This study reveals evidence that miRNA may play an important role and that gossypol's efficacy is in fact a multi-component system that is interconnected in its overall mechanism of action.

Inhibitory and oxidative effects of gossypol on MCF7 Breast Cancer cells *in vitro*

A Thesis

Presented To

The Faculty of the Department of Biology

East Carolina University

In Partial Fulfillment

of the Requirements for the Degree

Master of Science in Molecular Biology and Biotechnology

by

William Brandon Winfrey

20 August 2013

Inhibitory and oxidative effects of gossypol on MCF7 Breast Cancer cells in vitro

by

William Brandon Winfrey

APPROVED BY:

DIRECTOR OF THESIS: _____

Baohong Zhang, PhD

COMMITTEE MEMBER: _____

Anthony Capehart, PhD

COMMITTEE MEMBER: _____

Xiaoping Pan, PhD

COMMITTEE MEMBER: _____

Jarrett Whelan, PhD

CHAIR OF THE DEPARTMENT OF BIOLOGY:

Jeff McKinnon, PhD

DEAN OF THE GRADUATE SCHOOL:

Paul J. Gemperline, PhD

ACKNOWLEDGEMENTS

I want to start off by thanking Dr. Zhang for letting me work in his lab and for always leading by example. He is one of the hardest working people I know and he inspires everyone around him to achieve their best. I also want to thank my committee members Dr. Anthony Capehart, Dr. Xiaoping Pan and Dr. Jarrett Whelan for being my professors and mentors as well as my committee members. You all put your hearts and souls into what you do and I consider myself lucky to have had the opportunity to learn from each one of you.

I would be remiss not to mention the overwhelming support from my fellow lab members especially Fuliang Xie and Faten Taki. Without your support there would be no graduation. I am truly thankful for all you have done and all the ideas we bounced off each other and for the time you spent doing so.

Mostly, I want to thank God, for giving me the strength and ability to persevere and for giving me a loving family who I can always count on.

TABLE OF CONTENTS

LIST OF TABLES.....	viii
LIST OF FIGURES.....	ix-x
LIST OF ABBREVIATIONS.....	xi-xii
CHAPTER 1: REVIEW OF BREAST CANCER, MCF7 CELL LINE, GOSSYPOL, MICRORNAS, OXIDATIVE STRESS AND CANCER.....	1
Breast Cancer	1
MCF7 Cell Line.....	2
Gossypol.....	3
MCF7 and gossypol.....	4
Oxidative Stress and Cancer.....	5
MicroRNAs.....	6
Hypothesis.....	8
Objectives.....	9
References.....	10
CHAPTER 2: EFFECTS OF GOSSYPOL ON THE GROWTH, PROLIFERATION, CELL CYCLE PROGRESSION AND CELL DEATH OF MCF-7 BREAST CANCER CELLS.....	19-22 23
Abstract.....	23
Introduction.....	24
Materials and Methods.....	25
Cell Line and Cell Culture.....	25-26
Gossypol Treatment and Dose Response.....	26

Cell Cycle Analysis.....	26-27
RNA Extraction, Reverse Transcription, Real Time PCR.....	27-28
Results	
Proliferation of MCF-7 cells is inhibited by gossypol.....	29
Cell Cycle analysis.....	29
qRT-PCR analysis.....	30
Cell Death.....	31
Discussion.....	32-35
References.....	44-46
CHAPTER 3: CHAPTER 3: GOSSYPOL ALTERS MIRNA EXPRESSION OF	
MCF-7 BREAST CANCER CELLS.....	47
Abstract.....	47
Introduction.....	48-49
Materials and Methods.....	49
Cell line and Cell Culture.....	49
Gossypol Treatment.....	49-50
RNA Isolation.....	50
MicroRNA Microarray.....	51-52
Statistical analysis of microarray data.....	52
qRT-PCR of miRNA expression.....	52-53
Target Prediction and Functional analysis.....	53-54
Results	
Gossypol alters the miRNA expression of MCF-7 cells	

Microarray.....	55
qRT-PCR.....	55
miRNA targets.....	55-56
Discussion.....	56-58
References.....	71-73
CHAPTER 4: EFFECTS OF GOSSYPOL ON OXIDATIVE STRESS.....	74
Abstract.....	74
Introduction.....	75-77
Materials and Methods.....	77
Cell line and Cell Culture.....	77
Gossypol Treatment.....	77-78
RNA Extraction, Reverse Transcription, Real Time PCR.....	78-79
Treatment and Sample Preparation for Protein assays.....	80
Catalase assay.....	80-81
SOD assay.....	81
GCL and GSH assay.....	81-83
Results	
qRT-PCR.....	83
Catalase assay.....	84
SOD assay.....	84
GCL and GSH assay.....	84-85
Discussion.....	85
References.....	94-95

LIST OF TABLES

Table 1.1: Estimated New Cancer Cases and Deaths (US, 2012).....	12
Table 2.1: ICs of gossypol on MCF-7.....	36
Table 3.1: Table demonstrating the 11 miRNAs chosen for further analysis	59
Table 3.2: Pathways associated with the 11 miRNAs chosen for further study....	60
Table 3.3: Network using commonly targeted genes at least 8/11 miRNAs.....	61

LIST OF FIGURES

Figure 1.1: Diagram of the chemical structure of gossypol.....	13
Figure 1.2: A general overview of miRNA biogenesis.....	14
Figure 1.3: Risk Factors for ROS in Cancer.....	15
Figure 1.4: Wide Spectrum of Responses to ROS.....	16
Figure 1.5: Multiple pathways to cell death mediated by levels of ROS.....	17
Figure 1.6: Biological pathways and their miRNA targets in breast cancer.....	18
Figure 2.1: The effect of gossypol on MCF-7 cell proliferation.....	37
Figure 2.2: Effect of gossypol on cell cycle.....	38
Figure 2.3: qRT-PCR analysis of genes related to proliferation and cell cycle....	39
Figure 2.4: qRT-PCR analysis of genes relating to cell death.....	40
Figure 2.5: Representation of the cell death-inducing effects of BH3 mimetics...	41
Figure 2.6: Nutraceuticals targeting various aspects of cancer progression.....	42
Figure 2.7: Figure describing the alteration of microRNA expression.....	43
Figure 3.1: Microarray log2 graphs fold change of significantly altered miRNAs..	62
Figure 3.2: Microarray heat map of miRNA fold change.....	63
Figure 3.3: Microarray heat map of fold change of 11 chosen miRNAs	64
Figure 3.4: Fold change of qRT-PCR analysis of 11 chosen miRNAs.....	65
Figure 3.5: Genes commonly targeted by at least 8 of the 11 miRNAs.....	66
Figure 3.6: Directed acyclic graph of enriched pathways.....	67
Figure 3.7: MicroRNAs, Chromatin, Stress and Expression.....	68
Figure 3.8: Model of how let-7 and miR-200 contribute to tumor progression.....	69
Figure 3.9: Summary of the major targets found in literature of miRNAs.....	70

Figure 4.1: A schematic of the major antioxidant enzymes in mammalian cells...	87
Figure 4.2: Schematic for the method used to determine the SOD activity.....	88
Figure 4.3: Effect of gossypol on genes relating to oxidative stress.....	89
Figure 4.4: Catalase enzyme activity measured per milligram protein.....	90
Figure 4.5: SOD activity/mg (0.1 μ M, 3 μ M) concentrations.....	91
Figure 4.6: GCL activity and GSH level responses to treatment with gossypol...	92
Figure 4.7: GSH standard curve.....	93

LIST OF ABBREVIATIONS

TNF	Tumor Necrosis Factor
IGFBPs	Insulin Like Growth Factor BPs
ROS	Reactive Oxygen Species
TRBP	Trans Activating Binding Protein
PACT	Protein Kinase R Activating Protein
Ago	Argonaute Protein
GW182	Glycine Tryptophan Repeats 182
CCND1	Cyclin D1
PDCD4	Programmed Cell Death 4
DMSO	Dimethyl Sulfoxide
ESR1	Estrogen Receptor Alpha
EDTA	Ethylenediamine tetra-acetic acid
RPMI	Roswell Park Memorial Institute
FBS	Fetal Bovine Serum
LOEC	Lowest Observed Effective Concentration
qRT-PCR	Quantitative Real Time PCR
miRNA	MicroRNA
dNTP	Deoxyribonucleotide triphosphate
GO	Gene Ontology
cDNA	Complementary DNA
PBS	Phosphate Buffered Saline
RNS	Reactive Nitrogen Species
PB	Phosphate Buffer
XO	Xanthine Oxidase

DETAPAC	Diethylenetriaminepentaacetic acid
NBT	Nitro blue tetrazolium
SSA	5-Sulfosalicylic acid dihydrate
GC	Gamma-glutamylcysteine
NDA	Naphthalene Dicarboxaldehyde
PEITC	Phenylethyl isothiocyanate
BSO	Buthionine Sulfoximine
As ₂ O ₃	Arsenic Trioxide
MgCl ₂	Magnesium Chloride Hexahydrate

Chapter 1: Review of Breast Cancer, MCF7 Cell Line, Gossypol, MicroRNAs, Oxidative Stress and Cancer

Breast Cancer

Cancer is the second most common cause of death in the US, exceeded only by heart disease, accounting for nearly 1 of every 4 deaths [Cancer.org]. In 2012, about 577,190 Americans are expected to die of cancer, more than 1,500 people a day (Table 1) [Cancer.org]. Of these, breast cancer is the most diagnosed cancer among women, and the second leading cause of death in women, second only to lung cancer [Cancer.org]. An estimated 1,384,000 females were diagnosed with breast cancer globally in 2008 [8].

Breast cancer is screened for by mammograms in asymptomatic women in an attempt to diagnose at an early stage. Early detection is important due to the strong correlation between stage at diagnosis and mortality [8]. Additionally, in most cases as the size of the tumor increases, so does the likelihood of lymph node invasion, leading to poor long-term survival.

Incidence rates of breast cancer are the highest of any cancer amongst females in most regions of the world, with the exception of several countries in Eastern and Western Africa and parts of Central and South America and Southern Asia [8]. In developed countries, breast cancer is almost two and a half times more common. This large regional variation is thought to occur for many reasons, most of which are centered on lifestyle. Women in more developed countries have fewer children, give birth at an older age and are less likely to breastfeed [9]. Obesity, alcohol consumption, use of oral contraceptives and hormone replacement therapy are other factors

associated with higher incidence rates in developed countries [9]. Globally, 89% of breast cancers are diagnosed from the age of 40 and above [10].

Survival for breast cancer is higher than most other types of cancers. However, longer term survivors experience an ongoing survival deficit due to relapses and metastases [8]. One of the most important determinants of survival is stage at diagnosis. In the United States between 2001 and 2007, the 5-year relative survival percentages varied from 99% for localized tumors, 84% regional disease and 23% for distant stage disease [11].

MCF-7 Cell Line

MCF-7 cell line has proven to be a great model for human breast cancer studies *in vitro* [12]. MCF-7 is an adherent epithelial cell line that was first isolated in 1970 from the breast tissue of a 69-year old Caucasian woman (blood type: O, Rh positive) diagnosed with metastatic breast carcinoma [13]. Two mastectomies were performed, the first removing a tumor on the right breast determined benign and the second on the left breast determined malignant mammary adenocarcinoma 7 and 5 years respectively post diagnosis. Local recurrences appeared on the left chest wall immediately after postoperative radiotherapy. Radiotherapy and hormonotherapy controlled the recurrences for 3 years. Eventually in 1970, widespread erythematous recurrences appeared on the left anterior chest wall of which nodules were removed and placed in culture. Two months after the nodules were removed; the patient developed a pleural effusion. From this pleural effusion, cells were cultured and stabilized to eventually become the MCF-7 cell line [13].

Culturing the nodules was unsuccessful due to the overgrowth of fibroblasts, but from the pleural effusion culture the primary cell type remained epithelial. Eventually after the culture stabilized, it retained several characteristics of differentiated mammary epithelium, including ability to process estradiol via cytoplasmic estrogen receptors and the capability of forming domes. Although this cell line expresses estrogen receptors they are not estrogen dependent. The mean chromosome number for this cell line is 85 subtetraploid composed of 26 metacentrics, 35 subtelocentrics and 18 acrocentrics [13]. Growth of MCF7 cells is inhibited by tumor necrosis factor alpha (TNF alpha). Secretion of IGFBP's can be modulated by treatment with anti-estrogens [5, 14]. MCF-7 has an average doubling time of about 29 hours and possesses the wnt 7h+ oncogene [7].

Gossypol

The structural composition of gossypol was identified by chemists from bulk samples of cottonseed oil as long ago as 1886 [15]. It has a chemical formula of: $C_{30}H_{30}O_8$ [16]. The atropisomers (+/-) ratio varies among cotton species [17]. It is composed of two aldehyde, six hydroxyl, and two alkyl-naphthalene groups as seen in Figure 1.1. The resulting polarity from the two groups makes it soluble in many organic solvents like DMSO, and the alkyl-naphthalene groups are the reason its insoluble in water [18]. Gossypol exists in three different tautomeric forms depending on the solvent. In alkaline solvents, or with DMSO as a solvent, gossypol is in equilibrium between the, ketol, aldehyde and hemi-acetal forms [19]. Gossypol is a highly reactive molecule that is found in free or bound form. The bound structure is non-toxic, but can inactivate or reduce the bound target (e.g. enzyme). Correlating with the amino-carboxyl group

distance, gossypol more efficiently reacts with amino acids at PHs with a range between 5.7-7.5 [20]. Together, these properties make gossypol a highly reactive, unstable, anti-oxidative as well as pro-oxidative chemical.

Gossypol exists naturally in the cotton plant, and in high concentrations within the cotton seeds [7]. Gossypol has many biological and agricultural properties including anticancer activity [7]. Gossypol has appeared previously in literature inhibiting the growth of several cancer cell lines in a number of ways including uncoupling oxidative phosphorylation [21], inhibiting cytoplasmic and mitochondrial enzymes involved in energy production [22], decreases in BCL-2 and BCL-XL [23-25], depletion of cellular ATP [26] and inhibiting key nuclear enzymes involved in DNA replication and repair like DNA Polymerase Alpha and topoisomerase [27, 28]. Due to its structure, gossypol acts as a nonspecific enzyme inhibitor *in vitro* and has been shown to also effect many cellular functions, such as ion transport, macromolecular synthesis, and properties of glycolysis, lipid membranes, respiration and glucose uptake [3]. Initially, gossypol was studied as a contraceptive agent used in China which disrupted spermatogenesis by inhibiting lactate dehydrogenase-X [7]. It also was found to interfere with steroidogenesis in testicular Leydig cells and hindered the function of primary cultures of Leydig and Sertoli cells [7]. Additionally, it is found to have antisteroidogenic effects in female reproductive cells by suppressing adenylatecyclase and 3 Rhydroxysteroid dehydrogenase [2].

MCF-7 and gossypol

MCF-7 has proven to be an excellent breast cancer model for cytotoxic studies using a variety of chemotherapeutics [29-32]. In fact, many of these studies involving

treatment with gossypol are focused on using the MCF-7 model [2, 3, 33]. Gossypol has proven to be a potent inducer of cell death in MCF-7. Its important to use the term cell death because gossypol has been implicated not only in apoptosis, but it is also known to induce autophagy and necrosis as well. [2, 23, 34, 35]. However, global studies on these pathways with the inclusion of miRNAs as a possible regulator of gossypol's effects have never previously been recorded.

ROS, Antioxidants and Cancer

ROS, produced in the body, play a major role in various cell-signaling pathways. Studies have shown that ROS generation is associated with risk factors of chronic diseases like: stress, tobacco, environmental pollutants, radiation, viral infection, diet and bacterial infection (Figure 1.3) [36, 37].

ROS production can lead to a variety of cellular responses (Figure 1.4). Interestingly, although excess ROS from a variety of sources contributes to the formation of many cancers, they also mediate the effects of many chemotherapeutic agents [38]. ROS have been implicated in the chemopreventive and anti-tumor action of nutraceuticals derived from many natural products used in traditional medicine. Therefore, it is understood that there are both cancer-suppressing as well as cancer-promoting mechanisms to reactive oxygen species [38].

In general, ROS inducing chemotherapies are very effective initially, but with time cancer cells tend to develop a strong resistance to ROS through up regulation of their antioxidant defense system. This resistance is mediated through enzymes like catalase and superoxide dismutase which scavenge free radicals and prevent damage and activation of apoptotic signaling pathways [39, 40]. If gossypol inhibits this resistance,

then combination of drug therapy with ROS inducing chemotherapeutics can overcome this limitation.

ROS have been implicated as an effector resulting in multiple pathways leading to cell death (Figure 1.5). Autophagy is one of the first lines of defense when cells are faced with oxidative stress. In this defensive strategy, cells utilize selective lysosomal self-digestion of intracellular components to maintain cellular homeostasis. However, when faced with higher levels of ROS, cells often resort instead to activating the autophagy induced cell death pathways [41-43]. ROS induced apoptosis can be initiated by death receptors (extrinsic pathway) [4] or through mitochondria (intrinsic pathway) [38]. In the extrinsic pathway, ROS are generated by the Fas ligand and are in turn required for Fas phosphorylation and activation [38]. Intrinsically, ROS function to open the permeability transition pore of mitochondria by activating pore-destabilizing proteins (Bcl-2-associated X protein, Bcl-2) and inhibiting pore-stabilizing proteins (Bcl-2 and Bcl-xL) [44]. Additionally, if ROS levels are high enough, cells will undergo necrosis. ROS are key players in the propagation and execution phases of necrotic cell death, damaging proteins, lipids and DNA either directly or indirectly, which results in disruption of organelle and cell integrity. When cells undergo necrosis, they initiate pro-inflammatory signaling cascades by actively releasing inflammatory cytokines and by emptying their contents when they lyse [45-48]. This makes it very interesting to see how the miRNAs in this study affect ROS mediated reactions.

MiRNA

Within the last 10 years, a novel gene regulator was discovered in humans. This discovery began in 1993 in *C. elegans*. Lin-4 was shown to be involved in gene

regulation via an RNA-RNA antisense interaction [49]. Later, miRNAs were ubiquitously found in all eukaryotic organisms [50]. Currently 1100 miRNAs have been sequenced in humans (microRNA.org). Initially reported as a control mechanism for developmental timing [51], we now know their roles are much more diverse, and extend to many physiological and pathophysiological processes [52-56].

MiRNA is a non-coding RNA that is an important regulatory molecule in both plants and animals. MiRNAs are ~18-22 nucleotides long and are transcribed in the nucleus mainly by RNA Polymerase II. Most miRNAs seem to be solitary and are expressed under the control of their own promoters within the intergenic region of the genome [57, 58]. However, miRNAs in the introns of protein coding genes may use the same promoter as the proximal gene [57].

The biogenesis of miRNAs (Figure 1.2) begins in the nucleus where they are transcribed into a primary miRNA (pri-miRNA) mainly by RNA polymerase II, although a minor group of miRNAs associated with Alu repeats can be transcribed by RNA polymerase III [59]. The pri-miRNA can harbor a single pre-miRNA or a cluster of pre-miRNAs. In the nucleus, pri-miRNA is cleaved into miRNA precursor (pre-miRNA) by the Microprocessor complex (minimally composed of Drosha and DGCR8) which interacts with helicases p68 and p72 [60, 61]. The pre-miRNA is exported through the nuclear pore complex to the cytoplasm by Exportin5/RanGTP. Once pre-miRNA is in the cytoplasm, a second RNase III or “dicer” in conjunction with TRBP or PACT cleaves the stem of the pre-miRNA. The miRNA duplex is then loaded into the Ago protein within RISC, where one half of the duplex is preferentially retained. This complex contains an Ago protein and GW182, which is required for gene silencing [60, 61].

miRNAs regulate gene expression by translational repression and mRNA cleavage through binding to the 3' untranslated region (UTR) of a specific mRNA transcript [57, 59, 60]. The complementarity between the miRNA and its prospective mRNA will decide whether the mRNA is cleaved or translationally repressed [62]. In general, a fully complementary strand will cause cleavage while a partially complementary strand will induce translational inhibition (Figure 1.2).

MiRNA and Breast Cancer

As one would imagine from observing the strong regulatory function of miRNA, current literature demonstrates that some miRNAs regulate a variety of processes important in cancer formation like: cell proliferation and apoptosis [15, 16]. Recently, like in many other cancers, breast cancers were found to have unique miRNA expression profiles [63]. Due to this aberrant expression, researchers are using these profiles as a diagnostic tool. In fact, some studies demonstrate using circulating miRNAs within blood plasma to create a profile as a non-invasive and accurate method for diagnosing breast cancer [64, 65].

In breast cancer, miRNAs have been shown to play an important role in many different important biological pathways (Figure 1.6). A few of these which are interesting in the context of this study are: ESR1 (Estrogen Receptor 1) targeted by miR-206 which is down-regulated in breast cancer [66-68], CCND1 (Cyclin D1) targeted by miR-17p and miR-20a which are down-regulated in breast cancer [69, 70], PDCD4(Programmed Cell Death 4)[71]; targeted by miR-21 which is known to be up-regulated in breast cancer [72, 73].

Due to this differential miRNA expression in breast cancer and their influence on its progression or suppression, researchers have looked to miRNA as a possible mechanism of cancer therapies [74, 75]. There is still much to learn about the exact role each miRNA plays and how to manipulate their expression in order to treat breast cancer. However, the aberrant expression of miRNA in breast cancer coupled with the abnormal expression of their corresponding targets suggests miRNA may play an important role in determining how breast cancer is initiated and how it progresses.

MiRNA and Oxidative Stress

Although well documented in plants, few studies focus on miRNAs role in regulating cellular antioxidant defense systems in animals. However, many studies show that miRNA expression profiles indeed change in response to oxidative stress and help modulate the cellular response to this stress [76-78].

In one study, miR-17* suppressed the tumorigenicity of prostate cancer via inhibiting mitochondrial antioxidant enzymes MnSOD (manganese superoxide dismutase) and GPX (glutathione peroxidase) [79]. Because of the diverse roles of miRNA in gene regulation and the importance of ROS mediated mechanisms in cancer therapy it would be interesting to study the link between miRNA and these oxidative stress pathways.

Hypothesis and Objectives

I hypothesize that treating MCF-7 cells with gossypol not only effects cell growth, proliferation, cell death and cell cycle progression, but also reduces their natural

resistance to ROS. In addition, I believe oxidative stress has a large role in the induction of this cell death and that one or several antioxidant enzymes mediating MCF-7's defense against these ROS will be down-regulated via miRNA targeting. To test this hypothesis, the following specific objectives will be achieved in this thesis project:

Objective 1: Observe the effects of gossypol on cell growth, proliferation, cell cycle progression and cell death

As described in the methods section, assays will be used to demonstrate the deleterious effects on cells in response to varying concentrations of gossypol. Using a combination of dose response assays, cell cycle analysis and gene expression data, a more accurate representation of gossypol's global inhibitory effects will be achieved.

Objective 2: Analyze the differential expression of miRNA in response to gossypol

First, we performed a microarray analysis of all human miRNAs, then 5 of the most up-regulated and 6 of the most down-regulated miRNAs were chosen for further analysis by qRT-PCR.

Objective 3: Detect gossypol's effects on oxidative stress and the antioxidant enzymes involved

qRT-PCR analysis of key genes relating to oxidative stress will be performed. Then, protein assays for several of these genes will be performed to assess gossypol's effects at the protein level.

Objective 4: Determine the relationship between the differentially expressed miRNAs, their targets and the global effects on each pathway studied

Connecting gossypol's effects on a phenotypic, genotypic, and protein level will help provide a more complete picture of why gossypol is effective. From this data, a better

understanding of how gossypol should be used and how miRNA is involved in its efficacy will be formed.

Table 1.1: Estimated New Cancer Cases and Deaths (US, 2012) (www.cancer.org)

	Estimated New Cases			Estimated Deaths		
	Both SexesTotal	Male	Female	Both SexesTotal	Male	Female
All Sites	1,638,910	848,170	790,740	577,190	301,820	275,370
Breast	229,060	2,190	226,870	39,920	410	39,510

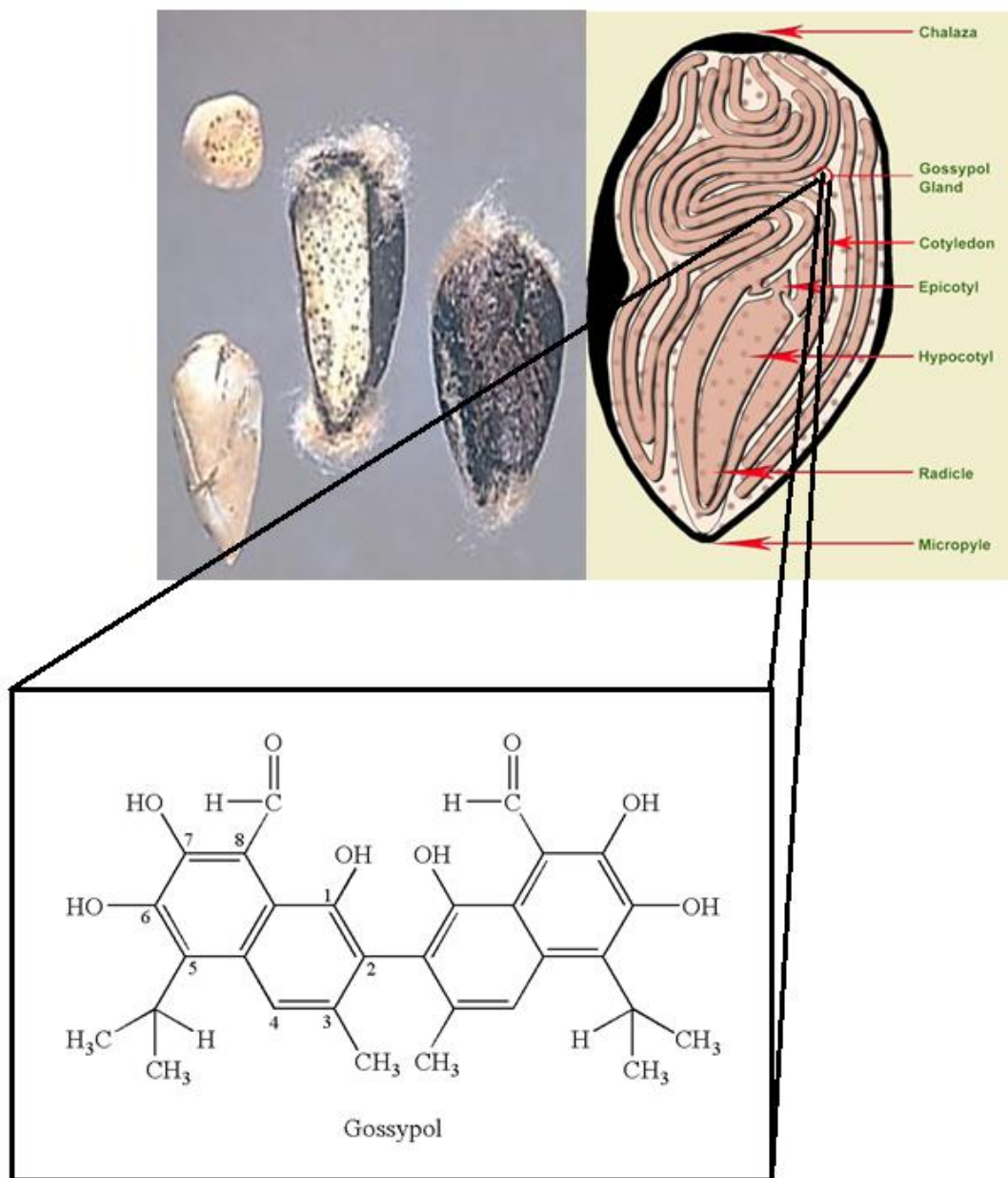


Figure 1.1: Diagram of the physical makeup of a cotton seed and the chemical structure of gossypol, a polyphenolic aldehyde. Image from freepatentsonline.com

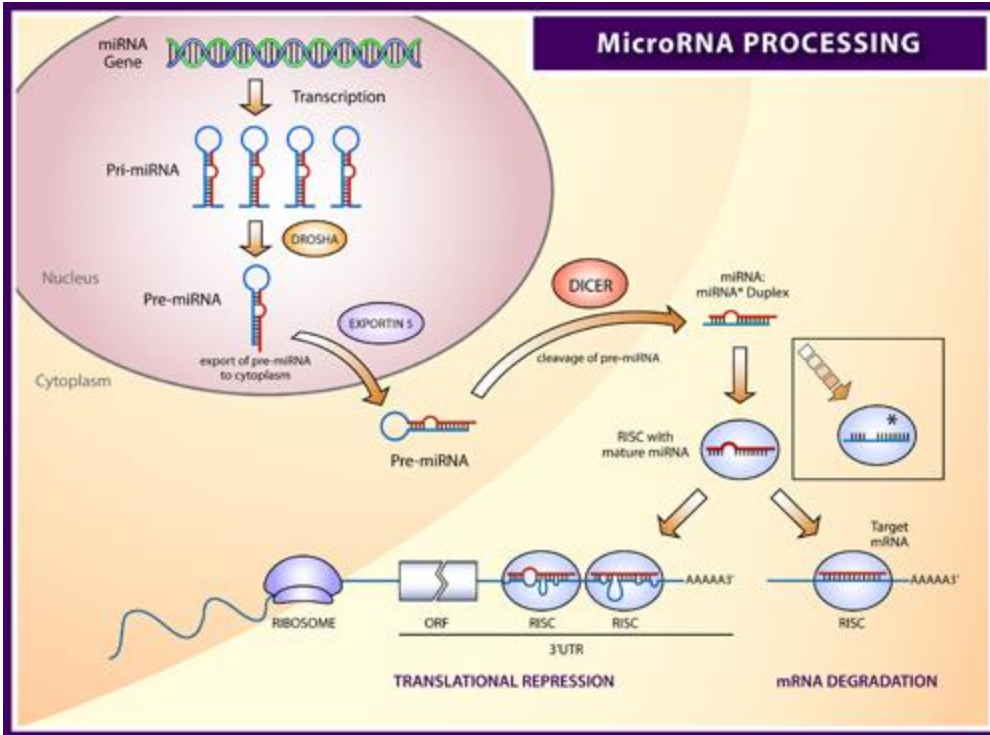


Figure 1.2: A general overview of miRNA biogenesis. Image from wordpress.com

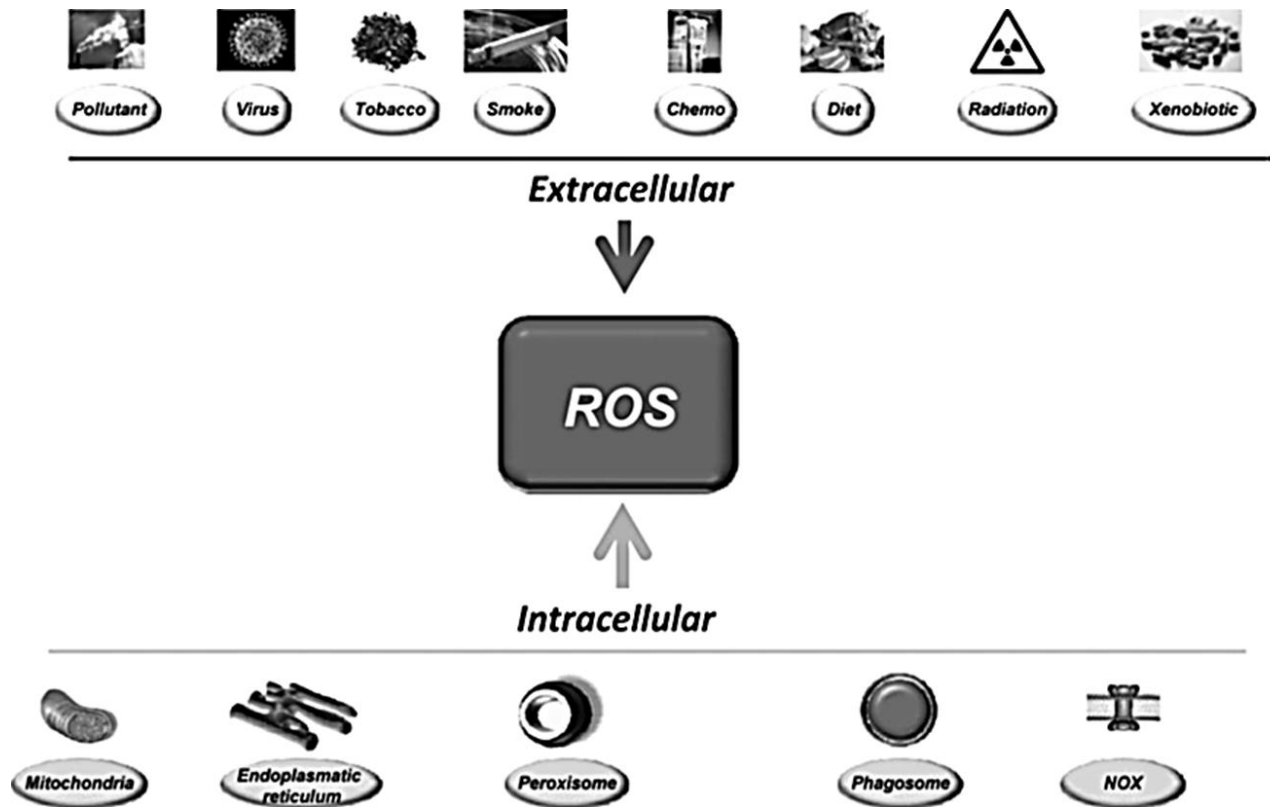


Figure 1.3: Risk Factors for ROS in Cancer [38]. This figure demonstrates both the intracellular and extracellular inducers of ROS.

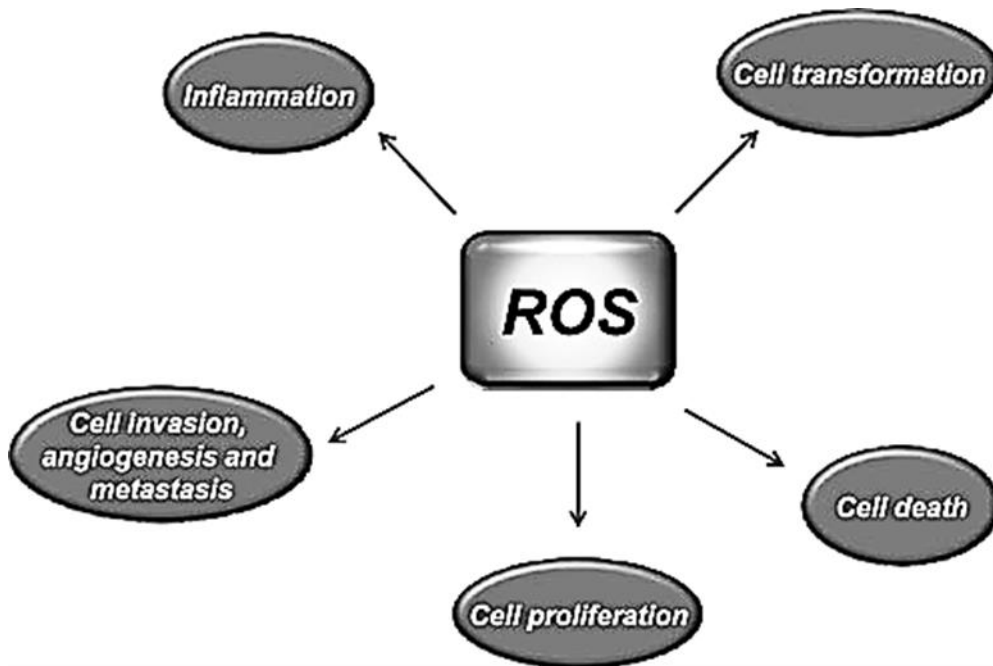


Figure 1.4: Wide Spectrum of Responses to ROS [38]

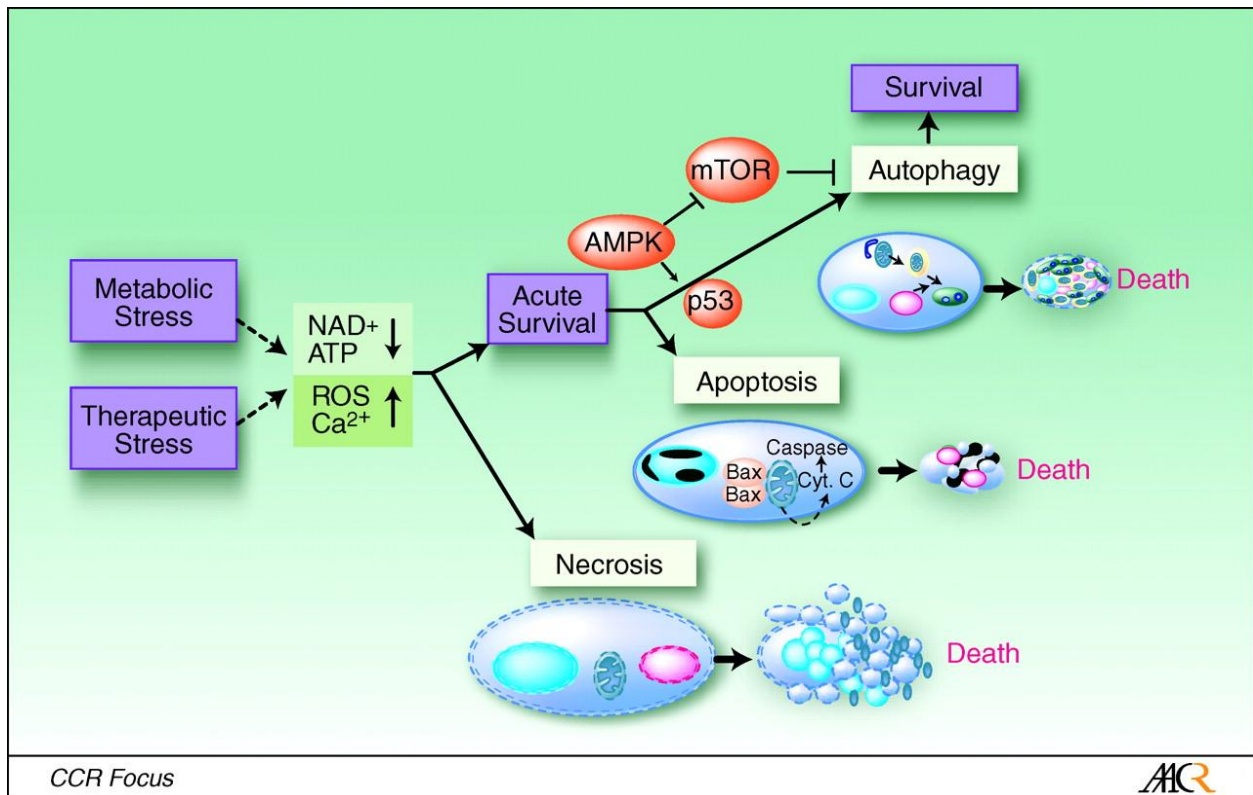


Figure 1.5: Multiple pathways to cell death mediated by levels of ROS [80]. As shown, varying levels of ROS induce varying pathways to cell death.

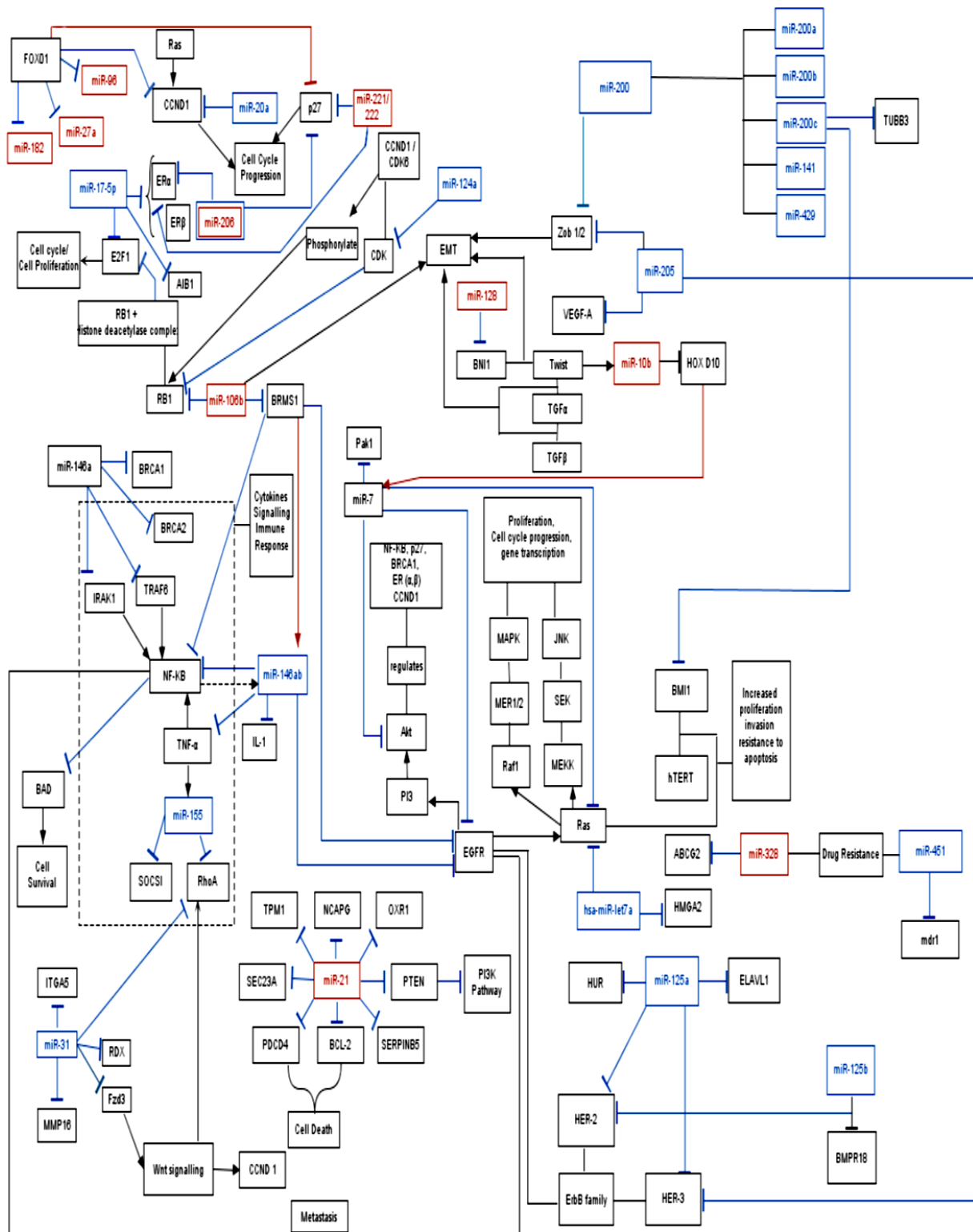


Figure 1.6: Various biological pathways and their reported miRNA targeting in breast cancer [72].

1. Barba-Barajas, M., et al., *Gossypol induced apoptosis of polymorphonuclear leukocytes and monocytes: involvement of mitochondrial pathway and reactive oxygen species*. Immunopharmacol Immunotoxicol, 2009. **31**(2): p. 320-30.
2. Gilbert, N.E., et al., *Antiproliferative activity of gossypol and gossypolone on human breast cancer cells*. Life Sci, 1995. **57**(1): p. 61-7.
3. Jaroszewski, J.W., O. Kaplan, and J.S. Cohen, *Action of gossypol and rhodamine 123 on wild type and multidrug-resistant MCF-7 human breast cancer cells: 31P nuclear magnetic resonance and toxicity studies*. Cancer Res, 1990. **50**(21): p. 6936-43.
4. Sung, B., et al., *Gossypol induces death receptor-5 through activation of the ROS-ERK-CHOP pathway and sensitizes colon cancer cells to TRAIL*. J Biol Chem, 2010. **285**(46): p. 35418-27.
5. Yan, F., et al., *A novel water-soluble gossypol derivative increases chemotherapeutic sensitivity and promotes growth inhibition in colon cancer*. J Med Chem, 2010. **53**(15): p. 5502-10.
6. Kitada, S., et al., *Discovery, characterization, and structure-activity relationships studies of proapoptotic polyphenols targeting B-cell lymphocyte/leukemia-2 proteins*. J Med Chem, 2003. **46**(20): p. 4259-64.
7. Wang, X., et al., *Gossypol--a polyphenolic compound from cotton plant*. Adv Food Nutr Res, 2009. **58**: p. 215-63.
8. Youlden, D.R., et al., *The descriptive epidemiology of female breast cancer: an international comparison of screening, incidence, survival and mortality*. Cancer Epidemiol, 2012. **36**(3): p. 237-48.
9. Porter, P., *"Westernizing" women's risks? Breast cancer in lower-income countries*. N Engl J Med, 2008. **358**(3): p. 213-6.
10. Ferlay, J., et al., *Estimates of worldwide burden of cancer in 2008: GLOBOCAN 2008*. International Journal of Cancer, 2010. **127**(12): p. 2893-917.
11. Howlader, N., et al., *SEER cancer statistics review, 1975–2008*. Bethesda, MD: National Cancer Institute, 2011.
12. Simstein, R., et al., *Apoptosis, chemoresistance, and breast cancer: insights from the MCF-7 cell model system*. Exp Biol Med (Maywood), 2003. **228**(9): p. 995-1003.
13. Soule, H.D., et al., *A human cell line from a pleural effusion derived from a breast carcinoma*. J Natl Cancer Inst, 1973. **51**(5): p. 1409-16.
14. Engel, L.W. and N.A. Young, *Human breast carcinoma cells in continuous culture: a review*. Cancer Res, 1978. **38**(11 Pt 2): p. 4327-39.
15. Longmore, J., *Cotton-seed oil: Its colouring matter and mucilage, and description of a new method of recovering the loss occurring in the refining process*. J. Soc. Chem. Ind.(Lond.), 1886. **5**: p. 200–206.
16. Clark, E.P., *Studies on gossypol*. Journal of Biological Chemistry, 1927. **75**(3): p. 725-739.
17. Cass, Q.B., et al., *Gossypol enantiomer ratios in cotton seeds*. Phytochemistry, 1991. **30**(8): p. 2655-2657.
18. Markman, A.L. and V.P. Rzhikhin, *Gossypol and its derivatives*. The U. S. Department of Agriculture and the National Science Foundation, Washington, DC, 1968.
19. Adams, R., T.A. Geissman, and J.D. Edwards, *Gossypol, a pigment of cottonseed*. Chemical reviews, 1960. **60**: p. 555-74.
20. Cater, C. and C. Lyman, *Reaction of gossypol with amino acids and other amino compounds*. Journal of the American Oil Chemists' Society, 1969. **46**(12): p. 649-653.
21. Abou-Donia, M.B. and J.W. Dieckert, *Gossypol: uncoupling of respiratory chain and oxidative phosphorylation*. Life Sci, 1974. **14**(10): p. 1955-63.

22. Ueno, H., et al., *Interaction of gossypol with sperm macromolecules and enzymes*. Contraception, 1988. **37**(3): p. 333-41.
23. Gao, P., et al., *The Bcl-2 homology domain 3 mimetic gossypol induces both Beclin 1-dependent and Beclin 1-independent cytoprotective autophagy in cancer cells*. J Biol Chem, 2010. **285**(33): p. 25570-81.
24. Lian, J., D. Karnak, and L. Xu, *The Bcl-2-Bec1 interaction in (-)-gossypol-induced autophagy versus apoptosis in prostate cancer cells*. Autophagy, 2010. **6**(8): p. 1201-3.
25. Voss, V., et al., *The pan-Bcl-2 inhibitor (-)-gossypol triggers autophagic cell death in malignant glioma*. Mol Cancer Res, 2010. **8**(7): p. 1002-16.
26. Keniry, M.A., C. Hollander, and C.C. Benz, *The effect of gossypol and 6-aminonicotinamide on tumor cell metabolism: a 31P-magnetic resonance spectroscopic study*. Biochem Biophys Res Commun, 1989. **164**(2): p. 947-53.
27. Adlakha, R.C., et al., *Modulation of 4'-(9-acridinylamino)methanesulfon-m-anisidide-induced, topoisomerase II-mediated DNA cleavage by gossypol*. Cancer Res, 1989. **49**(8): p. 2052-8.
28. Hou, D.X., et al., *Involvement of reactive oxygen species-independent mitochondrial pathway in gossypol-induced apoptosis*. Arch Biochem Biophys, 2004. **428**(2): p. 179-87.
29. Al-Akoum, M., S. Dodin, and A. Akoum, *Synergistic cytotoxic effects of tamoxifen and black cohosh on MCF-7 and MDA-MB-231 human breast cancer cells: an in vitro study*. Can J Physiol Pharmacol, 2007. **85**(11): p. 1153-9.
30. Gil, J.F., T.N. Augustine, and M.J. Hosie, *Anastrozole and RU486: Effects on estrogen receptor alpha and Mucin 1 expression and correlation in the MCF-7 breast cancer cell line*. Acta Histochem, 2013.
31. Wang, J.W., et al., *Contrast-enhanced US quantitatively detects changes of tumor perfusion in a murine breast cancer model during adriamycin chemotherapy*. Acta Radiol, 2013.
32. Li, W.Y., et al., *Emodin induces cytotoxic effect in human breast carcinoma MCF-7 cell through modulating the expression of apoptosis-related genes*. Pharm Biol, 2013.
33. Ligueros, M., et al., *Gossypol inhibition of mitosis, cyclin D1 and Rb protein in human mammary cancer cells and cyclin-D1 transfected human fibrosarcoma cells*. Br J Cancer, 1997. **76**(1): p. 21-8.
34. Ye, W., et al., *Induction of apoptosis by (-)-gossypol-enriched cottonseed oil in human breast cancer cells*. Int J Mol Med, 2010. **26**(1): p. 113-9.
35. Niu, X., et al., *Apogossypolone induces autophagy and apoptosis in breast cancer MCF-7 cells in vitro and in vivo*. Breast Cancer, 2012.
36. Inoue, M., et al., *Mitochondrial generation of reactive oxygen species and its role in aerobic life*. Curr Med Chem, 2003. **10**(23): p. 2495-505.
37. del Rio, L.A., et al., *Metabolism of oxygen radicals in peroxisomes and cellular implications*. Free Radic Biol Med, 1992. **13**(5): p. 557-80.
38. Gupta, S.C., et al., *Upsides and downsides of reactive oxygen species for cancer: the roles of reactive oxygen species in tumorigenesis, prevention, and therapy*. Antioxid Redox Signal, 2012. **16**(11): p. 1295-322.
39. Renschler, M.F., *The emerging role of reactive oxygen species in cancer therapy*. Eur J Cancer, 2004. **40**(13): p. 1934-40.
40. Reuter, S., et al., *Oxidative stress, inflammation, and cancer: how are they linked?* Free Radic Biol Med, 2010. **49**(11): p. 1603-16.
41. Scherz-Shouval, R., et al., *Reactive oxygen species are essential for autophagy and specifically regulate the activity of Atg4*. EMBO J, 2007. **26**(7): p. 1749-60.

42. Gong, K., et al., *Autophagy-related gene 7 (ATG7) and reactive oxygen species/extracellular signal-regulated kinase regulate tetrandrine-induced autophagy in human hepatocellular carcinoma*. J Biol Chem, 2012. **287**(42): p. 35576-88.
43. Li, L., G. Ishdorj, and S.B. Gibson, *Reactive oxygen species regulation of autophagy in cancer: implications for cancer treatment*. Free Radic Biol Med, 2012. **53**(7): p. 1399-410.
44. Martindale, J.L. and N.J. Holbrook, *Cellular response to oxidative stress: Signaling for suicide and survival**. Journal of Cellular Physiology, 2002. **192**(1): p. 1-15.
45. Festjens, N., T. Vanden Berghe, and P. Vandenabeele, *Necrosis, a well-orchestrated form of cell demise: signalling cascades, important mediators and concomitant immune response*. Biochim Biophys Acta, 2006. **1757**(9-10): p. 1371-87.
46. Morgan, M.J., Y.S. Kim, and Z.G. Liu, *TNFalpha and reactive oxygen species in necrotic cell death*. Cell Res, 2008. **18**(3): p. 343-9.
47. Lu, C.C., et al., *Chrysophanol induces necrosis through the production of ROS and alteration of ATP levels in J5 human liver cancer cells*. Mol Nutr Food Res, 2010. **54**(7): p. 967-76.
48. Higuchi, M., et al., *Regulation of reactive oxygen species-induced apoptosis and necrosis by caspase 3-like proteases*. Oncogene, 1998. **17**(21): p. 2753-60.
49. Lee, R.C., R.L. Feinbaum, and V. Ambros, *The C. elegans heterochronic gene lin-4 encodes small RNAs with antisense complementarity to lin-14*. Cell, 1993. **75**(5): p. 843-54.
50. He, L. and G.J. Hannon, *MicroRNAs: small RNAs with a big role in gene regulation*. Nat Rev Genet, 2004. **5**(7): p. 522-31.
51. Ambros, V., *A hierarchy of regulatory genes controls a larva-to-adult developmental switch in C. elegans*. Cell, 1989. **57**(1): p. 49-57.
52. Ambros, V., *MicroRNA pathways in flies and worms: growth, death, fat, stress, and timing*. Cell, 2003. **113**(6): p. 673-6.
53. Aukerman, M.J. and H. Sakai, *Regulation of flowering time and floral organ identity by a MicroRNA and its APETALA2-like target genes*. Plant Cell, 2003. **15**(11): p. 2730-41.
54. Chen, C.Z., et al., *MicroRNAs modulate hematopoietic lineage differentiation*. Science, 2004. **303**(5654): p. 83-6.
55. Kim, V.N., *MicroRNA biogenesis: coordinated cropping and dicing*. Nat Rev Mol Cell Biol, 2005. **6**(5): p. 376-85.
56. McManus, M.T., *MicroRNAs and cancer*. Semin Cancer Biol, 2003. **13**(4): p. 253-8.
57. Lizarraga, D., et al., *Benzo[a]pyrene-induced changes in microRNA-mRNA networks*. Chem Res Toxicol, 2012. **25**(4): p. 838-49.
58. Ambros, V., *The functions of animal microRNAs*. Nature, 2004. **431**(7006): p. 350-5.
59. Kim, V.N., J. Han, and M.C. Siomi, *Biogenesis of small RNAs in animals*. Nat Rev Mol Cell Biol, 2009. **10**(2): p. 126-39.
60. Libri, V., et al., *Regulation of microRNA biogenesis and turnover by animals and their viruses*. Cell Mol Life Sci, 2013.
61. Yang, J.S. and E.C. Lai, *Alternative miRNA biogenesis pathways and the interpretation of core miRNA pathway mutants*. Mol Cell, 2011. **43**(6): p. 892-903.
62. Behm-Ansmant, I., et al., *mRNA degradation by miRNAs and GW182 requires both CCR4:NOT deadenylase and DCP1:DCP2 decapping complexes*. Genes Dev, 2006. **20**(14): p. 1885-98.
63. Iorio, M.V., et al., *MicroRNA gene expression deregulation in human breast cancer*. Cancer Res, 2005. **65**(16): p. 7065-70.
64. Heneghan, H.M., et al., *Circulating microRNAs as novel minimally invasive biomarkers for breast cancer*. Ann Surg, 2010. **251**(3): p. 499-505.
65. Zhao, H., et al., *A pilot study of circulating miRNAs as potential biomarkers of early stage breast cancer*. PLoS One, 2010. **5**(10): p. e13735.

66. Adams, B.D., D.M. Cowee, and B.A. White, *The role of miR-206 in the epidermal growth factor (EGF) induced repression of estrogen receptor-alpha (ERalpha) signaling and a luminal phenotype in MCF-7 breast cancer cells.* Mol Endocrinol, 2009. **23**(8): p. 1215-30.
67. Adams, B.D., H. Furneaux, and B.A. White, *The micro-ribonucleic acid (miRNA) miR-206 targets the human estrogen receptor-alpha (ERalpha) and represses ERalpha messenger RNA and protein expression in breast cancer cell lines.* Mol Endocrinol, 2007. **21**(5): p. 1132-47.
68. Kondo, N., et al., *miR-206 Expression is down-regulated in estrogen receptor alpha-positive human breast cancer.* Cancer Res, 2008. **68**(13): p. 5004-8.
69. Trompeter, H.I., et al., *MicroRNAs MiR-17, MiR-20a, and MiR-106b act in concert to modulate E2F activity on cell cycle arrest during neuronal lineage differentiation of USSC.* PLoS One, 2011. **6**(1): p. e16138.
70. Cloonan, N., et al., *The miR-17-5p microRNA is a key regulator of the G1/S phase cell cycle transition.* Genome Biol, 2008. **9**(8): p. R127.
71. Frankel, L.B., et al., *Programmed cell death 4 (PDCD4) is an important functional target of the microRNA miR-21 in breast cancer cells.* J Biol Chem, 2008. **283**(2): p. 1026-33.
72. Kayani, M., et al., *Role of miRNAs in breast cancer.* Asian Pac J Cancer Prev, 2011. **12**(12): p. 3175-80.
73. Asangani, I., et al., *MicroRNA-21 (miR-21) post-transcriptionally downregulates tumor suppressor Pcd4 and stimulates invasion, intravasation and metastasis in colorectal cancer.* Oncogene, 2007. **27**(15): p. 2128-2136.
74. Iorio, M.V., et al., *MicroRNA profiling as a tool to understand prognosis, therapy response and resistance in breast cancer.* European Journal of Cancer, 2008. **44**(18): p. 2753-2759.
75. Liu, R., et al., *The prognostic role of a gene signature from tumorigenic breast-cancer cells.* New England Journal of Medicine, 2007. **356**(3): p. 217-226.
76. Thulasigam, S., et al., *miR-27b*, an oxidative stress-responsive microRNA modulates nuclear factor-kB pathway in RAW 264.7 cells.* Mol Cell Biochem, 2011. **352**(1-2): p. 181-8.
77. Sangokoya, C., M.J. Telen, and J.T. Chi, *microRNA miR-144 modulates oxidative stress tolerance and associates with anemia severity in sickle cell disease.* Blood, 2010. **116**(20): p. 4338-48.
78. Howell, J.C., et al., *Global microRNA expression profiling: curcumin (diferuloylmethane) alters oxidative stress-responsive microRNAs in human ARPE-19 cells.* Mol Vis, 2013. **19**: p. 544-60.
79. Xu, Y., et al., *miR-17* suppresses tumorigenicity of prostate cancer by inhibiting mitochondrial antioxidant enzymes.* PLoS One, 2010. **5**(12): p. e14356.
80. Amaravadi, R.K. and C.B. Thompson, *The roles of therapy-induced autophagy and necrosis in cancer treatment.* Clin Cancer Res, 2007. **13**(24): p. 7271-9.

Chapter 2: Effects of Gossypol on the Growth, Proliferation, Cell Cycle Progression and Cell Death of MCF-7 Breast Cancer Cells

Abstract

Breast cancer is the second leading cause of death for cancers among women. Treating breast cancer is often unsuccessful due to the resistance of the cancer to traditional chemotherapeutic drugs. Throughout scientific history we have harnessed the power of compounds created in nature for the benefit of human health and welfare. Gossypol, a polyphenolic aldehyde found in high concentrations in cotton seed, shows great promise as a natural chemotherapeutic drug. In this study we observed the global effects of treatment of MCF-7 breast cancer cells with multiple concentrations of gossypol 48 hours post treatment. The dose response curve revealed a significant decrease in cell proliferation in a direct relationship to the concentrations of the treatment. The IC_{50} (Inhibitory concentration 50%) value was calculated to be 4.52 μ M. Additionally, treatments with higher concentrations contained cells that were smaller and rounder compared with control cells, with some cells losing their adherence ability. Its clear gossypol has a strong effect on the cells and to further assess these effects, cell cycle analysis was performed followed by qRT-PCR of key apoptotic genes to further illustrate the global effects of gossypol.

Introduction

Chemotherapy with cytotoxic drugs and radiotherapy are common ways to treat and manage breast cancer. There are a wide variety of anticancer drugs used to treat breast cancer, most of which are synthetic that have targets ranging from inhibiting topoisomerases, raising ROS, to down-regulating the ESR. One of the major hurdles in treating breast cancer like most cancers, is although they may be sensitive to synthetic drugs initially, they gradually develop resistance to both chemotherapy and radiotherapy. This resistance in part, is due to the induction of multidrug resistant proteins or selection of cells expressing MDRs [1].

However, to combat this resistance, more natural chemotherapeutics are being used alone and in combination with synthetic drugs to overcome this resistance and lead to an overall more effective treatment with fewer side effects. A wide range of nutraceuticals have shown great promise by targeting various aspects of tumor progression (Figure 2.6). Gossypol in particular, is one such nutraceutical that has demonstrated the ability to reduce resistance to substances like TRAIL (and apoptosis inducing cytokine) through the ROS-ERK-CHOP pathway in colorectal cells [2]. Additionally, it has been used to combat the resistance to drugs like Tamoxifen [3] and Cisplatin [4]. One such study noting that when treated with Tamoxifen alone MCF-7 ADR cell growth was inhibited by 34% but when combined with gossypol reached an impressive 94% growth inhibition [3].

Negating its combination therapy success and ability to reduce drug resistance, gossypol used alone has proven to be a potent inducer of cell death. Its important to

use the term cell death because gossypol has been implicated not only in apoptosis, but it is also known to induce autophagy and necrosis as well [5-7]. Gossypol is a well-established inducer of cell death and understanding the correct concentrations to use is important in dictating the type of cell death, as well as the efficacy of different combination drug therapies to be used in the future.

Another important factor of chemotherapeutics is their abilities to target the regulation of the cell cycle. Many chemotherapeutic drugs as mentioned above sole mechanism of action are their ability to arrest cells in particular phases of the cell cycle. Since being used as a contraceptive agent in China, there has been great interest in gossypol's ability to arrest different cell lines in different phases of the cell cycle. Indeed literature demonstrates this ability in a variety of cell lines, of particular interest to this study are those arrested in the S phase [8-10].

The aim of this study was to focus on the physiological effects of gossypol in combination with the gene expression profile to create a better understanding of how gossypol is so effective at inhibiting MCF-7 cell growth and inducing cell death. Hemocytometer cell counts, flow cytometry, and qRT-PCR were performed to elucidate the effects of gossypol on cell proliferation, cell cycle progression and induction of cell death.

Materials and Methods

Cell Line and Cell Culture

MCF-7 breast cancer cells were purchased from ATCC and maintained at 37°C in a humidified 5%CO₂ and 95% air incubator. Roswell Park Memorial Institute medium

(RPMI) 1640 (GIBCO, Vienna, VA) media was used to culture the cells with 10% FBS (PAA Laboratories, Dartmouth, MA) and 4mg/ml human recombinant insulin (GIBCO). The media was changed at least every 48 hours, and cells were trypsinized and passaged once a week using 0.05% trypsin/0.02% EDTA (Sigma, St. Louis, MO).

Gossypol Treatment and Dose Response

Gossypol was purchased from Sigma-Aldrich (St. Louis, MO) and stored at -80°C in a dark tube impermeable to light. A stock solution of 100mM gossypol was mixed using DMSO as a solvent and vacuum filtered in a laminar flow hood to maintain sterility. 5×10^5 cells were plated into 12 well plates with 3 wells per treatment group including controls in RPMI media with 10% FBS and no antibiotics or antifungal compounds with a final volume of 2mL in each well. Cells were first incubated for 24 hours in RPMI media with no treatment to allow for adhesion and stability. Next, cells were treated at varying concentrations of gossypol using DMSO as a vehicle. To exclude potential effects of DMSO, 0.1% DMSO was used in both the treatment and vehicle control groups. After 48 h of exposure, cells were trypsinized and counted. Initially, 7 concentrations (500nM, 700nM, 1µM, 2µM, 3µM, 10µM) were chosen to assess the efficacy of gossypol and determine the IC_{50} and an appropriate treatment dosage for later assays. Upon examining this data in figure 2.1, we concluded it was necessary to do a smaller nM experiment (10nM, 100nM, 300nM) to determine the minimum concentration capable of eliciting a statistically significant change in cell ratio.

Cell Cycle Analysis

Cells were treated at varying concentrations of gossypol according to the same procedure as the dose response experiments. 48 hours post treatment, cells were

trypsinized and collected. Then, 0.7 mL of ice cold 100% ethanol was added in 0.3 mL cold PBS. Cells were incubated at -20°C for 30 minutes. Post-incubation, cells were centrifuged and the supernatant was removed. Next, 500uL of 50ug/mL propidium iodide staining solution containing 500 units/mL RNaseA in PBS was added to the pellet. Cells were then vortexed gently and incubated at 37°C for 30 minutes. Finally, cells were incubated at room temperature for 1 hour and analyzed by a Becton Dickson FACScan one laser 3-color cytometer.

RNA Extraction, Reverse Transcription, Real Time PCR

Cells were plated and treated according to the same procedure outlined in the dose response section. Post-treatment, cells were trypsinized, centrifuged, and then washed with PBS and the pellets were placed in 1.8mL micro centrifuge tubes. Next, RNA was extracted from cells according to the instructions of the mirVana™ miRNA Isolation Kit (Ambion, Austin, TX). First, a lysis binding buffer was used to denature the cells and stabilize the RNA. Then, RNA was separated from DNA and other cellular components via acid-phenol extraction. From this point, the sample was treated with molecular grade ethanol, followed by passing through a glass-filter. To improve purity, the filter was washed several times before eluting the RNAs with RNase free water. To quantify and evaluate the quality of the RNA, a NanoDrop ND-1000 Micro-Volume UVVis Spectrophotometer (NanoDrop Technologies, Wilmington, DE) was used and the quality of the RNA was determined by the absorbance ratios of 260/280 and 260/230. After collecting the RNA, 200 ng RNA was reverse transcribed to cDNA using the TaqMan microRNA Reverse Transcription kit from Applied Biosystems (Foster City, CA). For the RT primer, the poly-T primer was used to reverse transcribe protein

coding genes to cDNA. The reagents used for reverse transcription were: 0.15µL of 100mM dNTPs, 0.19µL RNase inhibitor (20U/µL), 1.5µL of reverse transcription buffer (10X), 2µL of primer mix (1 reverse: 1 forward: 3 poly(T)), and 1 µL of multiscribe reverse transcriptase (50U/µL) and RNase free water depending on the concentration of RNA in the sample will be added to make the final 15 uL reaction volume . A thermal cycler was used to perform the reverse transcription according to the parameters of 16 °C for 30 minutes followed by 42°C for 30 minutes, 85°C for 5 minutes and lastly hold at 4°C. The samples were then diluted in 85µL DNase/RNase free water to prepare the solution for qRT-PCR.

To evaluate expression levels of protein coding genes, results were analyzed after performing qRT-PCR on 384-well-plates using the ViiA™ 7 Real-Time PCR System (Applied Biosystem) using SYBR Green PCR master mix created by SuperArray Bioscience Corp. (Frederick, MD). Reverse and forward specific primers were designed and used in the quantification of protein coding genes. Next qRT-PCR was performed where each well contained a total of 15µL of reaction mixture composed of the combination of 7.5µL SYBR Green master mix, 5.5µL DNase/RNase free water, 1µL primer mix, 1µL cDNA. qRT-PCR was performed using at least 3 biological replicates and 3 technical replicates each to ensure accuracy. The technical aspects of the qRT-PCR program started by activating the enzyme for 10 minutes at 95°C then a denaturation step for 15 sec at 95°C followed by an annealing/extension step for 60 seconds at 60°C. The last 2 steps were repeated for 40 cycles.

Results

Proliferation of MCF-7 cells are inhibited by gossypol

Gossypol inhibited MCF-7 cell growth and proliferation in a dose dependent manner (Figure 2.1). The lowest observed effect concentration (LOEC) was 0.30 μ M. The IC₅₀ and IC₂₀ were determined to be 4.52 μ M and 0.70 μ M, respectively. Additionally, cells seemed unhealthy, smaller, rounder and many losing anchorage ability in a direct relationship to gossypol concentration.

Cell Cycle analysis by Flow Cytometry

Cell Cycle Analysis using Flow Cytometry is shown in figure 2.2. In the vehicle control, cells at different developmental stages show a normal distribution (75.01%G1, 14.96%G2, 10.03%S, and 1.53% apoptotic)with the highest percentage of cells in the G1 phase, which suggests the cells were in a normal healthy population. At the 0.1 μ M treatment, the cell population began to respond with a sharp increase of cells in G2 (34.31%) a drop in G1 to 61.97%, 3.71% in S followed by a slight increase in % apoptosis to 2.01%. Treatment with 1 μ M exhibited the highest % of cells undergoing apoptosis (10.82%) with an additionally large increase of cells in S phase to 19.82% and the lowest G1 percentage of the group (55.73%) with 24.45% of cells in the G2 phase. At 5 μ M treatment, the apoptosis data begins the downward trend of the biphasic curve and drops to 6.55%, followed by slight increases in G1 and decreases in S to 62.99% and 12.58%, respectively, G2 remained similar to the 1 μ M treatment and was 24.43%. Finally, to test the effects of an extreme dosage, a 10 μ M treatment was used and elicited a surprising response. Although the concentration was very high, the percentage of apoptosis was merely 0.23%, the highest percentage of cells in S phase (23.86%) was also in this group, indicating an arrest caused by gossypol. A significant

drop in G1 and G2 now at 57.75% and 18.39% respectively also occurred, supporting evidence for this S phase arrest.

qRT-PCR analysis

Gossypol caused differential expression of genes (Figure 2.3) involved in the regulation of cell cycle, proliferation, and growth and development. ATPase is an enzyme that helps maintain ionic homeostasis in cells as well as contributing to the energy cycling of ATP. According to figure 2.3, this gene was down-regulated in response to gossypol at all 4 treatment concentrations with a p value <0.001 using 3 biological replicates. ESR1 (Estrogen Receptor), a ligand-activated transcription factor is involved in several processes such as hormone binding, DNA binding, and activation of transcription. We observed an across the board down-regulation of this gene in response to all 4 concentrations of gossypol (p <0.001). GSK3 α and GSK3 β (glycogen synthase kinase 3 alpha and beta) is a multifunctional Serine/Threonine protein kinase that involved in regulating several regulatory proteins including glycogen synthase, and transcription factors, such as JUN. It also plays a role in the WNT and PI3K signaling pathways. According to the data both isoforms were down-regulated in response to all 4 treatment concentrations (p <0.001). Additionally, MAPK1 (mitogen activated protein kinase) was down regulated in a linear fashion as treatment concentrations of gossypol increased (Figure 2.3) with p values <0.01 . MAPK1 is involved in multiple pathways and control a large number of processes such as differentiation, proliferation, survival, development, stress response and apoptosis. In contrast, expression of RB1 appears to be stimulated by gossypol with its highest fold

change increase at the 0.1 μ M treatment. RB1 (retinoblastoma 1) is a known negative regulator of the cell cycle and was the first tumor suppressor gene discovered.

Cell Death

Apoptotic gene expression analysis demonstrates the effects of gossypol on genes relating to programmed cell death (Figure 2.4). BAK and BAX, the proteins required for mitochondrial permeabilizations were down-regulated slightly in response to all 4 concentrations of gossypol with p values <0.001. Additionally, Caspases 6 and 7 (executioner caspases) were downregulated in much the same way as BAK and BAX with similar p values <0.001. However, with the remaining genes, at the lowest 0.1 μ M treatment group, we see an up-regulation occurring in P53, PARP1, and PUMA with p values of 0.004, 0.0003, 0.040 respectively. The higher concentrations however, show a decrease in expression levels of these 4 genes.

Discussion

Initially, it was important to conduct a dose response experiment to determine the effective dosages of gossypol and observe the physiological response of MCF-7 cells at these varying concentrations. As shown in figure 2.1 gossypol elicited a statistically significant physiological response at concentrations as low as 300nM. According to this initial dose response data, it was easy to see gossypol was inhibiting the proliferation of MCF-7 cells in a dose dependent manner. Similar inhibition was observed in a study using gossypol as well as a gossypol derivative called gossypolone with DNA synthesis inhibited at concentrations of gossypol as low as 30nM in MCF-7 cells [11]. Using another natural polyphenol called curcumin (isolated from the the rhizome of the plant

Curcuma longa L.) to treat MCF-7 cells a similar dose dependent growth inhibition was observed measured by an MTT assay [12].

From this point, we assessed gossypol's effects on the regulation of the cell cycle, while simultaneously ascertaining the apoptotic effects of the drugs per the sub G_0 population using flow cytometric analysis. Looking at figure 2.2, we see an interesting biphasic relationship to % of cells undergoing apoptosis. As the concentration of gossypol increases to $1\mu\text{M}$ the % of cells undergoing apoptosis concurrently increases to a maximum of 10.82%. As the concentrations increase from $1\mu\text{M}$ however, the % of apoptosis begins to decrease to 6.55% at $5\mu\text{M}$ to a barely registering 0.23%. This suggests that other than apoptosis, there are other forms of cell death possibly at work, namely necrosis and autophagy. Current literature demonstrates that gossypol indeed has the capacity to induce other forms of cell death like autophagy [5, 6, 13, 14] and necrosis [15-17] depending on the concentration. Additionally, this data provided information on how gossypol was altering the regulation of the cell cycle. Based on figure 2.2 we see when MCF-7 cells treated with the higher concentrations of gossypol the cells tend to diverge from their normal proportions and a direct relationship between treatment concentration and percentages of cells in S phase of the cell cycle is observed. Previous reports of gossypol induced S phase arrest include: CLL cells [18], HeLa cells [8, 19] and rat spermatocytes [20]. Additionally, similar S phase arrest was seen in treatments using TW-37 a small molecule BCL-2 inhibitor designed based on the structure of gossypol in 7 different human pancreatic cell lines [21]. Other polyphenols that induced S phase arrest are: grape resveratrol in SK-Mel-28 melanoma cells [22], and Piceatannol, a natural analog of resveratrol [23].

Analysis of genes relating to cell cycle regulation, proliferation, and growth and development was performed to shed light on the physiological and cell cycle regulatory responses elicited by gossypol at a genetic level. As seen in figure 2.3, gossypol tends to down-regulate the genes involved in growth and proliferation (ATPase, ESR1, GSK3 α , GSK3 β , and MAPK1) and up-regulated RB1 almost 3 fold at the 0.1 μ M treatment. Its easy to understand how down-regulating these growth/proliferation genes is important in being successful in the treatment of breast cancer. Accordingly, many current chemotherapeutics target these pathways specifically [24-26]. RB1 is a strong regulator of the cell cycle; its up-regulation indicates that MCF-7 cells cell cycle regulation is being affected by treatment with gossypol [27]. In response to cytotoxic stress, RB1 can act to inhibit DNA replication and keep cells arrested in their respective phases of the cell cycle [27, 28]. The data in figure 2.2 demonstrates a clear manipulation of cell cycle progression in MCF-7 cells in response to gossypol treatment and agrees nicely with the genotypic data in figure 2.3.

Additionally, qRT-PCR was performed on genes related to apoptosis. From the data shown in figure 2.4 we see down-regulation of Bak and Bax as well as a concurrent down-regulation of caspases 6 and 7. Caspase 3 was not studied due to the lack of expression in MCF-7 cells [29]. This down-regulation is interesting due to the apparent apoptosis induction shown in figure 2.2, as well as the data from the dose response (Figure 2.1) combined with the physical appearance of the cells. Similar caspase down-regulation was shown in a phase II study of AT-101 (gossypol) in chemotherapy-sensitive recurrent extensive stage small cell lung cancer (ES-SCLC) [30]. With the genes P53, PARP1, and PUMA we see an increase in gene expression

at the lower treatment concentrations, particularly the 0.1 μ M concentration followed by a down-regulation consistent with the other apoptotic genes at the higher concentrations. This data suggests that the mechanism by which cell death occurs may be more complex than previously suggested in earlier studies. Instead of a clear cut example of apoptosis, it is more likely that multiple pathways to cell death are induced by treatment with gossypol.

Gossypol demonstrates strong effects on the growth, cell death, cellular proliferation, and cell cycle progression of MCF-7 cells. According to the data, cell cycle progression, growth and development and the mediators between the two seem to be intertwined with the effects of gossypol on physiological change and induction of cell death. It appears that the higher concentrations of gossypol are toxic to the cells. By various mechanisms gossypol has been shown to induce autophagy, apoptosis and necrosis [2, 5-7, 31, 32] It is well established that in many instances autophagy and apoptosis induced cell death are interrelated with BH3 domain containing proteins playing a large role in both pathways as seen in figure 2.5 [33]. Since gossypol is a BH3 mimetic [32], this scenario seems more likely considering the common element between the two pathways is Bcl-2 as seen in figure 2.5 [32, 33]. In summary, gossypol inhibits proliferation of MCF-7 cells, arresting them in the S phase of the cell cycle, while at the same time inducing cell death and gross morphological changes. (data not shown)

From the data we conclude that treating MCF-7 cells with gossypol disrupts cell proliferation, cell cycle progression and promotes cell death in a concentration dependent manner. When analyzing these results at a physiological and genetic level,

we can also observe how miRNA may play a role in regulating genes that play a part in why gossypol is so effective. When cells were treated with gossypol, the expressions of several miRNAs were shown to be altered in response (figure 3.4). For this study we will focus on miR-206, miR-15b (up-regulated) and miR-96 (down-regulated). Figure 2.7 describes some of the pathways known to be affected by these miRNAs found throughout literature. miR-206 has been shown to be a potent repressor of ESR1 [34-36], a gene shown to be down-regulated in this study (figure 2.3). Also found to be up-regulated, studies have shown miR-15b targets BCL-2 [37, 38], a survival protein that is well established as being down-regulated in response to gossypol [6, 39, 40]. Finally, miRNA 96 was shown to be down-regulated in response to gossypol and has been associated with a targeting of the FOXO pathway [41, 42]. MiR-96 acts as an oncomir suppressing FOXO1 in MCF-7 cells causing levels of FOXO1 to be very low. The FOXO1 transcription factor act to regulate genes involved in the apoptotic response, cell cycle checkpoints, and cellular metabolism and is a putative tumor suppressor [41]. Gossypol acts to stimulate a variety of mechanisms that synergistically contribute to its efficacy. This study demonstrates a clearer picture of how gossypol acts to inhibit MCF-7 cell proliferation and induce cell death and introduces the first evidence of gossypol's efficacy being linked to its alteration of miRNA expression.

Table 2.1. ICs of gossypol on MCF-7

IC	LOEC	IC5	IC10	IC20	IC50
Gossypol (nM)	300	134	267	700	4520

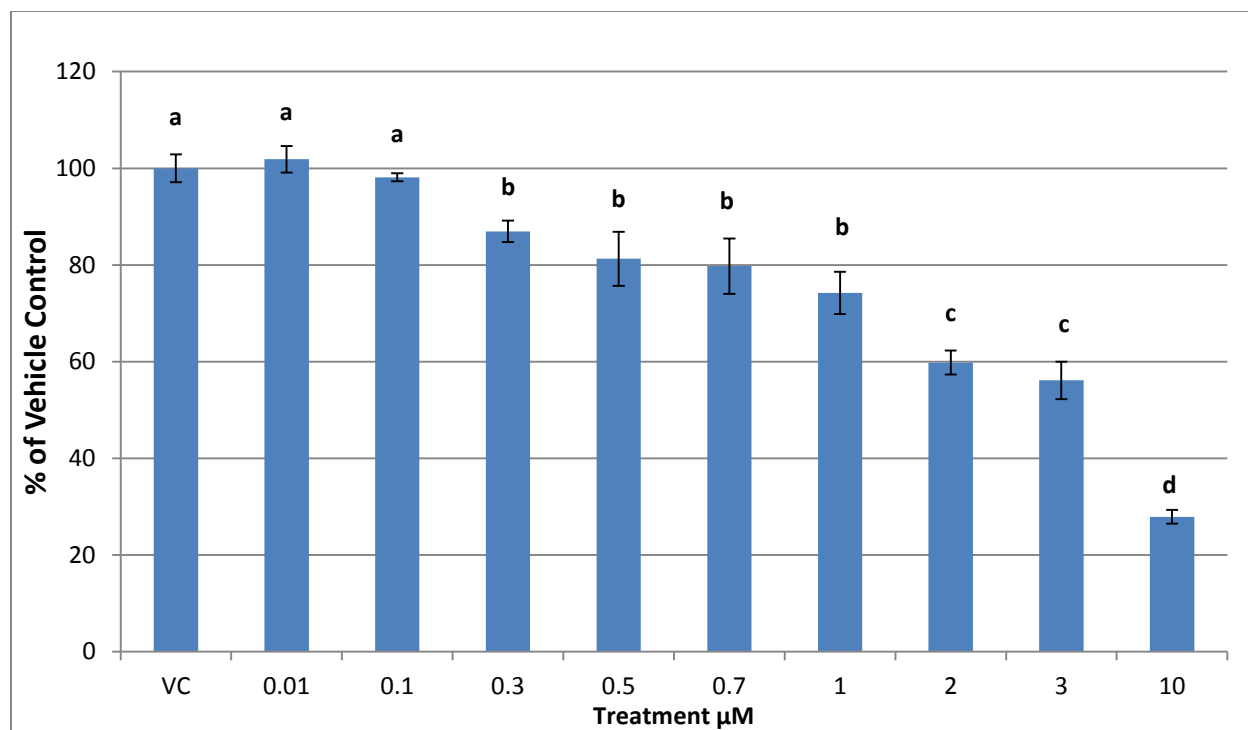


Figure 2.1: The effect of gossypol on MCF-7 cell proliferation 48 hours post treatment (Different letters=statistically significant difference $P < 0.05$).

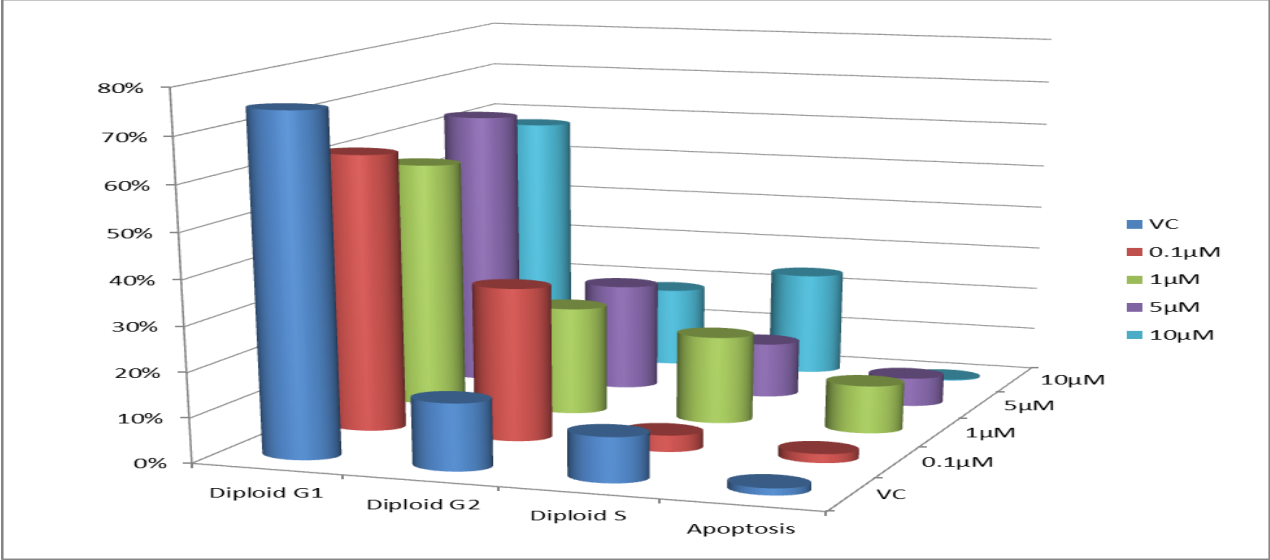


Figure 2.2: Effect of gossypol on cell cycle. MCF-7 cells post-treatment with five different gossypol concentrations after 48 hours

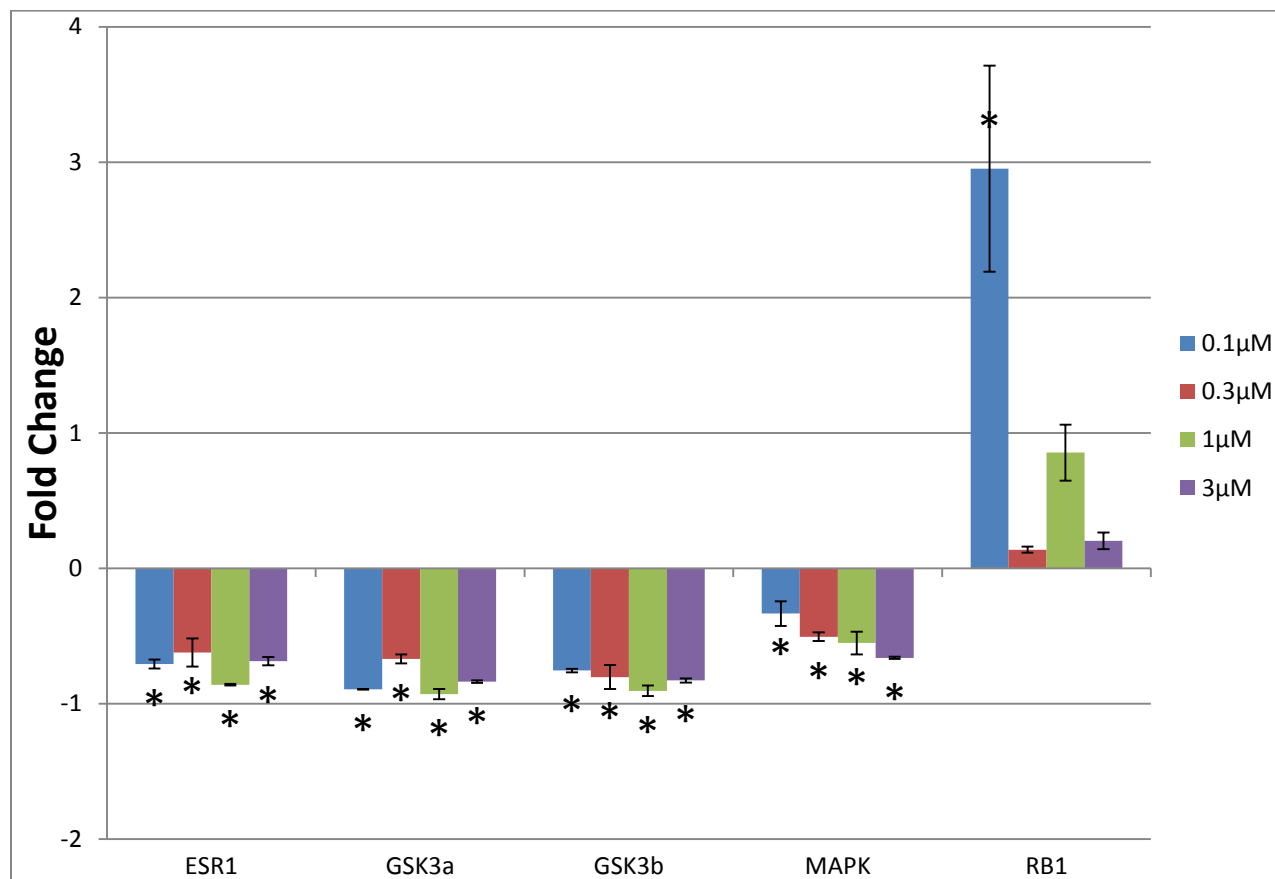


Figure 2.3: qRT-PCR analysis of gossypol's effect on the expression of protein coding genes related to a variety of processes including: cell cycle regulation, growth and development and cellular proliferation (* = $p < 0.05$ compared to VC).

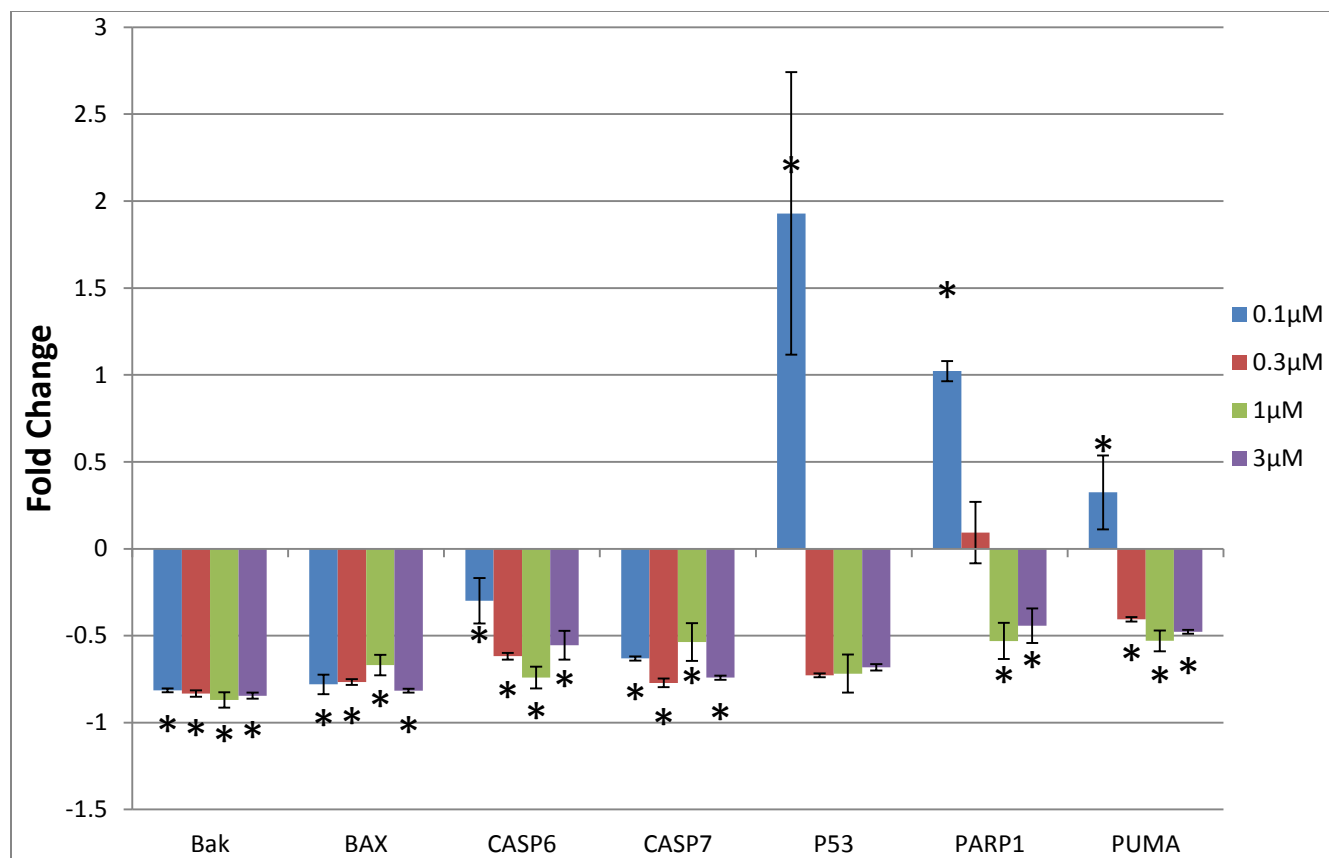


Figure 2.4: qRT-PCR analysis of gossypol's effect on genes relating to cell death. A general trend of down-regulation was observed in response to gossypol. (* = $p < 0.05$ compared to VC)

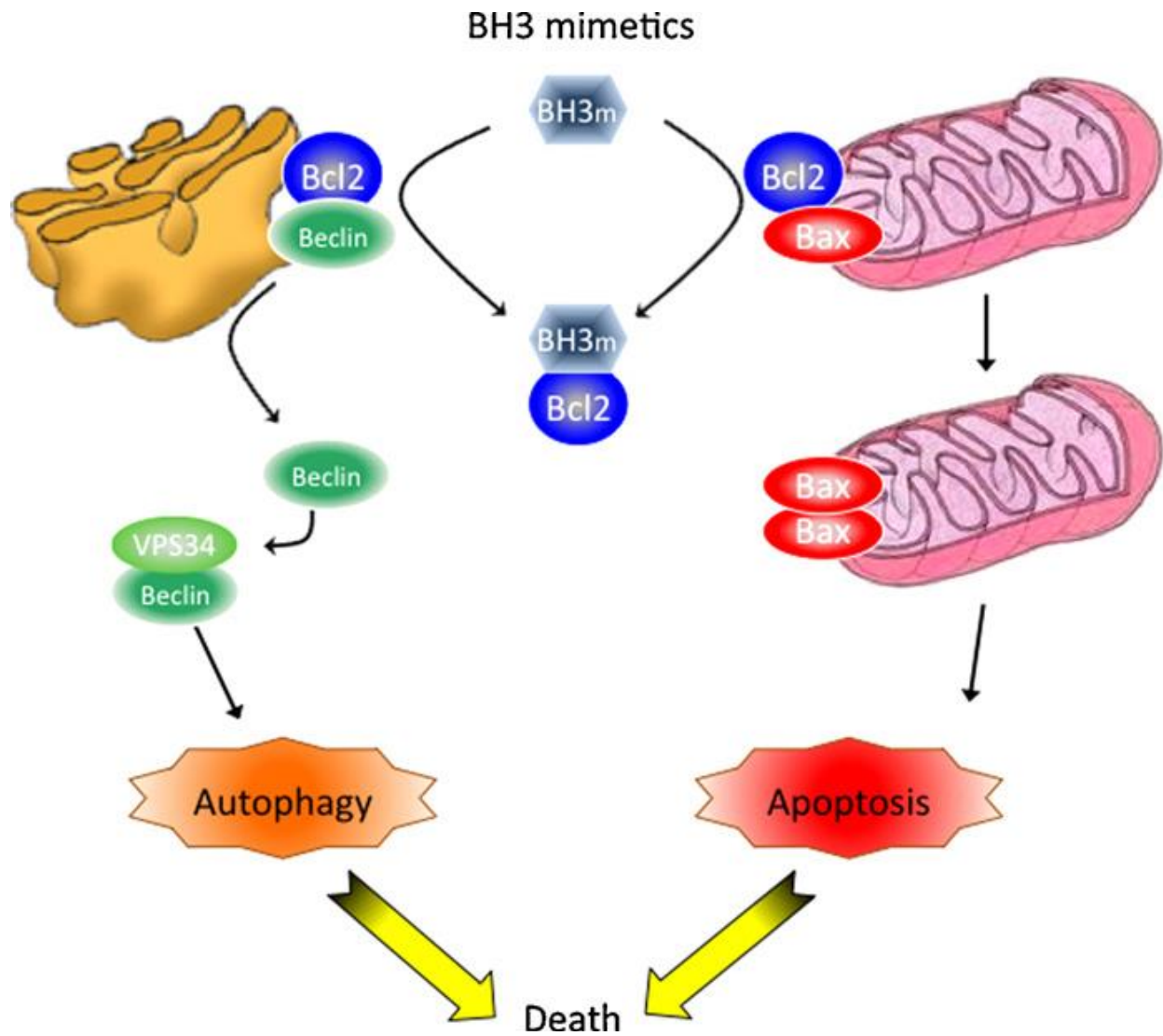


Figure 2.5: Representation of the cell death-inducing effects of BH3 mimetics. This figure illustrates the dual contribution of apoptosis and autophagy to induce cell death mediated by BH3 mimetics [33].

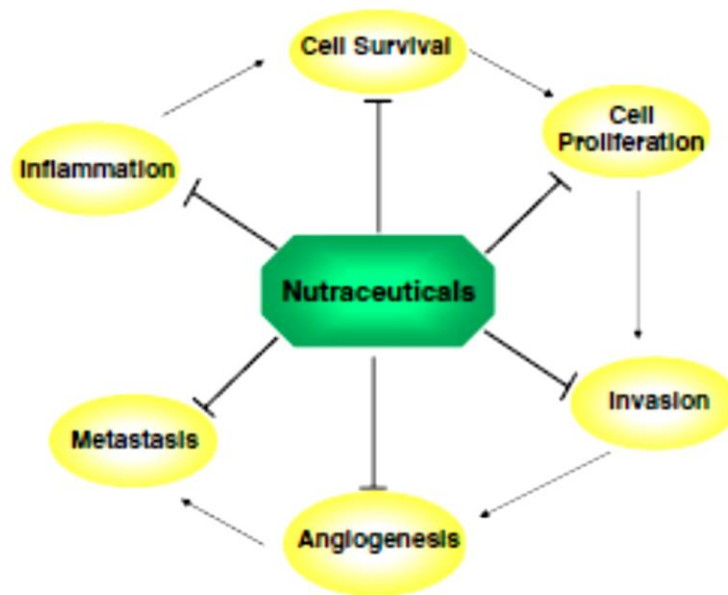


Figure 2.6: Nutraceuticals targeting various aspects of cancer progression [34].

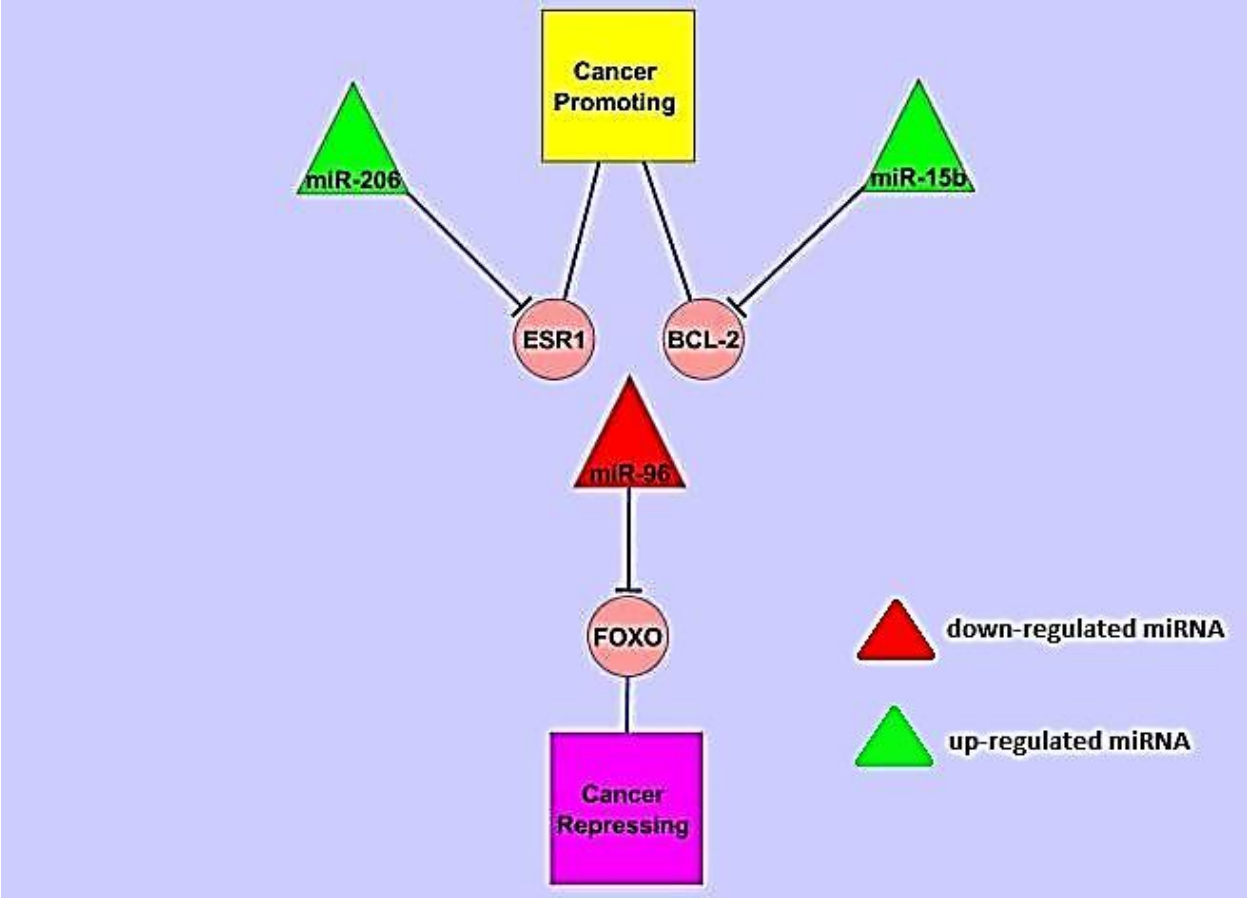


Figure 2.7: Figure describing how the alteration of microRNA expression by gossypol treatment may contribute to the effectiveness of gossypol to inhibit MCF-7 cell proliferation and promote cell death.

References

1. Gupta, S.C., et al., Upsides and downsides of reactive oxygen species for cancer: the roles of reactive oxygen species in tumorigenesis, prevention, and therapy. *Antioxid Redox Signal*, 2012. 16(11): p. 1295-322.
2. Sung, B., et al., Gossypol induces death receptor-5 through activation of the ROS-ERK-CHOP pathway and sensitizes colon cancer cells to TRAIL. *J Biol Chem*, 2010. 285(46): p. 35418-27.
3. Ye, W., et al., Modulation of multidrug resistance gene expression in human breast cancer cells by (-)-gossypol-enriched cottonseed oil. *Anticancer Res*, 2007. 27(1A): p. 107-16.
4. Bauer, J.A., et al., Reversal of cisplatin resistance with a BH3 mimetic, (-)-gossypol, in head and neck cancer cells: role of wild-type p53 and Bcl-xL. *Mol Cancer Ther*, 2005. 4(7): p. 1096-1104.
5. Lian, J., et al., A natural BH3 mimetic induces autophagy in apoptosis-resistant prostate cancer via modulating Bcl-2-Beclin1 interaction at endoplasmic reticulum. *Cell Death Differ*, 2011. 18(1): p. 60-71.
6. Voss, V., et al., The pan-Bcl-2 inhibitor (-)-gossypol triggers autophagic cell death in malignant glioma. *Mol Cancer Res*, 2010. 8(7): p. 1002-16.
7. Tang, H., et al., Oxidative stress induces monocyte necrosis with enrichment of cell-bound albumin and overexpression of endoplasmic reticulum and mitochondrial chaperones. *PLoS One*, 2013. 8(3): p. e59610.
8. Wang, Y. and P.N. Rao, Effect of gossypol on DNA synthesis and cell cycle progression of mammalian cells in vitro. *Cancer Res*, 1984. 44(1): p. 35-8.
9. Sun, J., et al., Apogossypolone inhibits cell growth by inducing cell cycle arrest in U937 cells. *Oncol Rep*, 2009. 22(1): p. 193-8.
10. Hu, Z.Y., et al., ApoG2 induces cell cycle arrest of nasopharyngeal carcinoma cells by suppressing the c-Myc signaling pathway. *J Transl Med*, 2009. 7: p. 74.
11. Gilbert, N.E., et al., Antiproliferative activity of gossypol and gossypolone on human breast cancer cells. *Life Sci*, 1995. 57(1): p. 61-7.
12. Simon, A., et al., Inhibitory effect of curcuminoids on MCF-7 cell proliferation and structure-activity relationships. *Cancer Lett*, 1998. 129(1): p. 111-116.
13. Niu, X., et al., Apogossypolone induces autophagy and apoptosis in breast cancer MCF-7 cells in vitro and in vivo. *Breast Cancer*, 2012.
14. Gao, P., et al., The Bcl-2 homology domain 3 mimetic gossypol induces both Beclin 1-dependent and Beclin 1-independent cytoprotective autophagy in cancer cells. *J Biol Chem*, 2010. 285(33): p. 25570-81.
15. Haschek, W., et al., Cottonseed meal (gossypol) toxicosis in a swine herd. *Journal of the American Veterinary Medical Association*, 1989. 195(5): p. 613.
16. Herman, R.L., Effects of gossypol on rainbow trout *Salmo gairdneri* Richardson. *Journal of Fish Biology*, 1970. 2(4): p. 293-303.
17. T.-L. R. and H. K.-H., Gossypol activates pancreatic polyamine catabolism in normal rats and induces acute pancreatitis in transgenic rats over-expressing spermidine/spermine N 1-acetyltransferase. *Scandinavian journal of gastroenterology*, 2003. 38(7): p. 787-793.
18. Balakrishnan, K., et al., Gossypol, a BH3 mimetic, induces apoptosis in chronic lymphocytic leukemia cells. *Blood*, 2008. 112(5): p. 1971-1980.
19. Rosenberg, L.J., et al., Inhibition of DNA polymerase α by gossypol. *Biochimica et Biophysica Acta (BBA)-Gene Structure and Expression*, 1986. 866(4): p. 258-267.
20. Zhang, S., et al., Biological activity in the repopulating rat spermatocyte after the withdrawal of gossypol treatment: I. The activity for DNA synthesis. *Contraception*, 1989. 40(2): p. 233-242.

21. Wang, Z., et al., TW-37, a small-molecule inhibitor of Bcl-2, inhibits cell growth and induces apoptosis in pancreatic cancer: involvement of Notch-1 signaling pathway. *Cancer Res*, 2009. 69(7): p. 2757-2765.
22. Larrosa, M., F.A. Tomás-Barberán, and J.C. Espín, Grape polyphenol resveratrol and the related molecule 4-hydroxystilbene induce growth inhibition, apoptosis, S-phase arrest, and upregulation of cyclins A, E, and B1 in human SK-Mel-28 melanoma cells. *Journal of Agricultural and Food Chemistry*, 2003. 51(16): p. 4576-4584.
23. Wolter, F., et al., Piceatannol, a natural analog of resveratrol, inhibits progression through the S phase of the cell cycle in colorectal cancer cell lines. *The Journal of nutrition*, 2002. 132(2): p. 298-302.
24. Roberts, P.J. and C.J. Der, Targeting the Raf-MEK-ERK mitogen-activated protein kinase cascade for the treatment of cancer. *Oncogene*, 2007. 26(22): p. 3291-310.
25. Jacobs, K.M., et al., GSK-3beta: A Bifunctional Role in Cell Death Pathways. *Int J Cell Biol*, 2012. 2012: p. 930710.
26. Ougolkov, A.V. and D.D. Billadeau, Targeting GSK-3: a promising approach for cancer therapy? *Future Oncol*, 2006. 2(1): p. 91-100.
27. Chinnam, M. and D.W. Goodrich, RB1, development, and cancer. *Curr Top Dev Biol*, 2011. 94: p. 129-69.
28. Wiman, K.G., The retinoblastoma gene: role in cell cycle control and cell differentiation. *FASEB J*, 1993. 7(10): p. 841-5.
29. Janicke, R.U., MCF-7 breast carcinoma cells do not express caspase-3. *Breast Cancer Res Treat*, 2009. 117(1): p. 219-21.
30. Baggstrom, M.Q., et al., A phase II study of AT-101 (Gossypol) in chemotherapy-sensitive recurrent extensive-stage small cell lung cancer. *J Thorac Oncol*, 2011. 6(10): p. 1757-60.
31. Wang, J., et al., Gossypol induces apoptosis in ovarian cancer cells through oxidative stress. *Mol Biosyst*, 2013. 9(6): p. 1489-97.
32. Lian, J., D. Karnak, and L. Xu, The Bcl-2-Bcl-1 interaction in (-)-gossypol-induced autophagy versus apoptosis in prostate cancer cells. *Autophagy*, 2010. 6(8): p. 1201-3.
33. Notte, A., L. Leclere, and C. Michiels, Autophagy as a mediator of chemotherapy-induced cell death in cancer. *Biochem Pharmacol*, 2011. 82(5): p. 427-34.
34. Adams, B.D., D.M. Cowee, and B.A. White, The role of miR-206 in the epidermal growth factor (EGF) induced repression of estrogen receptor-alpha (ERalpha) signaling and a luminal phenotype in MCF-7 breast cancer cells. *Mol Endocrinol*, 2009. 23(8): p. 1215-30.
35. Adams, B.D., H. Furneaux, and B.A. White, The micro-ribonucleic acid (miRNA) miR-206 targets the human estrogen receptor-alpha (ERalpha) and represses ERalpha messenger RNA and protein expression in breast cancer cell lines. *Mol Endocrinol*, 2007. 21(5): p. 1132-47.
36. Kondo, N., et al., miR-206 Expression is down-regulated in estrogen receptor alpha-positive human breast cancer. *Cancer Res*, 2008. 68(13): p. 5004-8.
37. Xia, L., et al., miR-15b and miR-16 modulate multidrug resistance by targeting BCL2 in human gastric cancer cells. *International Journal of Cancer*, 2008. 123(2): p. 372-379.
38. Zhu, W., et al., miR-181b modulates multidrug resistance by targeting BCL2 in human cancer cell lines. *International Journal of Cancer*, 2010. 127(11): p. 2520-2529.
39. Ni, Z., et al., Natural Bcl-2 inhibitor (-)- gossypol induces protective autophagy via reactive oxygen species-high mobility group box 1 pathway in Burkitt lymphoma. *Leuk Lymphoma*, 2013.
40. Yan, F., et al., A novel water-soluble gossypol derivative increases chemotherapeutic sensitivity and promotes growth inhibition in colon cancer. *J Med Chem*, 2010. 53(15): p. 5502-10.
41. Guttilla, I.K. and B.A. White, Coordinate regulation of FOXO1 by miR-27a, miR-96, and miR-182 in breast cancer cells. *Journal of Biological Chemistry*, 2009. 284(35): p. 23204-23216.

42. Lin, H., et al., Unregulated miR-96 induces cell proliferation in human breast cancer by downregulating transcriptional factor FOXO3a. *PLoS One*, 2010. 5(12): p. e15797.
43. Gupta, S.C., et al., Regulation of survival, proliferation, invasion, angiogenesis, and metastasis of tumor cells through modulation of inflammatory pathways by nutraceuticals. *Cancer Metastasis Rev*, 2010. 29(3): p. 405-34.

Chapter 3: Gossypol Alters miRNA Expression of MCF-7 Breast Cancer Cells

Abstract

Gossypol is a relatively new nutraceutical chemotherapeutic currently undergoing clinical trials for use in treating various forms of cancer. Although the drug has shown effectiveness, the mechanism of action is poorly understood. MicroRNAs (miRNAs) are a recently identified group of small non-coding RNAs that play an important role in gene regulation through their targeting of mRNAs for cleavage or inhibiting their translation. When cells are treated with a variety of chemotherapeutics or other drugs that induce genotoxic stress, miRNA expression profiles change in response and are thought to modulate the effectiveness of drugs and in some cases promote resistance. In this study, using a combined advanced microarray and qRT-PCR technologies, we demonstrate a change in expression of miRNAs in response to gossypol in the MCF-7 cell line. According to target analysis and previous studies, many of these miRNAs whose expression profiles changed have been implicated in processes relating to tumor suppressing as well as oncogenic activity.

Introduction

Chemotherapy with cytotoxic drugs and radiotherapy are common ways to treat and manage breast cancer. There are a wide variety of anticancer drugs used to treat breast cancer, most of which are synthetic that have targets ranging from inhibiting topoisomerases, raising ROS, to down-regulating the ESR etc. One of the major hurdles in treating breast cancer, like most cancers, is that they gradually develop resistance to both chemotherapy and radiotherapy although they may be sensitive to synthetic drugs initially. This resistance is due in part, to the induction of multidrug resistant proteins [1].

Relatively new in its application as a chemotherapeutic, the molecular mechanism behind the functionality of gossypol remains to be elucidated. Indeed gossypol has been shown to alter the expression of a variety of protein coding genes that regulate pathways like cell death [2-7], cell cycle [8-12] and oxidative stress [5, 13]. We hypothesize that microRNA (miRNA), short non-coding RNAs that are an important regulatory molecule in both plants and animals, play an important role in gossypol's efficacy. miRNAs are ~18-22 nucleotides long and are transcribed in the nucleus mainly by RNA Polymerase II [14, 15].

These molecules regulate gene expression by translational repression, mRNA cleavage, mRNA decay by rapid deadenylation [15-17] and in some cases translational activation [16, 17]. The majority of miRNAs function by binding to the 3' untranslated region (UTR) of a specific mRNA transcript. The complementarity between the miRNA and its prospective mRNA will decide whether the mRNA is cleaved or translationally

repressed [18]. In general, a fully complimentary strand will cause cleavage while a partially complimentary strand will induce translational inhibition [18].

Polymerase II promoters, which include miRNA genes, many times contain toxicologically sensitive enhancer regions [15]. Due to this sensitivity, miRNAs are thought to be involved in the response of cells to genotoxic stress in a variety of pathways [15, 19]. Studies demonstrate that a variety of drugs alter the expression profiles of miRNAs in MCF-7 and other cell lines [20-23]. However, currently there are no studies that provide insight on the effects of gossypol on the miRNA expression profile of MCF-7 cells *in vitro*.

Materials and Methods

Cell line and cell culture

Human MCF-7 breast cancer cells were obtained from ATCC, cultured and kept at 37°C in a 5% CO₂ and 95% humidified air incubator. MCF-7 cells were passaged and grown in Roswell Park Memorial Institute medium (RPMI) 1640 (GIBCO, Vienna, VA) with 10% FBS (PAA Laboratories, Dartmouth, MA), and supplemented with 4 mg/ml human recombinant insulin (GIBCO). The culture media was replaced every 48 hours, and the cells were passaged at least once a week by trypsinizing the cells using 0.05% trypsin/0.02% EDTA (Sigma, St. Louis, MO).

Gossypol treatment

Gossypol, purchased from Sigma-Aldrich (St. Louis, MO), and was kept at -80°C in a dark 1.8mL tube completely impermeable to light. Directly after purchase, a stock

solution of 100mM gossypol was made using DMSO as a proper solvent as it is insoluble in water and vacuum filtered the solution in a laminar flow hood to maintain sterility. 5×10^5 cells were plated into 12 well plates using 3 wells per treatment group (biological replicates) including vehicle controls in RPMI media supplemented with 10% FBS and absent of the use of antibiotics or antifungal compounds composing a final volume of all reagents to be 2mL. After this, cells were incubated for 24 hours in just RPMI media without treatment allowing cells to properly adhere and stabilize. Cells were exposed to gossypol at various concentrations. Using 0.1% DMSO to dissolve gossypol, it was important to use the same amount of DMSO into vehicle control and treatment groups to help exclude the potential effects of DMSO on the cells.

RNA Isolation

After treatment, MCF-7 cells were trypsinized, centrifuged, and washed with PBS and the remaining pellet was transferred to 1.8mL micro-centrifuge tubes. RNA was extracted from the cells according to the mirVana™ miRNA Isolation Kit. Briefly, samples were denatured using lysis binding buffer contained in the kit. Then, acid-phenol extraction was used to separate RNA from DNA and other cellular components. After this, ethanol was added to samples and the solution was passed through a glass-filter. Before eluting with RNase free water, the RNA was washed several times with wash solution.

Using the NanoDrop ND-1000 Micro-Volume UVVis Spectrophotometer (NanoDrop Technologies, Wilmington, DE), RNA was quantified in ng/ μ l and evaluated using the absorbance ratios of 260/280 and 260/230 to assess quality.

MicroRNA Microarray

LC Sciences (Houston, TX) was contracted to perform the miRNA microarray. We sent approximately 5mg samples of total RNA to LC Sciences for analysis. Total RNA samples were size fractionated using the YM-100 Microcon centrifugal filter (Millipore, Billerica, MA) and screened for RNA sequences with <30 nt. These screened small RNA were extended at 3'-end with a poly(A) tail placed there by poly(A) polymerase, then an oligonucleotide tag to the poly(A) tail was fused by ligation for later fluorescent staining. Two tags (Cy3 and Cy5) were used for two different RNA samples (vehicle control and gossypol treated RNA samples). Both RNA samples were hybridized overnight on top of an mParaflo™ microfluidic chip utilizing a microcirculation pump (Atactic Technologies, Inc., Houston, TX). The microfluidic chips contained positive control probes, detection probes and negative control probes. Detection probes were created *in situ* by photogenerated reagent (PGR) chemistry. Probes were composed of nucleotide coding sequences that were chemically modified and complementary to the 871 target miRNAs listed in the Sanger's miRNA miRBase, and additionally a spacer segment of polyethylene glycol was used to extend the coding sequence away from the substrate. To ensure uniformity of conditions and sample labels, a combined total of 50 positive and negative control probes were used. The chemical modifications were done to help balance the melting temperatures of hybridization. The RNA hybridization process was completed using 100 ml of 6X SSPE buffer (0.9M NaCl, 6mM EDTA, 60mM Na₂HPO₄, pH 6.8) containing 25% formamide at 348C. Post-hybridization, control and gossypol treated cells were dyed using tag-conjugating dyes Cy3 and Cy5, respectively. To collect the fluorescent images, an Axon GenePix 4000B Microarray Scanner (Molecular Device, Union City, CA) was used.

Then the images were digitized using Array-Pro image Analysis software (Media Cybernetics, Bethesda, MD). To avoid dye bias, dye switching between control and treated RNA samples in order was performed. For accuracy, every miRNA was analyzed four times followed by the controls being repeated 4–16 times.

Statistical analysis of microarray data

The statistical analysis of the microarray data was performed by subtracting the background while normalizing the signals using a locally weighed regression (LOWESS) filter according to Bolstad et al. (2003). Detectable miRNAs were filtered by the following criteria: spot $CV < 0.5$ (where $CV = \frac{\text{standard deviation}}{\text{signal intensity}}$); signal intensity higher than $3X$ (background standard deviation); and signals from no less than two out of four replicates above the detection level. Statistical analysis was performed to identify miRNAs with expression differences between control and gossypol treated MCF-7 cells. The ratio between the two sets of signals (control and treated) was calculated and presented in \log_2 scale for each miRNA. miRNAs were then sorted by their differential ratios. Readings of miRNAs with $p\text{-values} < 0.01$ and $\log_2 \text{ratio} > 0.5$ were considered significantly differentially expressed.

qRT-PCR of miRNA expression

TaqMan microRNA Reverse Transcription kit from Applied Biosystems (Foster City, CA) was used to reverse transcribe miRNAs to cDNAs. miRNA-specific stem-loop primer was used to reverse transcribe miRNAs to cDNA with a total of 200 ng RNAs. The composition of the other components were as follows: 0.15 μL of 100mM dNTPs, 0.19 μL RNase inhibitor (20U/ μL), 1 μL f primer and 1 μL multiscribe reverse transcriptase (50U/ μL), 1.5 μL reverse transcription buffer (10X), and an amount of

RNase free water dependent on the RNA concentration in the sample was added to make the final 15 μ L reaction volume. A thermal cycler was programmed to perform the reverse transcription according to the settings of: 16 °C-30 minutes followed by 42°C-30 minutes, 85°C-5 minutes and finally holding the temperature upon completion at 4°C. The sample was then diluted with 85 μ L DNase/RNase-free water to prepare the cDNA products for qRT-PCR.

Five of the most up-regulated and six of the most down-regulated miRNAs were chosen for further analysis. Expression levels of miRNAs were analyzed after performing qRT-PCR using 384-well-plates used by the ViiA™ 7 Real-Time PCR System (Applied Biosystem) with SYBR Green PCR master mix (SuperArray Bioscience Corp, Frederick, MD). Specific forward primers as well as miRNA universal reverse primers for miRNAs were used for quantification. Each reaction contained a total solution of 15 μ L composed of 5.5 μ L DNase/RNase free water, 7.5 μ L SYBR Green master mix, 1 μ L cDNA, and 1 μ L of primer mix. At least 3 biological replicates with 3 technical replicates for each reaction was run. The program used for qRT-PCR began with the enzyme activation phase with a duration of 10 min at 95°C, followed directly by the denaturation phase for 15 sec at 95°C and lastly an annealing or extension step with a duration of 60 sec at a temperature of 60°C. The final 2 steps were repeated for 40 cycles.

Target Prediction and Functional analysis

A step by step process was used for miRNA-pathway enrichment. Initially, target prediction was performed for the 11 chosen miRNAs using TargetScan. Duplicates were removed and a list was generated that ranked 4,728 different gene targets. From this

point the genes were ordered from most to least commonly targeted genes. This list was used and inputted into DAVID. Functional annotation clustering was run with the highest stringency. Out of 213 clusters, only 5 clusters with enrichment values ≥ 3 were used for subsequent analysis. Next, genes were extracted from these enriched clusters and their order was maintained for analysis using GOrilla gene ontology software. The single ranked gene list was used to perform process-analysis whose output was summarized as 'Directed Acyclic Graph'. This presentation demonstrates the relationship between the pathways predicted to be altered in response to gossypol. Each enriched pathway had an enrichment score ($E=(b/n)/(B/N)$) where "b" is the number of genes in the intersection; "n" is the number of genes in the top of the user's input list; "B" is the total number of genes associated with a specific GO term; "N" is the total number of genes), a p-value, and a corrected p-value (FDR).

Next, a gene based target prediction shown in figure 3.5 and table 3.3 was based on targetscan. This network was constructed using genes that are commonly targeted by at least 8 of the 11 miRNAs chosen for further analysis. 2 genes (CCND2 and HIPK2) were predicted to be targeted by 9 of the 11 miRNAs of interest (SS change in expression levels). 3 genes (IGF1, NUFIP2, and ELL2) were predicted to be targeted by 8 miRNAs.).

Results

Gossypol alters the miRNA expression of MCF-7 cells

Microarray

Treatment with gossypol significantly altered the miRNA expression profile of MCF-7 cells. 891 miRNAs were analyzed in this microarray study in response to gossypol. Of the 891, many were discarded due to either low signal intensity or unacceptable statistical significance values ($P > 0.01$). After this filter, there were 52 miRNAs that were up-regulated and 33 miRNAs down-regulated in response to gossypol (Figure 3.1). Of these miRNAs, 5 of the most up-regulated and 6 of the most down-regulated were chosen for further analysis by qRT-PCR, these miRNAs are shown in table 3.1 and figures 3.3 and 3.4.

qRT-PCR

qRT-PCR data confirmed our miRNA microarray data and the miRNAs were differentially expressed in a dosage-dependent manner

The expression of miRNAs 141, 15b, 197, 206 and 320c were significantly up-regulated in response to treatment with gossypol. MiR-29c was significantly down-regulated at all concentrations and miRNA 96 was shown to be significantly down-regulated at the 0.3 μ M concentration.

miRNA targets

Targetscan was used as the primary means to predict miRNA targets of the miRNAs in this study. From this analysis we observed multiple biological pathways targeted by miRNAs including: hemophilic cell adhesion, nervous system development, cell-cell adhesion, biological adhesion, cell adhesion, system development, angiogenesis, and neuron migration as seen in figure 3.2 and table 3.6.

Next, targeting was used to construct a network using genes that are commonly targeted by at least 8 of the 11 miRNAs chosen for further analysis. 2 genes (CCND2

and HIPK2) were predicted to be targeted by 9 of the 11 miRNAs of interest (SS change in expression levels). 3 genes (IGF1, NUFIP2, and ELL2) were predicted to be targeted by 8 miRNAs.) as shown in figure 3.5. The relative function of each of these co-targeted genes is listed in table 3.3.

Discussion

miRNAs are proven to be an important regulatory element in cancer and have the ability to function as both oncogenes and tumor suppressors [24-26]. Currently, researchers are investigating ways to use these small noncoding RNAs as therapy for cancer treatments. Its interesting to see how altering the expression of existing miRNAs in response to gossypol may contribute to the overall mechanism of action and efficacy of the nutraceutical.

This study reveals the first information about the alteration of miRNA expression in response to gossypol ever done in human breast cancer cells. Its well-known that a variety of toxological stressors induce changes in miRNA expression which in turn mediate a response as shown in figure 3.7 [20, 21, 23, 27, 28].

Interestingly, miRNAs that show altered gene expression in both the microarray and the multiple dose qRT-PCR analysis have been implicated previously to affect a variety of biological pathways related to cancer including many of those predicted by Targetscan (Tables 3.2 and 3.3 and Figures 3.5 and 3.6). In particular, miR-141 of the miR-200 miRNA family was found to be one of the most up-regulated in both the microarray study and qRT-PCR study. Previous literature demonstrates that this miRNA is likely to be involved in targeting two E box factors ZEB1 and ZEB2 which are

both key regulators within a complex network of transcriptional repressors that regulate the expression of E-cadherin and a number of master regulators of epithelial polarity [29-31]. Due to this targeting, miRNA 200 family has been implicated to be involved as both a marker and a powerful regulator of epithelial-to-mesenchymal transition (EMT) [32, 33]. These effects can be seen in figure 3.8 which additionally shows the targets of the let-7 family which in our microarray study (let-7f) was shown to be up-regulated also as seen in figure 3.1 [33].

Additionally up-regulated miRNAs from this study seen in literature are miR-15b, miR-206 and miR-320c. Current literature suggests that miR-15b likely targets BCL-2 a well-known mechanism of gossypol's ability to initiate cell death and cyclins contributing to controlling cell cycle progression [23, 34, 35]. miR-206 is well documented in its role in suppressing the human estrogen receptor alpha (ER α) [36-38]. Numerous studies demonstrate that their expression is inversely related and some support evidence of a double negative feedback loop between the two. Additionally, it has been shown that ER+ breast cancers express far lower amounts of miR-206 than normal cells. miR-320c has been implicated as a biomarker for gastric cancer. When miR-320c is expressed at very low levels studies show this is a strong indicator of gastric cancer, with some demonstrating this expression pattern in liver and brain cancers as well [39-41].

miRNAs that were significantly down-regulated miRNAs in this study are miR-29c and miR-96. MiR-29c, which was down-regulated in all 4 dosages of gossypol when compared to the vehicle control (figure 3.4), has been looked at as a possible biomarker for breast cancer as well as a contributor to drug resistance [42-44]. Although only down-regulated in the 0.3 μ M treatment group, miR-96 up-regulation has been

associated with the proliferation and anchorage-independent growth of breast cancer cells as well as preventing apoptosis induction via the FOXO1 pathway [45, 46].

Taken together, it is clear that gossypol induces an aberrant change in expression of a variety of miRNAs. The miRNAs chosen for further analysis affect a variety of different biological pathways involved in cancer progression (figure 3.5 and 3.6). Figure 3.9 demonstrates miRNAs that exhibited altered expression in response to gossypol treatment and their known targets found throughout literature and mentioned above. From this data, we see how changes in miRNA expression levels in response to gossypol contribute to its overall efficacy. Additionally, the miRNA targeting data with the most enriched pathways relating to cell adhesion (table 3.2) combined with 2 out of the 5 confirmed up-regulated miRNAs (figure 3.4 and 3.9) targeting the EMT pathway presents evidence gossypol may be an effective treatment for preventing cancer progression and metastasis.

Table 3.1: Table demonstrating the 11 miRNAs chosen for further analysis by qRT-PCR and the total amounts of predicted mRNA targets for each.

miRNA	Number of predicted targets
hsa-let-7f	819
hsa-miR-141	531
hsa-miR-15b	968
hsa-miR-197	140
hsa-miR-19a	938
hsa-miR-206	584
hsa-miR-30e	1080
hsa-miR-320b	539
hsa-miR-320c	539
hsa-miR-96	787
hsa-miR-29c	1078

Table 3.2: Pathways associated with the 11 miRNAs chosen for further study in order from highest to lowest enrichment values ($E=(b/n)/(B/N)$ where “b” is the number of genes in the intersection; “n” is the number of genes in the top of the user’s input list; “B” is the total number of genes associated with a specific GO term; “N” is the total number of genes), a p-value, and a corrected p-value (FDR).

Description	P-value	FDR q-value	Enrichment (N, B, n, b)
homophilic cell adhesion	1.31E-18	6.84E-16	12.69 (203,16,14,14)
nervous system development	1.09E-14	3.15E-12	11.28 (203,18,12,12)
cell-cell adhesion	5.30E-16	1.97E-13	10.15 (203,20,14,14)
biological adhesion	2.85E-12	6.74E-10	6.34 (203,32,14,14)
cell adhesion	2.85E-12	6.18E-10	6.34 (203,32,14,14)
system development	3.02E-10	5.61E-08	6.34 (203,32,12,12)
cell development	4.82E-06	5.02E-04	3.69 (203,10,55,10)
angiogenesis	8.48E-05	4.70E-03	3.17 (203,9,64,9)
neuron migration	3.43E-05	2.29E-03	3.12 (203,10,65,10)

Table 3.3: This network was constructed using genes that are commonly targeted by at least 8 of the 11 miRNAs chosen for further analysis. 2 genes (CCND2 and HIPK2) were predicted to be targeted by 9 of the 11 miRNAs of interest (SS change in expression levels). 3 genes (IGF1, NUFIP2, and ELL2) were predicted to be targeted by 8 miRNAs.).

ID	Gene Name	Summary of Functions
CCND2	cyclin D2	cell cycle, cell cycle control, cell division, complete proteome, cyclin, polymorphism, G1/S-specific cyclin-D2
ELL2	elongation factor, RNA polymerase II, 2	3d-structure, complete proteome, elongation factor, nucleus, phosphoprotein, polymorphism, Transcription, transcription regulation
HIPK2	homeodomain interacting protein kinase 2	alternative splicing, apoptosis, atp-binding, complete proteome, cytoplasm, isopeptide bond, kinase, nucleotide-binding, nucleus, phosphoprotein, polymorphism, serine/threonine-protein kinase, transcription, transcription regulation, transferase, ubl conjugation
IGF1	insulin-like growth factor 1 (somatomedin C)	3d-structure, alternative splicing, amidated carboxyl end, complete proteome, deafness, direct protein sequencing, disulfide bond, growth factor, plasma, polymorphism, secreted, signal
NUFIP2	nuclear fragile X mental retardation protein interacting protein 2	acetylation, complete proteome, cytoplasm, direct protein sequencing, nucleus, phosphoprotein, RNA-binding

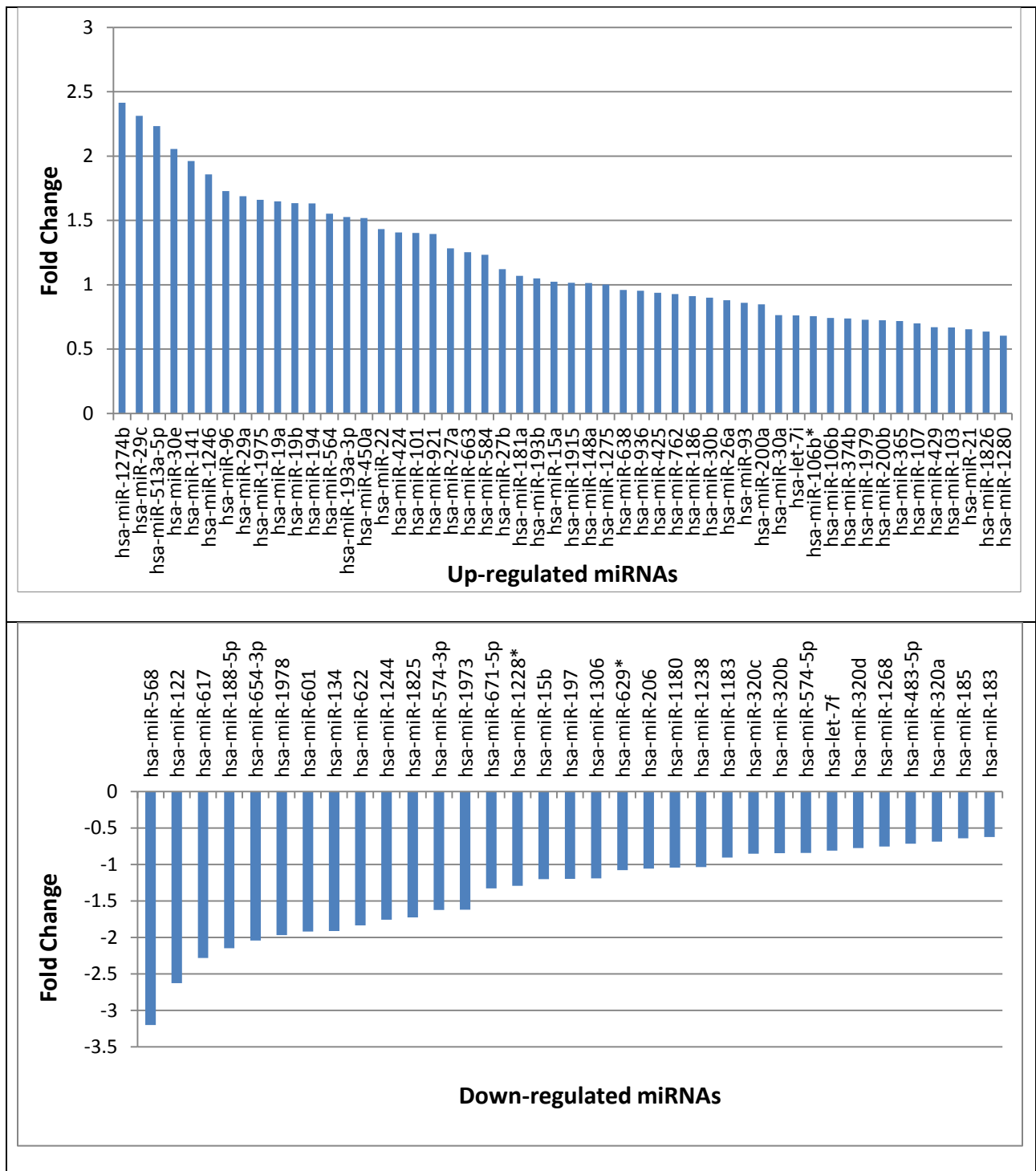


Figure 3.1: Log₂ graphs demonstrating fold change in expression of significantly altered miRNAs between gossypol treated and non-treated MCF-7 cells p<.001.

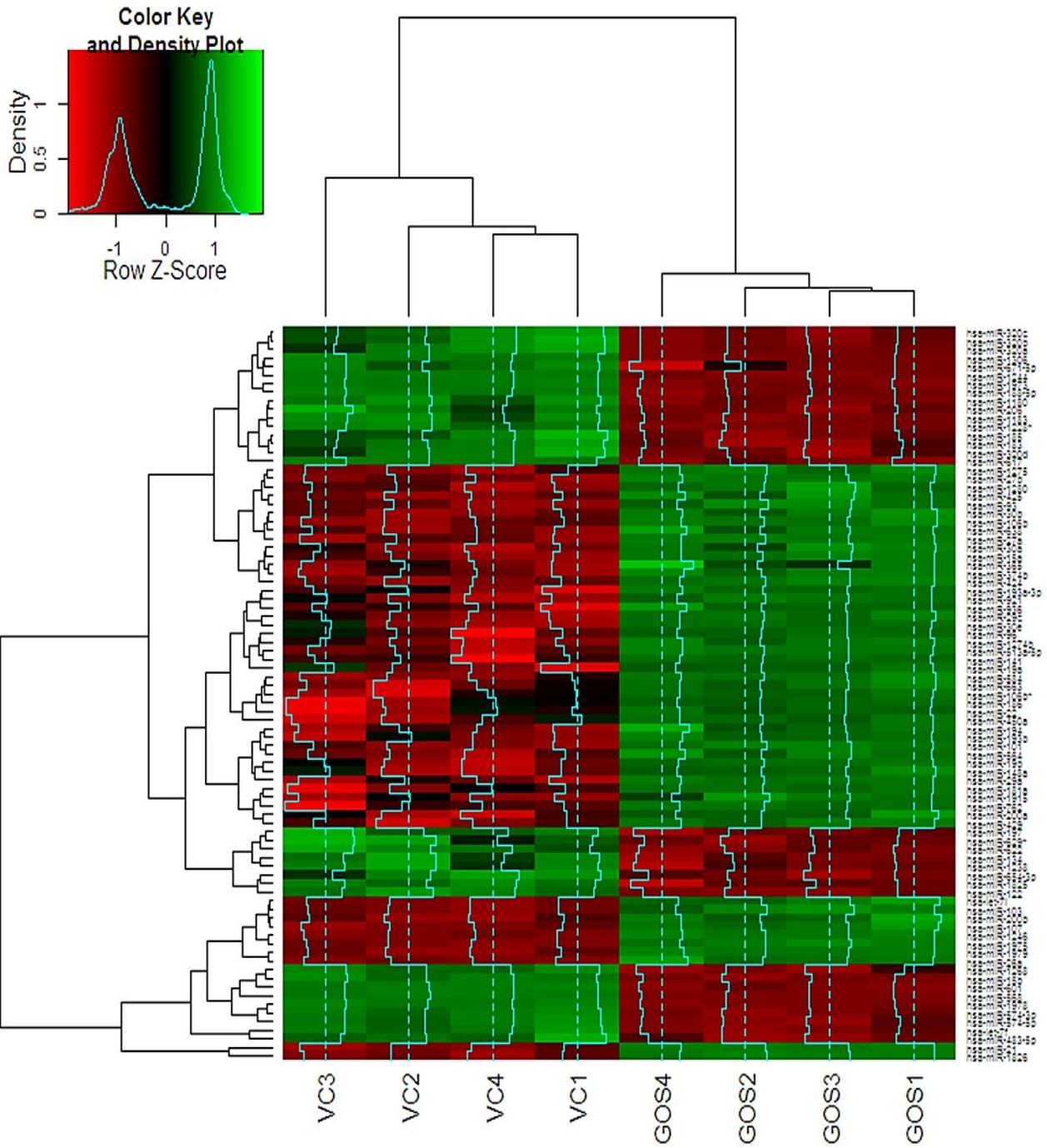


Figure 3.2: Heat map demonstrating fold change in expression of significantly altered miRNAs between gossypol treated and non-treated MCF-7 cells $p < .001$. The brighter the green in color represents higher up-regulation, while the brighter the red in color represents down-regulation.

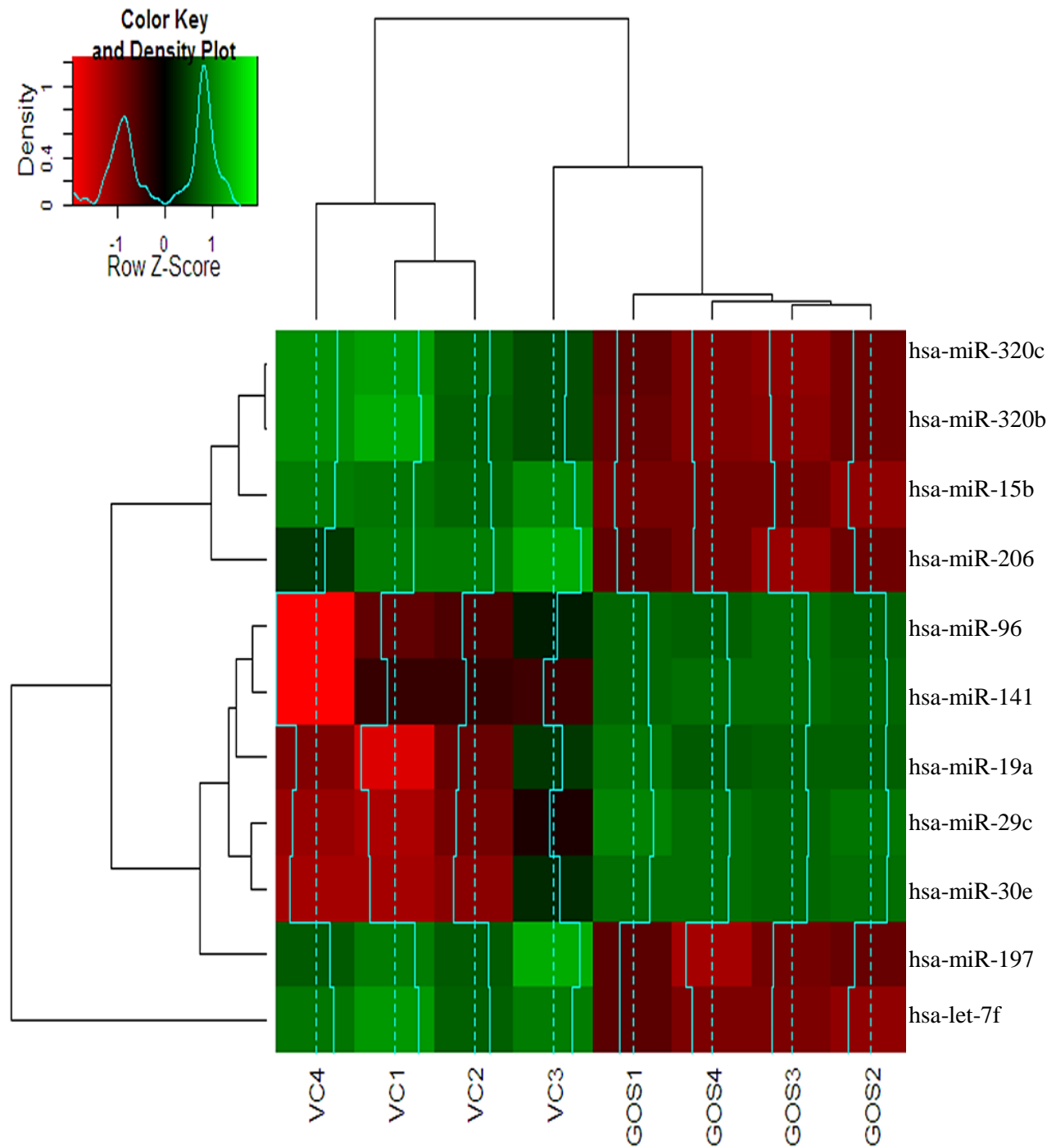


Figure 3.3: Heat map demonstrating fold change in expression of 11 miRNAs chosen for further study between gossypol treated and non-treated MCF-7 cells $p < .001$. The brighter the green in color represents higher up-regulation, while the brighter the red in color represents down-regulation.

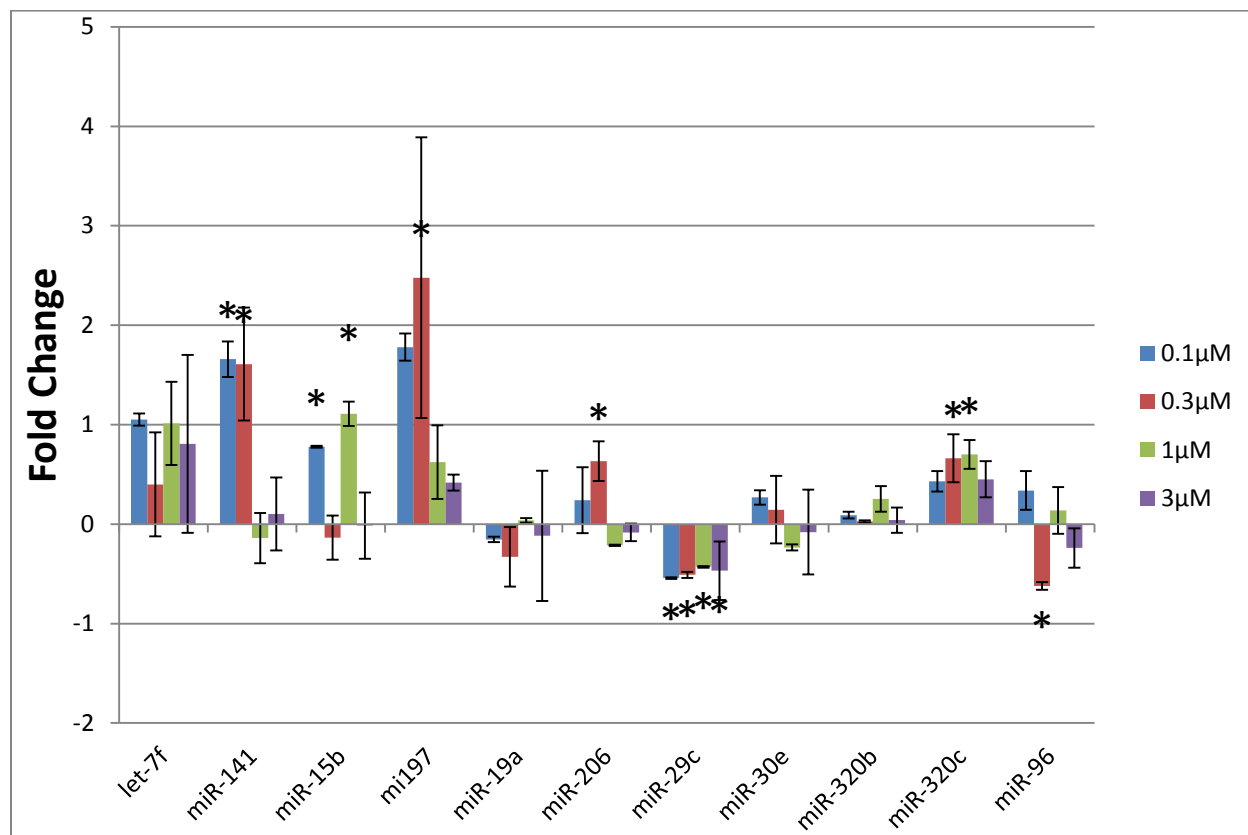


Figure 3.4: Fold change of qRT-PCR analysis of 11 chosen miRNAs at 4 different concentrations (0.1 μM; 0.3 μM; 1 μM; 3 μM) (* = p<0.05 compared to VC).

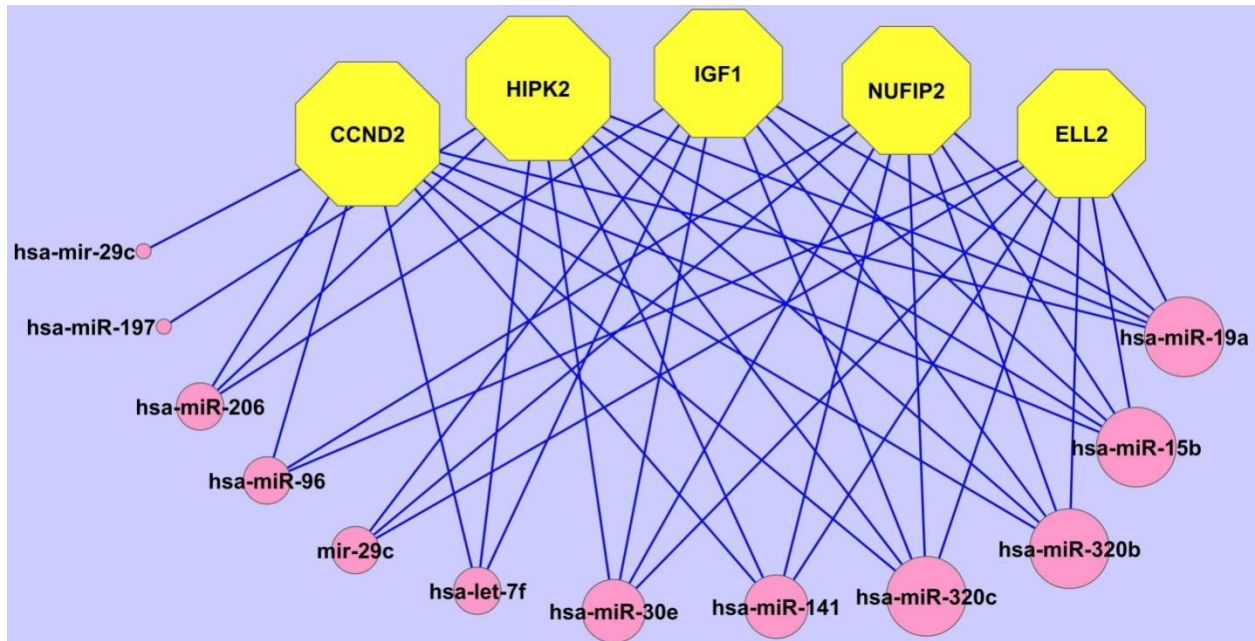


Figure 3.5: Network using genes that are commonly targeted by at least 8 of the 11 miRNAs chosen for further analysis. Hexagons are the protein coding genes, circles are the miRNAs. 2 genes (CCND2 and HIPK2) were predicted to be targeted by 9 of the 11 miRNAs of interest (SS change in expression levels). 3 genes (IGF1, NUFIP2, and ELL2) were predicted to be targeted by 8 miRNAs.). The node size is scaled such that it is proportional to the number of interactions. The highest being 9 (e.g. CCND2) and the lowest being 1 (e.g. hsa-miR-29c).

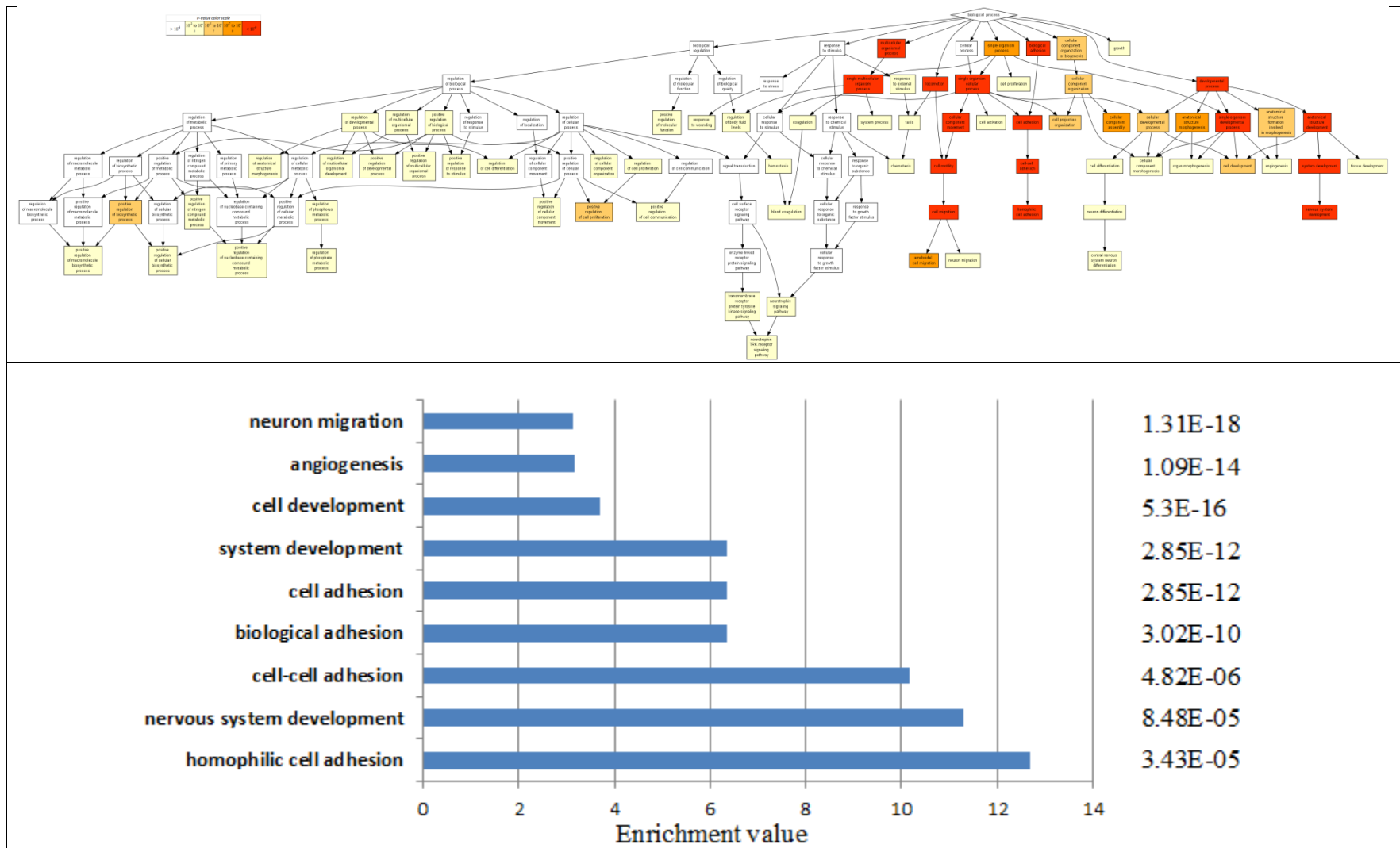


Figure 3.6: Directed acyclic graph that shows the relationship between enriched pathways predicted to be affected in response to gossypol.



Figure 3.7: MicroRNAs, Chromatin, Stress and Expression. Various stresses mediate multiple signaling pathways. MiRNAs that regulate Dicer and chromatin are components of stress pathways that regulate gene expression patterns (Image from roswellpark.edu).

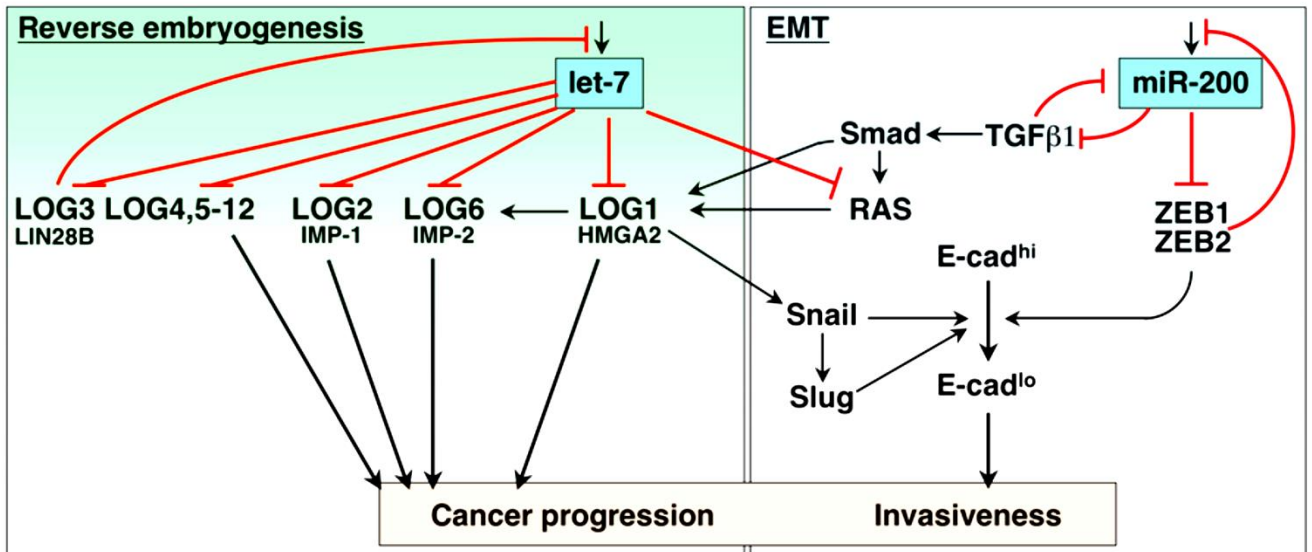


Figure 3.8: Model to illustrate how let-7 and miR-200 could each contribute to tumor progression, one by controlling let-7 regulated oncofetal genes (LOGs) and the other by regulating EMT and metastasis. Crosstalk exists between the pathways that regulate reverse embryogenesis and EMT [33].

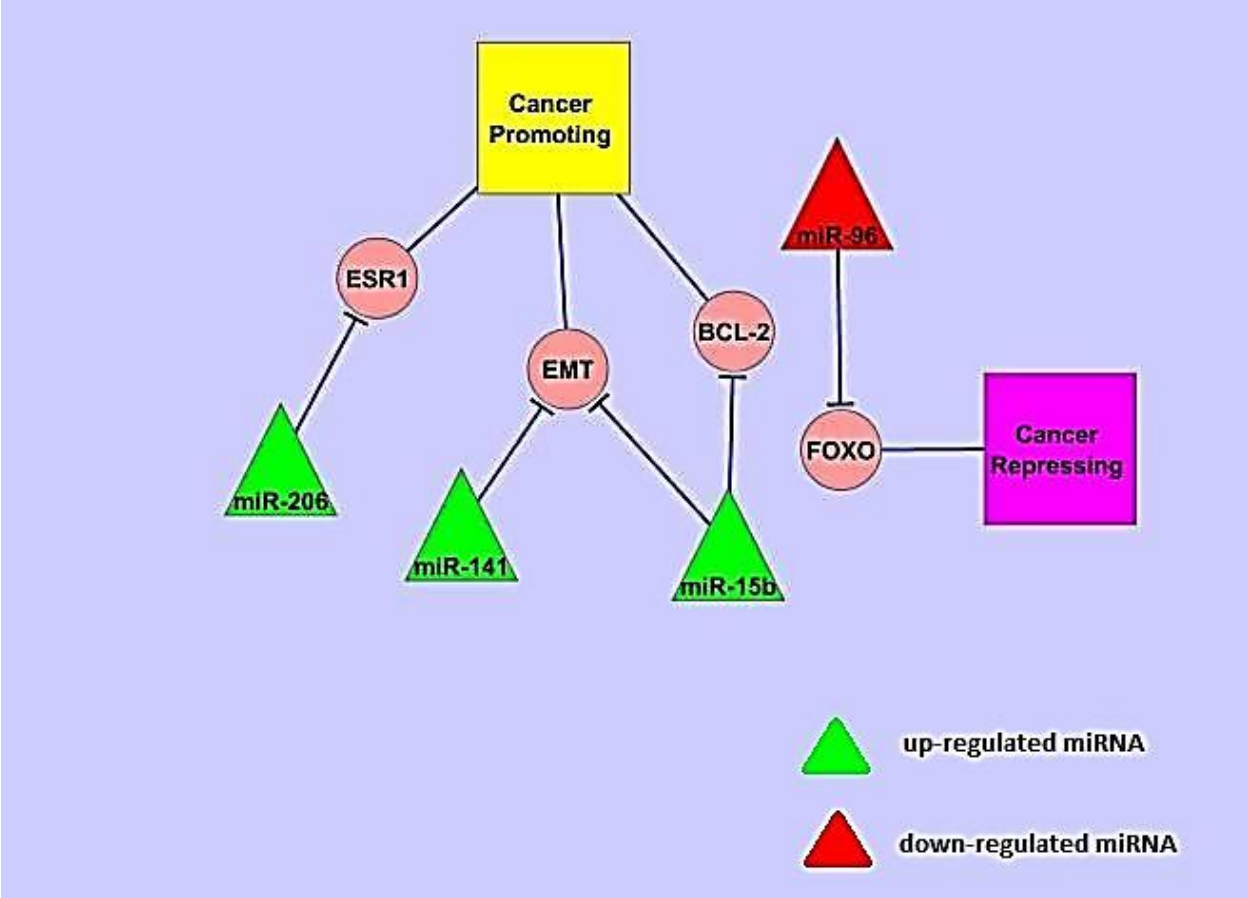


Figure 3.9: Summary of the major targets found in literature of miRNAs whose expression was altered in response to treatment with gossypol.

References

1. Gupta, S.C., et al., *Upsides and downsides of reactive oxygen species for cancer: the roles of reactive oxygen species in tumorigenesis, prevention, and therapy*. *Antioxid Redox Signal*, 2012. **16**(11): p. 1295-322.
2. Voss, V., et al., *The pan-Bcl-2 inhibitor (-)-gossypol triggers autophagic cell death in malignant glioma*. *Mol Cancer Res*, 2010. **8**(7): p. 1002-16.
3. Lian, J., et al., *A natural BH3 mimetic induces autophagy in apoptosis-resistant prostate cancer via modulating Bcl-2-Beclin1 interaction at endoplasmic reticulum*. *Cell Death Differ*, 2011. **18**(1): p. 60-71.
4. Ye, W., et al., *Modulation of multidrug resistance gene expression in human breast cancer cells by (-)-gossypol-enriched cottonseed oil*. *Anticancer Res*, 2007. **27**(1A): p. 107-16.
5. Sung, B., et al., *Gossypol induces death receptor-5 through activation of the ROS-ERK-CHOP pathway and sensitizes colon cancer cells to TRAIL*. *J Biol Chem*, 2010. **285**(46): p. 35418-27.
6. Barba-Barajas, M., et al., *Gossypol induced apoptosis of polymorphonuclear leukocytes and monocytes: involvement of mitochondrial pathway and reactive oxygen species*. *Immunopharmacol Immunotoxicol*, 2009. **31**(2): p. 320-30.
7. Ye, W., et al., *Induction of apoptosis by (-)-gossypol-enriched cottonseed oil in human breast cancer cells*. *Int J Mol Med*, 2010. **26**(1): p. 113-9.
8. Thomas, M., et al., *Effects of gossypol on the cell cycle phases in T-47D human breast cancer cells*. *Anticancer Res*, 1991. **11**(4): p. 1469-75.
9. Hu, Z.Y., et al., *ApoG2 induces cell cycle arrest of nasopharyngeal carcinoma cells by suppressing the c-Myc signaling pathway*. *J Transl Med*, 2009. **7**: p. 74.
10. Sun, J., et al., *Apogossypolone inhibits cell growth by inducing cell cycle arrest in U937 cells*. *Oncol Rep*, 2009. **22**(1): p. 193-8.
11. Wang, Y. and P.N. Rao, *Effect of gossypol on DNA synthesis and cell cycle progression of mammalian cells in vitro*. *Cancer Res*, 1984. **44**(1): p. 35-8.
12. Ligueros, M., et al., *Gossypol inhibition of mitosis, cyclin D1 and Rb protein in human mammary cancer cells and cyclin-D1 transfected human fibrosarcoma cells*. *Br J Cancer*, 1997. **76**(1): p. 21-8.
13. Wang, J., et al., *Gossypol induces apoptosis in ovarian cancer cells through oxidative stress*. *Mol Biosyst*, 2013. **9**(6): p. 1489-97.
14. Ambros, V., *The functions of animal microRNAs*. *Nature*, 2004. **431**(7006): p. 350-5.
15. Lizarraga, D., et al., *Benzo[a]pyrene-induced changes in microRNA-mRNA networks*. *Chem Res Toxicol*, 2012. **25**(4): p. 838-49.
16. Truesdell, S.S., et al., *MicroRNA-mediated mRNA translation activation in quiescent cells and oocytes involves recruitment of a nuclear microRNP*. *Sci Rep*, 2012. **2**: p. 842.
17. Vasudevan, S., Y. Tong, and J.A. Steitz, *Switching from repression to activation: microRNAs can up-regulate translation*. *Science*, 2007. **318**(5858): p. 1931-4.
18. Behm-Ansmant, I., et al., *mRNA degradation by miRNAs and GW182 requires both CCR4:NOT deadenylase and DCP1:DCP2 decapping complexes*. *Genes Dev*, 2006. **20**(14): p. 1885-98.
19. Taylor, E.L. and T.W. Gant, *Emerging fundamental roles for non-coding RNA species in toxicology*. *Toxicology*, 2008. **246**(1): p. 34-9.
20. Lema, C. and M.J. Cunningham, *MicroRNAs and their implications in toxicological research*. *Toxicol Lett*, 2010. **198**(2): p. 100-5.
21. Avissar-Whiting, M., et al., *Bisphenol A exposure leads to specific microRNA alterations in placental cells*. *Reprod Toxicol*, 2010. **29**(4): p. 401-6.

22. Sun, M., et al., *Curcumin (diferuloylmethane) alters the expression profiles of microRNAs in human pancreatic cancer cells*. *Mol Cancer Ther*, 2008. **7**(3): p. 464-73.
23. Shah, M.Y., et al., *5-Fluorouracil drug alters the microRNA expression profiles in MCF-7 breast cancer cells*. *J Cell Physiol*, 2011. **226**(7): p. 1868-78.
24. Huang, Q., et al., *The microRNAs miR-373 and miR-520c promote tumour invasion and metastasis*. *Nat Cell Biol*, 2008. **10**(2): p. 202-10.
25. Zhang, B., et al., *microRNAs as oncogenes and tumor suppressors*. *Dev Biol*, 2007. **302**(1): p. 1-12.
26. Zhang, H., et al., *Upregulation of microRNA-125b contributes to leukemogenesis and increases drug resistance in pediatric acute promyelocytic leukemia*. *Mol Cancer*, 2011. **10**: p. 108.
27. Hudder, A. and R.F. Novak, *miRNAs: effectors of environmental influences on gene expression and disease*. *Toxicol Sci*, 2008. **103**(2): p. 228-40.
28. Howell, J.C., et al., *Global microRNA expression profiling: curcumin (diferuloylmethane) alters oxidative stress-responsive microRNAs in human ARPE-19 cells*. *Mol Vis*, 2013. **19**: p. 544-60.
29. Gregory, P.A., et al., *The miR-200 family and miR-205 regulate epithelial to mesenchymal transition by targeting ZEB1 and SIP1*. *Nat Cell Biol*, 2008. **10**(5): p. 593-601.
30. Hurteau, G.J., et al., *Overexpression of the microRNA hsa-miR-200c leads to reduced expression of transcription factor 8 and increased expression of E-cadherin*. *Cancer Res*, 2007. **67**(17): p. 7972-6.
31. Park, S.M., et al., *The miR-200 family determines the epithelial phenotype of cancer cells by targeting the E-cadherin repressors ZEB1 and ZEB2*. *Genes Dev*, 2008. **22**(7): p. 894-907.
32. Gregory, P.A., et al., *An autocrine TGF-beta/ZEB/miR-200 signaling network regulates establishment and maintenance of epithelial-mesenchymal transition*. *Mol Biol Cell*, 2011. **22**(10): p. 1686-98.
33. Peter, M.E., *Let-7 and miR-200 microRNAs: guardians against pluripotency and cancer progression*. *Cell Cycle*, 2009. **8**(6): p. 843-52.
34. Xia, H., et al., *MicroRNA-15b regulates cell cycle progression by targeting cyclins in glioma cells*. *Biochem Biophys Res Commun*, 2009. **380**(2): p. 205-10.
35. Xia, L., et al., *miR-15b and miR-16 modulate multidrug resistance by targeting BCL2 in human gastric cancer cells*. *International Journal of Cancer*, 2008. **123**(2): p. 372-9.
36. Kondo, N., et al., *miR-206 Expression is down-regulated in estrogen receptor alpha-positive human breast cancer*. *Cancer Res*, 2008. **68**(13): p. 5004-8.
37. Adams, B.D., H. Furneaux, and B.A. White, *The micro-ribonucleic acid (miRNA) miR-206 targets the human estrogen receptor-alpha (ERalpha) and represses ERalpha messenger RNA and protein expression in breast cancer cell lines*. *Mol Endocrinol*, 2007. **21**(5): p. 1132-47.
38. Adams, B.D., D.M. Cowee, and B.A. White, *The role of miR-206 in the epidermal growth factor (EGF) induced repression of estrogen receptor-alpha (ERalpha) signaling and a luminal phenotype in MCF-7 breast cancer cells*. *Mol Endocrinol*, 2009. **23**(8): p. 1215-30.
39. Roth, P., et al., *A specific miRNA signature in the peripheral blood of glioblastoma patients*. *J Neurochem*, 2011. **118**(3): p. 449-57.
40. Yao, Y., et al., *MicroRNA profiling of human gastric cancer*. *Mol Med Rep*, 2009. **2**(6): p. 963-70.
41. Liu, R., et al., *A five-microRNA signature identified from genome-wide serum microRNA expression profiling serves as a fingerprint for gastric cancer diagnosis*. *Eur J Cancer*, 2011. **47**(5): p. 784-91.
42. Andorfer, C.A., et al., *MicroRNA signatures: clinical biomarkers for the diagnosis and treatment of breast cancer*. *Trends Mol Med*, 2011. **17**(6): p. 313-9.
43. Rukov, J.L. and N. Shomron, *MicroRNA pharmacogenomics: post-transcriptional regulation of drug response*. *Trends Mol Med*, 2011. **17**(8): p. 412-23.

44. Sarkar, F.H., et al., *Implication of microRNAs in drug resistance for designing novel cancer therapy*. Drug Resist Updat, 2010. **13**(3): p. 57-66.
45. Guo, Y., et al., *miR-96 regulates FOXO1-mediated cell apoptosis in bladder cancer*. Oncol Lett, 2012. **4**(3): p. 561-565.
46. Lin, H., et al., *Unregulated miR-96 induces cell proliferation in human breast cancer by downregulating transcriptional factor FOXO3a*. PLoS One, 2010. **5**(12): p. e15797.

Chapter 4: Effects of gossypol on oxidative stress in MCF-7 cells

Abstract

Many chemotherapy drugs today utilize the generation of reactive oxygen species (ROS) to induce cell death in cancer cells. In general, this strategy is very effective initially, but with time cancer cells tend to develop a strong resistance to ROS through up regulation of their antioxidant defense system. When treated with gossypol, a polyphenolic aldehyde found in high concentrations within cotton seed oil, many cancer cells are unable to procure this resistance and in many cases gossypol has been able to lower their resistance to other drugs [1-3]. In this study, using qRT-PCR technology followed by protein analysis of several key elements involved in oxidative stress, we examined if gossypol may indeed decrease the resistance of MCF-7 cells to ROS via their antioxidant defense systems. Our results indicate that gossypol does seem to have a profound effect on the antioxidant defenses of MCF-7 cells on both mRNA and protein levels. When treated with gossypol, MCF-7 cells exhibited signs of oxidative stress as well as an inability to deal with this stress using key antioxidant enzymes. This data combined with other studies leads us to believe that generation of ROS plays a big role in the efficacy of gossypol in treating breast cancer solitarily and may also be a big part of its success when combined with other chemotherapy drugs. This study helps to elucidate which candidate chemotherapeutics may be more effective in combination with gossypol.

Introduction

Oxidative stress is a common term used to describe the stress placed on cells due to an imbalance in the relationship between oxidants and their antioxidant defense systems. Oxidants are chemical compounds that are good electrophiles or that gain electrons easily when undergoing a redox reaction. Reactive oxygen species (ROS), reactive nitrogen species (RNS) and electrophilic metal ions have undergone extensive study in the biological science field. Important biological molecules like DNA, lipids and proteins, are nucleophilic due to their phosphate, sulfur and nitrogen enriched structures making them susceptible to electrophilic attack. These attacks result in DNA damage, lipid peroxidation and protein dysfunction [4].

ROS present in the body, play a major role in various cell-signaling pathways [5-7]. Studies have shown that ROS can be associated with risk factors of chronic diseases like cancer, such as tobacco, stress, radiation, environmental pollutants, viral infection, bacterial infection and diet that impact cells through the generation of ROS [8, 9].

Rather complexly, even though excess ROS from many different sources contributes to the induction of many cancers, they also seem to mediate the mechanism of action of many chemotherapeutic agents [10]. ROS have been associated with the anti-tumor and chemopreventive action of nutraceuticals that are extracted from many natural molecules used today in traditional medicine. With this knowledge, we understand that ROS can function as both cancer-suppressors and the function of cancer-promoters depends on the dosage of ROS [10].

In general, cancer treatment strategies utilizing ROS inducing chemotherapies show initially very successful results, but as time goes on cancer cells often develop a strong resistance to oxidative stressors by up-regulating their antioxidant defense systems (Figure 4.1). Some examples of key enzymes involved in this defense and related to this study are catalase (Cat) and superoxide dismutase (SOD) which act to eliminate free radicals and prevent DNA damage and the activation of apoptotic signaling pathways [11, 12]. If gossypol successfully inhibits this resistance, then new strategies using combination drug therapy with ROS inducing chemotherapeutics like 5-Fluorouracil or As_2O_3 can help overcome this limitation.

ROS have been demonstrated to be effector molecules of many pathways ending in cellular death (Figure 1.5) [13]. One of the first lines of defense when cells are faced with oxidative stress is autophagy. In this strategy of defense, cells can utilize a mechanism of selective lysosomal self-digestion of their intracellular components to help maintain cellular homeostasis. However, when exposed to higher levels of ROS, cells usually resort instead to the activation of autophagy induced cell death pathways [5, 7, 14]. ROS inducing apoptosis can be initiated by extracellular death receptors (extrinsic pathway) or through the intracellular mitochondrial signaling pathway (intrinsic pathway). With the extrinsic signaling pathway, ROS are induced by the Fas ligand and are required for Fas phosphorylation and activation [10]. In the intrinsic pathway, ROS act to open the permeability transition pore of mitochondria by utilizing the activating pore-destabilizing proteins (Bcl-2-associated X protein, Bcl-2) and inhibiting pore-stabilizing proteins (Bcl-2 and Bcl-xL) [6]. Additionally, in many cases if ROS levels are high enough, cells will undergo necrosis. ROS are key factors involved in the

propagation and execution phases of necrotic cell death, they can damage proteins, DNA and lipids either directly or indirectly, which can result in the disruption of the integrity of organelles and the cell as a whole. When cells are undergoing necrosis, they initiate a release of pro-inflammatory signaling cascades via the release of pro-inflammatory cytokines and by a sporadic emptying of their cellular contents upon lysing [15-18]. In this study, we investigated the effect of gossypol on oxidative stress-related proteins at both mRNA and enzyme activity levels in the human breast cancer line, MCF-7, *in vitro*.

Materials and Methods

Cell line and cell culture

Human MCF-7 breast cancer cells were ordered from ATCC and placed in a humidified 5%CO₂ and 95% air incubator at 37°C. Roswell Park Memorial Institute medium (RPMI) 1640 (GIBCO, Vienna, VA) media was used to grow MCF-7 cells and it was supplemented with 10% FBS (PAA Laboratories, Dartmouth, MA), and 4 mg/ml human recombinant insulin (GIBCO). A media change was performed at least every 48 hours, and the cells were trypsinized and passaged once a week by using 0.05% trypsin/0.02% EDTA (Sigma, St. Louis, MO).

Gossypol treatment

Gossypol was ordered from Sigma-Aldrich (St. Louis, MO) and kept at -80°C in a dark 1.8 mL micro-centrifuge tube impermeable to light. A 100 mM stock solution of gossypol was created using DMSO as the solvent and the entire procedure was

performed in a laminar flow hood and the solution was vacuum filtered to maintain sterility. To prepare cells for treatment, 5×10^5 cells were plated into 12 well plates with 3 wells per treatment group including controls in RPMI media with 10% FBS and no antifungal compounds or antibiotics with a final volume of 2mL in each well. Initially, cells were incubated for 24 hours in the RPMI media described above without treatment to allow for adhesion and stability. After stabilization and adherence, cells were treated with gossypol using DMSO as a vehicle. A 0.1% DMSO concentration was maintained in both the vehicle control and the treatments to exclude potential effects of DMSO.

RNA Extraction, Reverse Transcription, Real Time PCR

Forty-eight hours post-treatment, cells were trypsinized, centrifuged, washed with PBS and the pellet was placed in 1.8 mL micro-centrifuge tubes. RNA was extracted from cells using the mirVana™ miRNA Isolation Kit. The sample cells were denatured using a lysis binding buffer. Then, the RNA was separated from DNA and other cellular lipids and proteins via acid-phenol extraction. Next, ethanol was added to each sample, immediately followed by passing the solution through a glass-filter. To purify the RNA, several washes preceded the addition of elution solution used to elute the RNAs. To quantify and evaluate the quality of RNAs extracted, a NanoDrop ND-1000 Micro-Volume UVVis Spectrophotometer (NanoDrop Technologies, Wilmington, DE) was used to determine RNA concentration and the quality of the RNA which is based on the absorbance ratios of 260/280 and 260/230.

Next, reverse transcription was performed using TaqMan microRNA Reverse Transcription kit from Applied Biosystems (Foster City, CA) to create cDNAs. For protein coding genes, the poly-T primer was used. 200 ng RNAs was used for each

reverse transcription reaction. The other reagents within the reaction are as follows: 0.15 μ L of 100mM dNTPs, 2 μ L of poly (T) primer, 0.19 μ L RNase inhibitor (20U/ μ L), 1.5 μ L of reverse transcription buffer (10X), and 1 μ L of multiscribe reverse transcriptase (50U/ μ L) and RNase free water was added based on the concentration of RNA in the sample to make the final 15 μ L reaction volume. A thermal cycler was used to perform the reverse transcription reaction and was programmed as follows: 16 °C for 30 minutes followed by 42°C for 30 minutes, 85°C for 5 minutes and finally, a hold phase at 4°C. To prepare the cDNA for qRT-PCR, the sample was then diluted in 85 μ L DNase/RNase-free water.

qRT-PCR was conducted on 384-well-plates using the ViiA™ 7 Real-Time PCR System (Applied Biosystem) using SYBR Green PCR master mix (SuperArray Bioscience Corp,(Frederick, MD). To amplify cDNAs of the protein coding genes created in the previous step, forward and reverse specific primers were designed and used. Then, qRT-PCR was performed with each well containing a total of 15 μ L of total reaction mixture made up of the compilation of 7.5 μ L SYBR Green master mix, 1 μ L primer mix, 5.5 μ L DNase/RNase free water, 1 μ L cDNA. qRT-PCR was conducted with at less 3 biological replicates with a corresponding 3 technical replicates each. The actual program used for qRT-PCR began by activating the enzyme for 10 minutes at 95°C followed by a denaturation step for 15 seconds at 95°C, then by an annealing/extension step for 60 seconds at 60°C. The final 2 steps were repeated for 40 cycles.

Treatment and Sample Preparation for Protein Assays

Gossypol was purchased from Sigma-Aldrich (St. Louis, MO) and stored at -80°C. To maintain consistency, and provide the larger amount of cells necessary for protein assays, the same ratio of cells to surface area was used as all other assays. Instead of Corning 12-well plates, 9.35×10^6 cells were seeded in T-75 Corning Canted Neck Cell Culture Flasks, one biological replicate per flask. Cells were first incubated for 24 hours in RPMI media with no treatment to allow for adhesion and stability. Next, cells were treated at varying concentrations of gossypol using DMSO as a vehicle. Since 0.1% DMSO was used in each treatment group, the same amount of DMSO was also added to the control groups to exclude potential effects of DMSO. Forty eight hours post-treatment, media was removed and cells were washed three times with PBS free of Ca^{2+} and Mg^{2+} for 30 seconds. After the final wash, cells were removed using a rubber policeman and centrifuged at 200g 4°C in 1.5-mL centrifuge tubes. Supernatant was removed and cells were re-suspended in three times the pellet volume in Phosphate Buffer (PB, pH 7.8) and sonicated on ice for ~30 seconds at low power.

Protein concentrations of samples were calculated using the Thermo Scientific™ Pierce™ BCA Protein Assay according to the manufacturer's protocol and utilizing the 96-well Fisher Scientific Multiskan®. MCC/340 Microplate Reader measuring absorbance at 562 nm.

Catalase Assay

Catalase activity was measured according to a previous method with a small modification [19]. Catalase removes peroxide at an exponential rate. Using a Shimadzu UVmini-1240 UV/Visible Scanning Spectrophotometer, a kinetics program was set to record every 30 seconds at 240 nm for 2 minutes. The Spectrophotometer

was calibrated using a 3-mL quartz cuvette filled with 3-mL of Phosphate Buffer pH 7.8. Next, the biological replicates and the bovine liver catalase standard were mixed with the Hydrogen Peroxide working solution and the kinetics program was performed according to a previous protocol [20] using 3 biological replicates with 3 technical replicates.

SOD Assay

Xanthine-Xanthine Oxidase was used to generate superoxide and nitroblue tetrazolium (NBT) reduction was used as an indicator of superoxide production. SOD competes with NBT for superoxide; therefore, the percentage inhibition of NBT reduction is a measure of the amount of SOD present (Figure 4.2). A modified method was used to determine the activity of SOD per mg of protein using a 96-well Fisher Scientific Multiskan®. MCC/340 Microplate Reader. Reagents and Solutions needed for this assay were purchased and prepared according previous reported protocol [20]. A kinetics program was used to calculate the absorbance/minute of reduced NBT at 560nm. An XO control was prepared and adjusted with DETAPAC to a measurement between 0.02 and 0.025 absorbance/minute. Once properly calibrated, the control was used as a baseline for NBT reduction free from competition from superoxide. A serial dilution with Phosphate Buffer pH 7.8 was conducted for each sample using 3 biological replicates and 3 technical replicates to assess the % inhibition as a function of protein concentration.

GCL and GSH Assay

Reagents used in the study include sucrose, Tris base, ethylenediamine tetra-acetic acid (EDTA), boric acid, L-serine, magnesium chloride hexahydrate (MgCl₂),

adenosine 5'-triphosphate disodium (ATP), L-glutamic acid, L-cysteine, 5-sulfosalicylic acid dihydrate (SSA), sodium hydroxide (NaOH), naphthalene-2,3-dicarboxaldehyde (NDA), dimethyl sulfoxide (DMSO) and gamma- glutamylcysteine (GC). Sodium hydroxide was obtained from Fisher Scientific International Inc. (Fair Lawn, NJ, USA), while all others were purchased from Sigma Co. (St. Louis, MO, USA).

The GCL reaction cocktail contained 400mM Tris, 2mM EDTA, 20mM boric acid, 2mM L-serine, 40mM MgCl₂, 40mM ATP and L-glutamic acid, with a pH of 7.4. The concentration of glutamic acid in reaction cocktail was 40mM, and the concentration of cysteine was 30mM based on the previous report [21].

Fifty μ l of cell homogenate, 50 μ l of GCL reaction cocktail and 50 μ l of cysteine were added sequentially, then incubated for 30 minutes at 37°C, after which, 50 μ l of 200mM SSA were added to terminate the reaction. For GSH background measurement, 50 μ l of 200mM SSA were added prior to the addition of GCL reaction cocktail and cysteine.

The mixture was then centrifuged at 2,000g for 10 minutes at 4°C. The resulting supernatant was used for the following derivation. Twenty μ l of supernatant were loaded into a clear-bottomed black 96-well microplate, followed by the addition of 180 μ l of NDA solution (1:1:7 of 10mM NDA : 0.5M NaOH : 0.05M Tris with a pH of 10.0, v/v/v), the mixture was incubated in the dark at room temperature for 30 minutes. The fluorescence intensities of GSH-NDA and the sum of GC-NDA and GSH-NDA were measured at 485nm excitation and 538nm emission on a fluorescence plate reader (Molecular Devices, CA, USA, 1996), the difference was the GC-NDA content.

To assess the concentration of GSH in relation to the fluorescence, a standard curve was performed and is shown in figure 4.7. Using the standard curve, both GSH and GCL concentrations could be obtained due to their lack of difference in fluorescent activity as demonstrated by White [22].

A GSH standard curve was used for the quantification of both GCL and GSH in relation to fluorescence intensity. As shown in figure 4.7, a series of seven 2-fold dilutions were calculated beginning with 1000 μ M GSH and ending with 15.625 μ M GSH with the last and final point void of GSH. Three replicates of each concentration were used and the R^2 value for the standard curve was 0.9984 as seen in figure 4.7.

Results

qRT-PCR

Figure 4.3 shows the results from qRT-PCR analysis of key genes relating to oxidative stress in MCF-7 breast cancer cells after treatment at four concentrations (0.1 μ M, 0.2 μ M, 1 μ M, 3 μ M) of gossypol. We observed an overall downward trend in gene expression as the dosages of gossypol increased. Catalase (CAT), cytochrome p450 (CYP2U1), glutathione synthetase (GSS) and glutathione S-transferase theta 1 (GSTT1) all had similar patterns of a slight down-regulation in response to gossypol with significances of $p < 0.033$. With glutathione peroxidase (GPX1), nicotanimide adenine dinucleotide phosphate (NADPH) and superoxide dismutase (SOD1), we see a distinct up-regulation of the 0.1 μ M treatment followed by a pattern of decrease in expression as concentrations increased with p values < 0.013 .

Catalase Assay

Catalase activity decreases as treatment concentration with gossypol increases (Figure 4.4). This decrease is consistent with the gene expression data from the qRT-PCR analysis (Figure 4.3). The protein activity of catalase is expressed as U/mg protein with the vehicle control having an average activity of 2.99 U/mg; the 0.1 μ M gossypol treatment demonstrated an average activity of 2.29U/mg and finally the highest concentration of gossypol at 3 μ M exhibited the lowest average activity of 1.94 U/mg.

SOD assay

Similar to catalase, SOD activity was decreased proportionally to the concentration of gossypol treatment. The vehicle control displayed an average activity of 43.39 U/mg; the 0.1 μ M gossypol treatment exhibited an activity of 55.52 U/mg a slight but not statistically significant increase and at the highest concentration of gossypol 3 μ M, we observed a strong statistically significant ($p=0.01$) decrease to an average activity of 8.06 U/mg (Figure 4.5 D). Figures 4.5 A, B, C are graphs that show the % inhibition of NBT reduction versus μ g of protein for VC, 0.1 μ M and 3 μ M.

GCL and GSH assay

Gossypol treatment increased the activity of GCL and the levels of GSH at even the lowest treatment (0.1 μ M) and even further at the 3 μ M treatment. We saw that the increase in GCL activity and GSH levels correlated well, which beyond statistical tests is a good indicator the assay was effective due to their interrelatedness. Average GCL activity was 0.364 measured in nmole/minute/milligrams protein for the vehicle control; 0.591 at the 0.1 μ M gossypol treatment and finally 0.693 for the 3 μ M treatment. GSH

levels measured in $\mu\text{M}/\mu\text{g}$ in a similar manner had average levels of 1.80 for the vehicle control, 2.98 for the 0.1 μM gossypol treatment and finally 2.71 at the 3 μM treatment.

Discussion

In this study, we observed the down-regulation of many antioxidants in response to gossypol. However, with enzymes like SOD and GCL, a period of up-regulation seems to occur in response to gossypol treatment, with SOD at the lower concentration of 0.1 μM consistent at both the genotypic and protein level (figures 4.3, 4.5 respectively) and with GCL and levels of GSH at both treatment levels (figure 4.6: 0.1 μM , 3 μM). Although it would be more desirable from a combination therapy standpoint to see a complete down-regulation of all antioxidant defenses, this data does suggest that not only does gossypol reduce the efficacy of key antioxidants at the right concentration (3 μM) but that gossypol is simultaneously creating oxidants and stressing MCF-7 cells which is not unexpected due to its structure. Previous studies have shown gossypol is very capable at both inhibiting oxidative stress related enzymes as well as inducing oxidative stress [23-25].

An emerging strategy in cancer treatment is to enhance the oxidative stress placed on cancer cells by inhibiting elements of their antioxidant defense systems. Using anticancer agents that target SOD in particular has shown great promise in utilizing this strategy. 2-Methoxyestradiol [26-28] for metastatic breast cancer and prostate cancer, ATN-224 for prostate cancer [29] have undergone phase I and II clinical trials respectively as drugs that specifically inhibit superoxide dismutase enzyme activity in cancer cells. Some anticancer compounds also target the GSH system. β -

Phenylethyl isothiocyanate (PEITC) a mustard oil, was shown to deplete levels of GSH and inhibit the activity of GPx [30]. Buthionine Sulfoximine (BSO) specifically inhibits GCS which in turn inhibits GSH levels downstream. It was found to be safe and effective in a phase I study where it was combined with melphalan an alkylating chemotherapeutic [31]. BSO has also been used in combination with As_2O_3 in the successful treatment of advanced stage solid tumors [32].

Additionally, gossypol has been shown to induce cell death utilizing its oxidant generating ability in a variety of cell lines [24, 33, 34]. It appears from the results of this study that cells did in fact experience oxidative stress in response to gossypol and certain key antioxidants were simultaneously inhibited. Due to these results, a more accurate assessment of the oxidative effects of gossypol on MCF-7 breast cancer cells has been achieved. These results indicate the possibility of a dual role of gossypol inhibiting SOD and CAT, the main eliminators of superoxide and hydrogen peroxide respectively, and inducing cell death mediated by generation of ROS. Due to gossypol's unique ability to simultaneously inhibit these key antioxidant enzymes and induce oxidative stress, a combination therapy with a superoxide generating chemotherapy like As_2O_3 which has had success in treating leukemia [35, 36] and advanced solid stage tumors in combination with BSO [32] is suggested to optimize their results and possibly create a synergistic effect that is more successful than either drug solitarily.

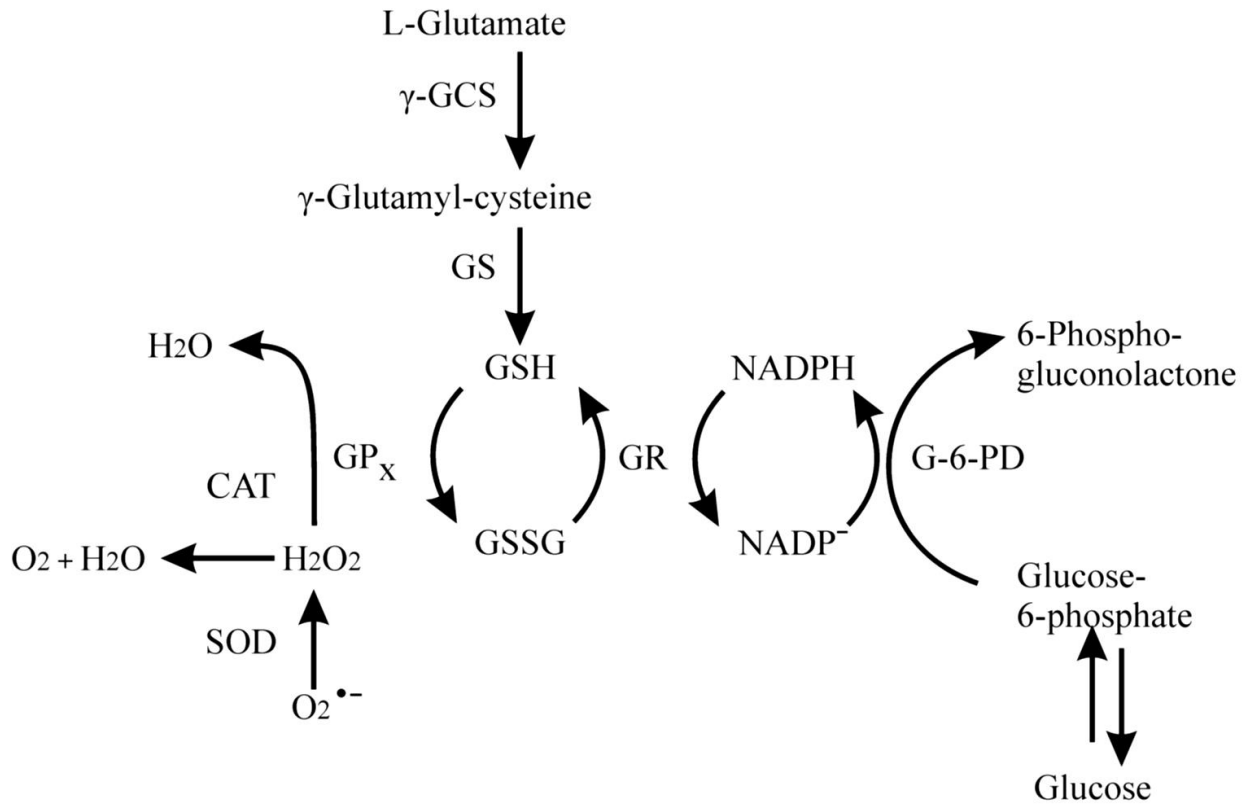


Figure 4.1: A schematic of the three major types of primary intracellular antioxidant enzymes in mammalian cells: SOD, catalase, and peroxidase. The SODs convert $O_2 \bullet^-$ into H_2O_2 , while the catalases and peroxidases convert H_2O_2 into water [20].

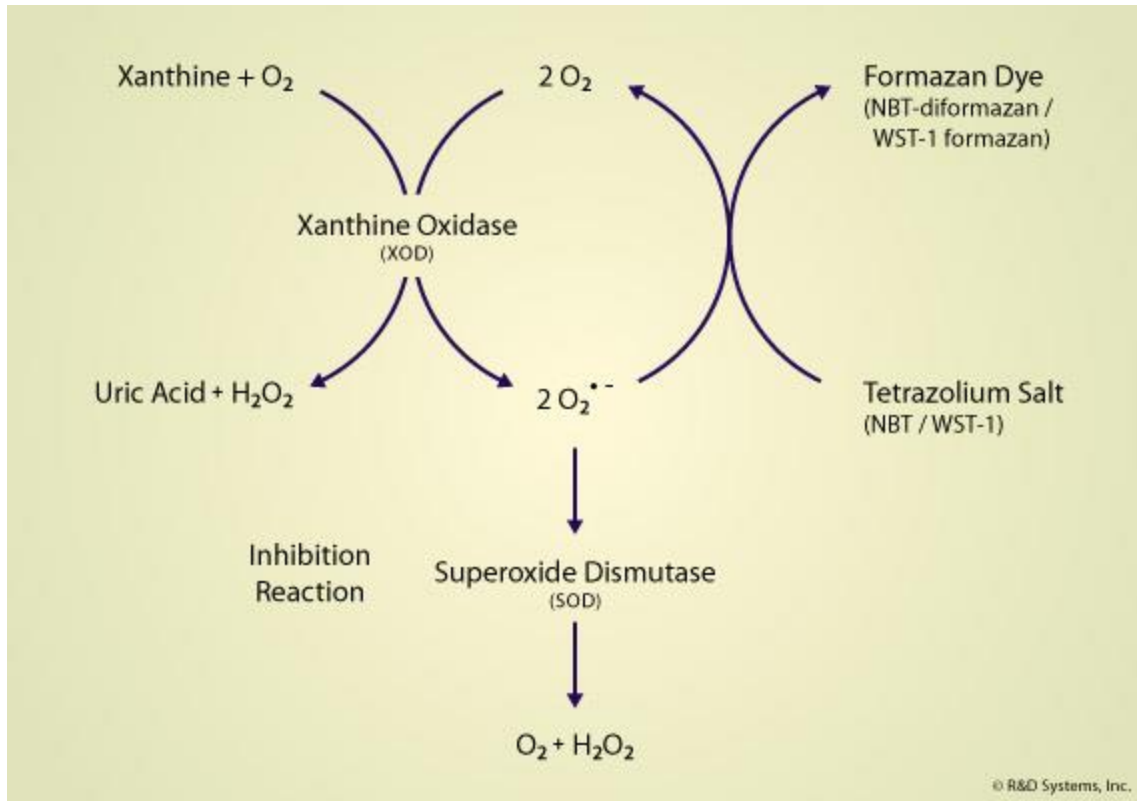


Figure 4.2: Schematic for the method used to determine the SOD activity utilizing the ability of SOD to inhibit the reduction of NBT. Under normal conditions, Xanthine Oxidase produces superoxide when substrates Xanthine and O₂ are present. However, when active Superoxide Dismutase is present it competes for Superoxide; thus inhibiting the normal rate at which NBT is reduced.

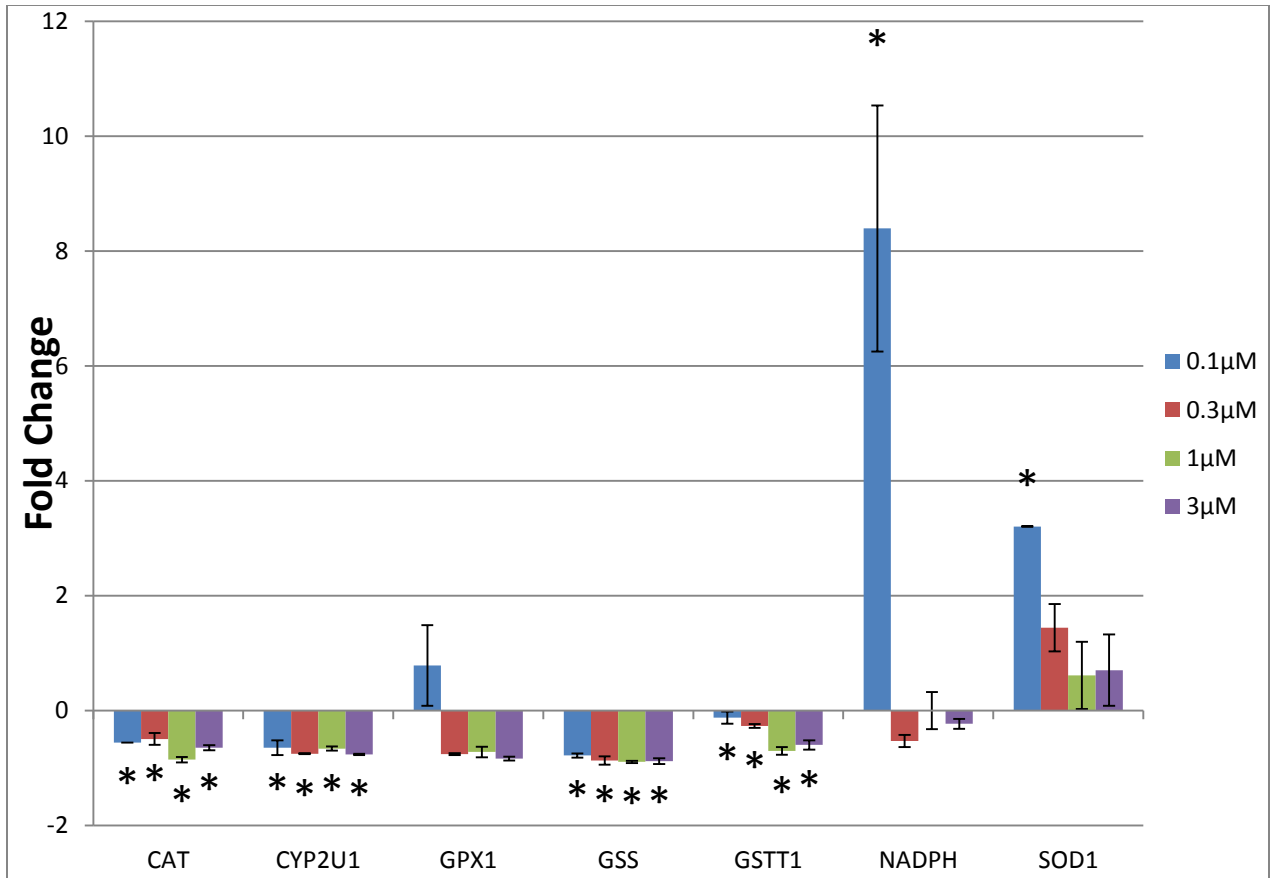


Figure 4.3: Effect of gossypol on the expression of genes relating to oxidative stress.

When treating with gossypol at 4 different concentrations (0.1 μM, 0.2 μM, 1 μM, and 3 μM), a general downward trend is observed that is proportional to the dose (* = p<0.05 compared to VC).

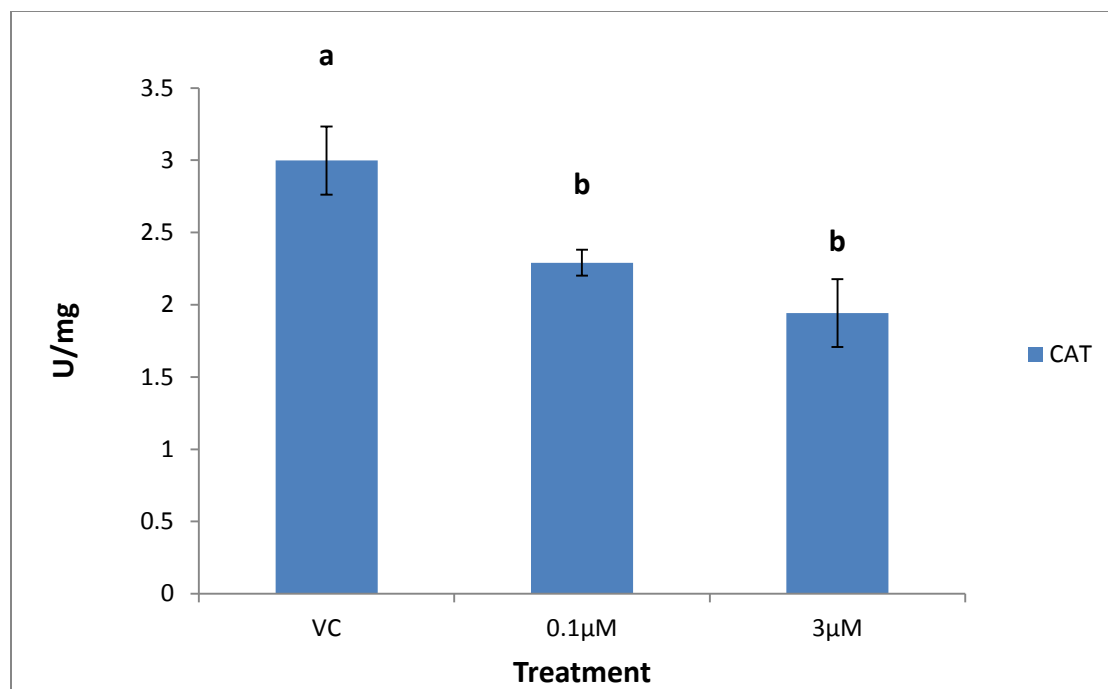


Figure 4.4: Catalase enzyme activity measured per milligram protein. Post-treatment with gossypol a downward trend of enzyme activity was observed proportional to the dosage of treatment. Catalase activity was measured by a spectrophotometric procedure measuring peroxide removal according to the method of Beers and Sizer [19] (Different letters=statistically significant difference $P < 0.05$).

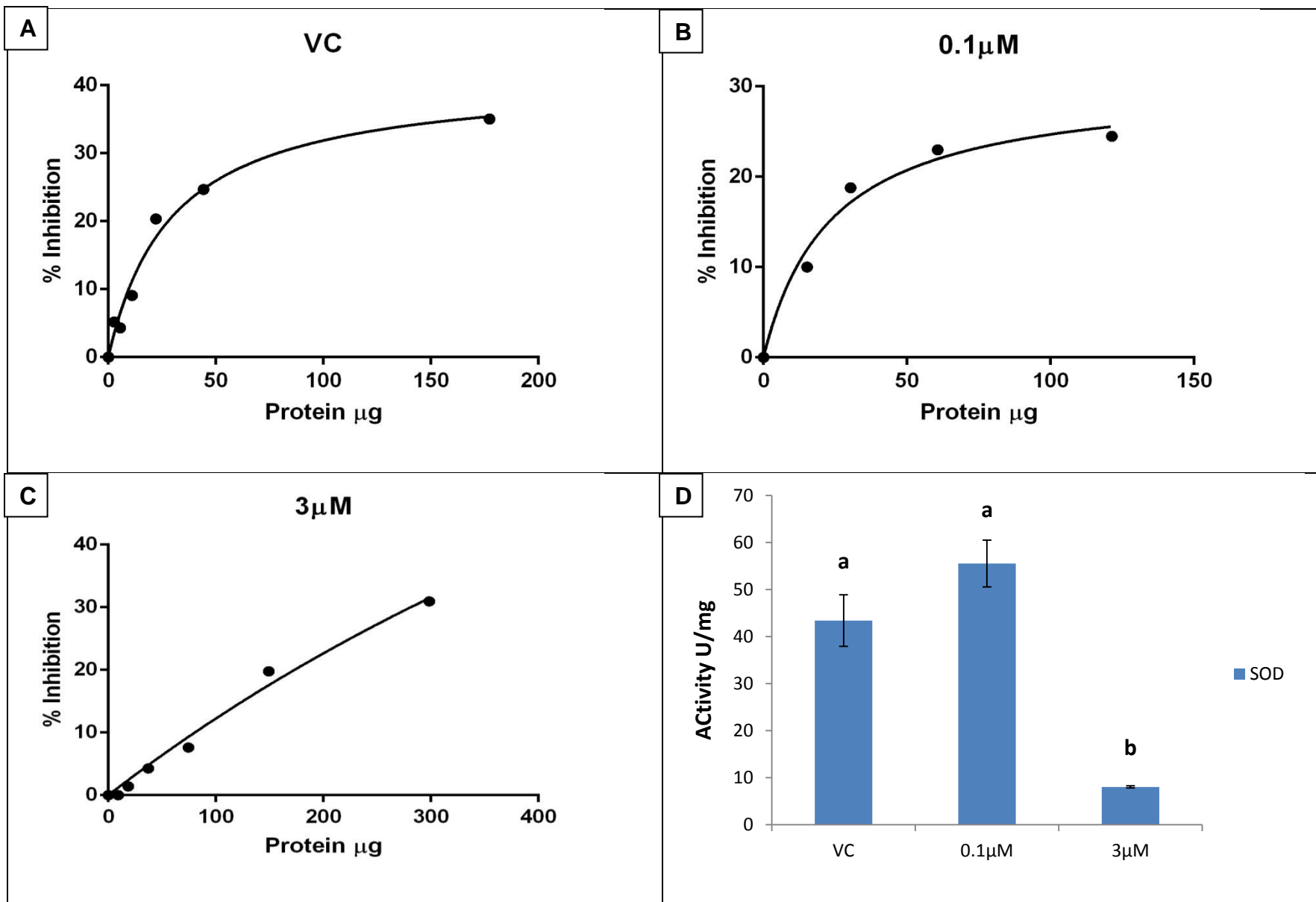


Figure 4.5: SOD activity/mg (0.1 μM , 3 μM) concentrations (Different letters=statistically significant difference $P < 0.05$).

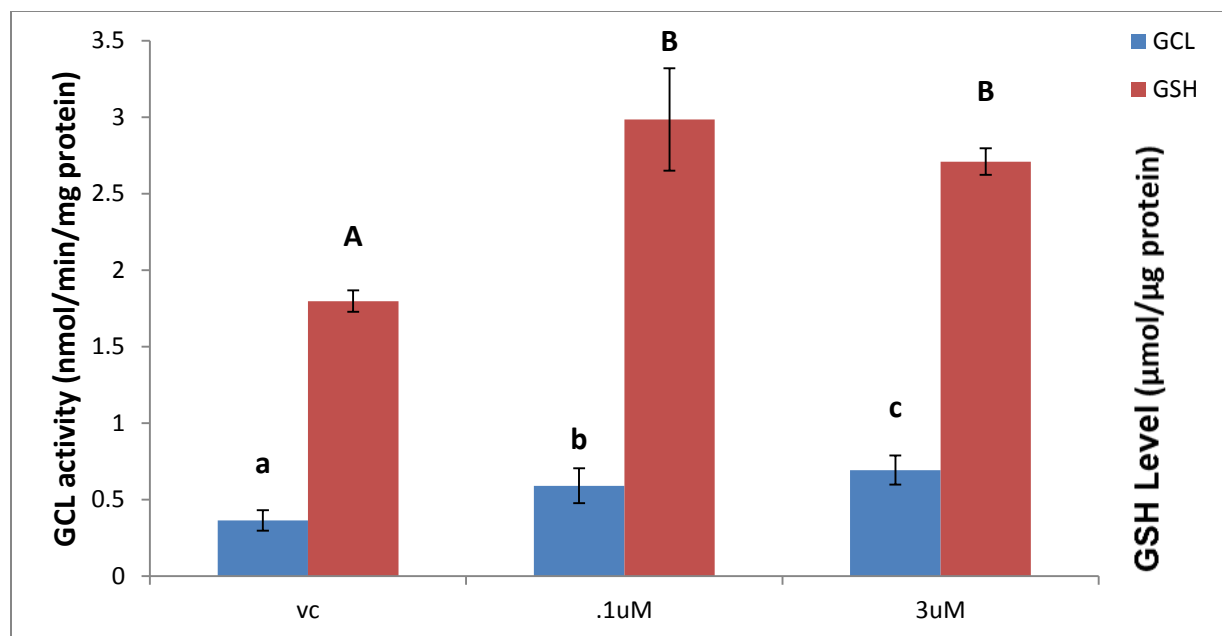


Figure 4.6: GCL activity and GSH level responses to treatment with gossypol (0.1 μM, 3 μM). Gossypol stimulates slightly the protein expression of GCL and GSH indicating a response to oxidative stress induced by the drug. (Different letters=statistically significant difference, capital letters comparing GSH levels and lower case letters for GCL activity P<0.05)

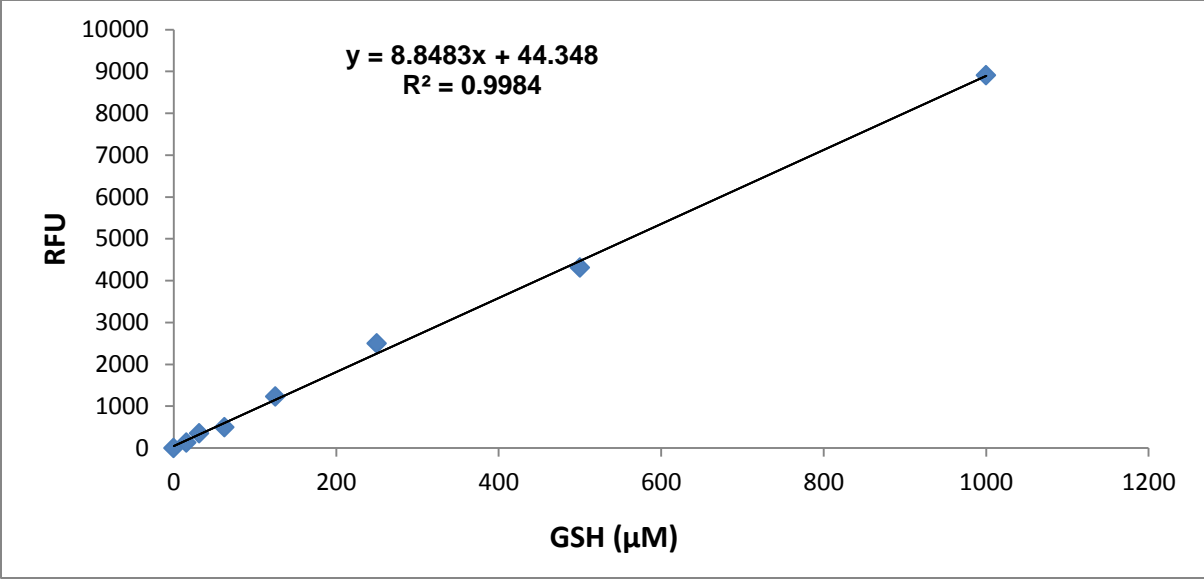


Figure 4.7: GSH standard curve conducted using 2 fold dilutions starting at 1000µM.

This curve helped to standardize the RFU per µM of GSH-NDA and GCL-NDA.

References

1. Lian, J., et al., *A natural BH3 mimetic induces autophagy in apoptosis-resistant prostate cancer via modulating Bcl-2-Beclin1 interaction at endoplasmic reticulum*. Cell Death Differ, 2011. **18**(1): p. 60-71.
2. Ye, W., et al., *Modulation of multidrug resistance gene expression in human breast cancer cells by (-)-gossypol-enriched cottonseed oil*. Anticancer Res, 2007. **27**(1A): p. 107-16.
3. Yan, F., et al., *A novel water-soluble gossypol derivative increases chemotherapeutic sensitivity and promotes growth inhibition in colon cancer*. J Med Chem, 2010. **53**(15): p. 5502-10.
4. Valko, M., et al., *Free radicals and antioxidants in normal physiological functions and human disease*. The international journal of biochemistry & cell biology, 2007. **39**(1): p. 44-84.
5. Li, L., G. Ishdorj, and S.B. Gibson, *Reactive oxygen species regulation of autophagy in cancer: implications for cancer treatment*. Free Radic Biol Med, 2012. **53**(7): p. 1399-410.
6. Martindale, J.L. and N.J. Holbrook, *Cellular response to oxidative stress: Signaling for suicide and survival**. Journal of Cellular Physiology, 2002. **192**(1): p. 1-15.
7. Scherz-Shouval, R., et al., *Reactive oxygen species are essential for autophagy and specifically regulate the activity of Atg4*. EMBO J, 2007. **26**(7): p. 1749-60.
8. Inoue, M., et al., *Mitochondrial generation of reactive oxygen species and its role in aerobic life*. Curr Med Chem, 2003. **10**(23): p. 2495-505.
9. del Rio, L.A., et al., *Metabolism of oxygen radicals in peroxisomes and cellular implications*. Free Radic Biol Med, 1992. **13**(5): p. 557-80.
10. Gupta, S.C., et al., *Upsides and downsides of reactive oxygen species for cancer: the roles of reactive oxygen species in tumorigenesis, prevention, and therapy*. Antioxid Redox Signal, 2012. **16**(11): p. 1295-322.
11. Renschler, M.F., *The emerging role of reactive oxygen species in cancer therapy*. Eur J Cancer, 2004. **40**(13): p. 1934-40.
12. Reuter, S., et al., *Oxidative stress, inflammation, and cancer: how are they linked?* Free Radic Biol Med, 2010. **49**(11): p. 1603-16.
13. Amaravadi, R.K. and C.B. Thompson, *The roles of therapy-induced autophagy and necrosis in cancer treatment*. Clin Cancer Res, 2007. **13**(24): p. 7271-9.
14. Gong, K., et al., *Autophagy-related gene 7 (ATG7) and reactive oxygen species/extracellular signal-regulated kinase regulate tetrandrine-induced autophagy in human hepatocellular carcinoma*. J Biol Chem, 2012. **287**(42): p. 35576-88.
15. Festjens, N., T. Vanden Berghe, and P. Vandenabeele, *Necrosis, a well-orchestrated form of cell demise: signalling cascades, important mediators and concomitant immune response*. Biochim Biophys Acta, 2006. **1757**(9-10): p. 1371-87.
16. Morgan, M.J., Y.S. Kim, and Z.G. Liu, *TNFalpha and reactive oxygen species in necrotic cell death*. Cell Res, 2008. **18**(3): p. 343-9.
17. Lu, C.C., et al., *Chrysophanol induces necrosis through the production of ROS and alteration of ATP levels in J5 human liver cancer cells*. Mol Nutr Food Res, 2010. **54**(7): p. 967-76.
18. Higuchi, M., et al., *Regulation of reactive oxygen species-induced apoptosis and necrosis by caspase 3-like proteases*. Oncogene, 1998. **17**(21): p. 2753-60.
19. Beers, R.F., Jr. and I.W. Sizer, *A spectrophotometric method for measuring the breakdown of hydrogen peroxide by catalase*. J Biol Chem, 1952. **195**(1): p. 133-40.
20. Weydert, C.J. and J.J. Cullen, *Measurement of superoxide dismutase, catalase and glutathione peroxidase in cultured cells and tissue*. Nat Protoc, 2010. **5**(1): p. 51-66.
21. Wu, H., et al., *Optimization and application of glutamate cysteine ligase measurement in wildlife species*. Ecotoxicol Environ Saf, 2009. **72**(2): p. 572-8.

22. White, C.C., et al., *Fluorescence-based microtiter plate assay for glutamate-cysteine ligase activity*. Anal Biochem, 2003. **318**(2): p. 175-80.
23. Bender, H.S., S.Z. Derolf, and H.P. Misra, *Effects of gossypol on the antioxidant defense system of the rat testis*. Arch Androl, 1988. **21**(1): p. 59-70.
24. Sung, B., et al., *Gossypol induces death receptor-5 through activation of the ROS-ERK-CHOP pathway and sensitizes colon cancer cells to TRAIL*. J Biol Chem, 2010. **285**(46): p. 35418-27.
25. Velasquez-Pereira, J., et al., *Reproductive effects of feeding gossypol and vitamin E to bulls*. J Anim Sci, 1998. **76**(11): p. 2894-904.
26. Huang, P., et al., *Superoxide dismutase as a target for the selective killing of cancer cells*. Nature, 2000. **407**(6802): p. 390-395.
27. James, J., et al., *Phase I safety, pharmacokinetic and pharmacodynamic studies of 2-methoxyestradiol alone or in combination with docetaxel in patients with locally recurrent or metastatic breast cancer*. Investigational new drugs, 2007. **25**(1): p. 41-48.
28. Sweeney, C., et al., *A phase II multicenter, randomized, double-blind, safety trial assessing the pharmacokinetics, pharmacodynamics, and efficacy of oral 2-methoxyestradiol capsules in hormone-refractory prostate cancer*. Clinical cancer research, 2005. **11**(18): p. 6625-6633.
29. Lin, J., et al. *A non-comparative randomized phase II study of 2 doses of ATN-224, a copper/zinc superoxide dismutase inhibitor, in patients with biochemically recurrent hormone-naive prostate cancer*. in *Urologic Oncology: Seminars and Original Investigations*. 2011. Elsevier.
30. Trachootham, D., et al., *Selective killing of oncogenically transformed cells through a ROS-mediated mechanism by β -phenylethyl isothiocyanate*. Cancer Cell, 2006. **10**(3): p. 241-252.
31. Bailey, H.H., et al., *Phase I study of continuous-infusion LS, R-buthionine sulfoximine with intravenous melphalan*. J Natl Cancer Inst, 1997. **89**(23): p. 1789-1796.
32. Maeda, H., et al., *Effective treatment of advanced solid tumors by the combination of arsenic trioxide and L-buthionine-sulfoximine*. Cell Death & Differentiation, 2004. **11**(7): p. 737-746.
33. Cheng, P., et al., *The novel BH-3 mimetic apogossypolone induces Beclin-1- and ROS-mediated autophagy in human hepatocellular carcinoma [corrected] cells*. Cell Death Dis, 2013. **4**: p. e489.
34. Ni, Z., et al., *Natural Bcl-2 inhibitor (-)- gossypol induces protective autophagy via reactive oxygen species-high mobility group box 1 pathway in Burkitt lymphoma*. Leuk Lymphoma, 2013.
35. Niu, C., et al., *Studies on treatment of acute promyelocytic leukemia with arsenic trioxide: remission induction, follow-up, and molecular monitoring in 11 newly diagnosed and 47 relapsed acute promyelocytic leukemia patients*. Blood, 1999. **94**(10): p. 3315-3324.
36. Shen, Z.-X., et al., *Use of arsenic trioxide (As₂O₃) in the treatment of acute promyelocytic leukemia (APL): II. Clinical efficacy and pharmacokinetics in relapsed patients*. Blood, 1997. **89**(9): p. 3354-3360.